UNIVERSITY OF NAIROBI
COLLEGE OF BIOLOGICAL AND PHYSICAL SCIENCES
SCHOOL OF PYSICAL SCIENCES

Evaluation of Hydrogeochemical Facies of the Barrier Volcanic Complex Geothermal Fluids in Developing a Conceptual Model

By:
LEAKEY OCHIENG AUKO
I56/70861/2011

A dissertation submitted in partial fulfillment of the requirements for the degree of Master of Science in Applied Geochemistry

JULY, 2013

Declaration

This thesis is my original work and has not been presented for a degree in any other university or any other award.

Signature_____ Date: _____

Mr. Leakey Ochieng Auko
Department of Geology,
School of Physical Sciences,
University of Nairobi

This thesis has been submitted for examination with my approval as the supervisor;

Signature_____ Date: _____

Prof. Daniel Olago

Department of Geology,
School of Physical Sciences,
University of Nairobi

Signature _____ Date: _____

Prof. Eric O. Odada

Department of Geology,
School of Physical Sciences,
University of Nairobi

Signature _____ Date: _____

Prof. Norbert Opiyo-Akech

Department of Geology,
School of Physical Sciences,
University of Nairobi

Declaration of Originality

Name of Student	Leakey Ochieng Auko
Registration Number	I56/70861/2011
College	College of Biological Physical Sciences
School	School of Physical Sciences
Department	Department of Geology
Course Name	Master of Science in Applied Geochemistry
Title of the Work	**Evaluation of Hydrogeochemical Facies of the Barrier Volcanic Complex Geothermal Fluids in Developing a Conceptual Model**

DECLARATION

1. I understand what Plagiarism is and I am aware of the University's policy in this regard
2. I declare that this thesis is my original work and has not been submitted elsewhere for examination, award of a degree or publication. Where other people's work, or my own work has been used, this has properly been acknowledged and referenced in accordance with the University of Nairobi's requirements.
3. I have not sought or used the services of any professional agencies to produce this work
4. I have not allowed, and shall not allow anyone to copy my work with the intention of passing it off as his/her own work
5. I understand that any false claim in respect of this work shall result in disciplinary action, in accordance with University Plagiarism Policy.

Signature _____

Date _____

Abstract

The Barrier Volcanic Complex (BVC) geothermal prospect is situated on the floor of the northern sector of the Kenya rift, immediately south of Lake Turkana. It is composed of four distinct polygenetic volcanic edifices; Kaloleyang, Likaiu East, Likaiu West and Kakorinya, which are characterised by a wide spectrum of lava types including basanite, basalt, hawaiite, mugearite, benmorite, trachyte, phonolite and pyroclastics. Geothermal manifestations occur in the form of fumaroles, silica sinters, Logipi hot springs and hydrothermally altered rocks characterised by argillic alteration deposits of alunite, kaolinite, and other clay minerals found in the areas of fumarolic activity in the Kakorinya caldera and its summit. The caldera is the youngest volcanic centre and has the most promising geothermal potential. This project presents the evaluation of the hydrogeochemical characteristics of the sampled seven Logipi hot springs and six Kakorinya fumaroles in the BVC with the aim of developing a conceptual model. It is inherent that the key to successful exploration, development (including drilling) and subsequent sustainable utilization and optimization of a geothermal resource is to clearly define and understand the nature, components and characteristics of the geothermal system. This is best achieved by developing a conceptual model. The Logipi thermal springs discharge waters of Na-Cl-HCO_3 facies suggesting peripheral waters, which indeed marks the outflow of the geothermal system as confirmed from the Na/K and HCO_3/SO_4 ratios as well as the $\delta^{18}O$ and $\delta^{2}H$ stable isotopes composition. The fumarole gas chemistry indicates a high atmospheric contamination, propelled by the interconnectivity of the various fissures, fractures and minor faults in the caldera or from dissolved air in shallow aquifers. Nevertheless, the discharge chemistry of fumaroles BF-01 and BF-04 suggest their proximity to the upflow zone. The study of the stable isotopes of $\delta^{18}O$ and $\delta^{2}H$ indicate that thermal waters in the BVC show a derivative recharge from Lake Turkana and meteoric waters from the rift flanks in varying proportions. The silica-enthalpy mixing model denotes a conductive cooling of the thermal waters before or after mixing that also lead to the low enthalpies (600kJ/kg) reflecting low temperature (142.5°C). The correlation plots of the conservative constituents and Na-HCO_3 correlation plots display a linear relationship hence confirming mixing between Lake Turkana waters, Lake Logipi thermal springs waters and ground water of Parkati well. A high temperature geothermal resource exists in the BVC with an estimated equilibrium reservoir temperature above 280^{o}C based on the gas geothermometers. Further geoscientific exploration methods should be carried out in order to affirm and validate the extent of the resource, thus refining the model.

Acknowledgement

First and foremost, I want to express my heartfelt gratitude to my supervisors; Prof. Olago, Prof. Odada and Prof. Opiyo for their invaluable encouragements, suggestions, comments and advice given towards the realization of this project. I am also particularly indebted to John Lagat, (Manager, Geothermal Resource Assessment), Charles Wanjie (Deputy Manager, Direct Use) and colleagues in Geothermal Development Company for the consent, support, discussions and data collections that made this project a success. I want to particularly thank the Chairman, Geology Department, University of Nairobi for the great advice that enabled me to reach this level in this project and my study. Finally, I want to thank my family and friends for their love, patience, support and encouragement.

Dedication

Larrimore and “ma femme”

Table of Contents

Declaration ii
Declaration of Originality iv
Abstract iv
Acknowledgement v
Dedication vi
Table of contents viii
List of Figures ix
List of Tables xi
List of Plates xi
List of abbreviations and symbols xii
List of Terms and Definition xiiiii

CHAPTER ONE 1
1.1 Introduction 1
1.2 The Problem Statement 2
1.3 Aim and Objectives 3
1.3.1 Main Aim 3
1.3.2 Specific Objectives 3
1.4 Justification and Significance of the Research 3
1.5 The Study area 5
1.5.1 General information of the area 5
1.5.2 Location and Description 6
1.5.3 Climate 6
1.5.4 Vegetation 6
1.5.5 Land Use and Land Resources 7
1.5.6 Physiography 7
1.5.7 Soils 8
1.5. 8 Surface and Groundwater Resources 9
1.6 Literature Review 10
1.6.1 Previous Work in the BVC 10
1.6.2 Chemical characteristics 12
1.6.3 Geothermomometry 16
1.6.4 Stable and radioactive isotope chemistry 18
1.6.5 Evaluation of mixing and boiling processes 19
1.6.6 Conceptual Model Approach 21
CHAPTER TWO 23
2.1 Geological and Structural setting 23

2.2 Structures 25
2.3 Hydrogeology 26

CHAPTER THREE 28
3.1 Materials and Methods 28
3.2 Desk Top Studies 28
3.3 Field Work 28
3.4 Laboratory Analyses 30
3. 5 Analytical Equipment 31
3.5.1 Atomic Absorption Spectrometer 31
3.5.2 UV-Visible Spectrophotometer 31
3.5.3 Ion Selective Electrode 31
3.5.4 Gas Chromatograph 32
3.6 Data Handling, Interpretation and Reporting 32

CHAPTER FOUR 34
4.1 Results 34
4.2 Chemical Characteristics of the Hot Spring Fluids 34
4.2.1 Piper Diagram of the Logipi springs 34
4.2.2 Cl-SO_4-HCO_3 Diagram 35
4.2.3 Relative Cl-Li-B Ternary Diagram 36
4.2.4 Relative Na-K-Mg 37
4.3 Fumarole Discharge chemistry 38
4.3.1 Fumarole Steam Condensate Chemistry 38
4.3.2 Fumarole Gas Chemistry 39
4.3.3 CH_4-CO_2-H_2S Ternary Diagram 40
4.4 Geothermometry 41
4.4.1 Solute Geothermometers 41
4.4.2 Na-K/Mg-Ca and K/Mg vs. K/Ca Diagram 44
4.4.3 The log (K^2/Mg) vs. log (SiO_2) Plot 46
4.4.4 Gas Geothermometer 47
4.5 Stable Isotope Characteristics 49
4.5.1 Isotopic Analysis of Hot Thermal Waters and Lake Turkana 50
4.5.2 Isotopic Analysis of Ambient Waters in the Turkana 51
4.6 Petrochemistry 52
4.6.1 Total Alkali-Silica Diagram 52
4.6.2 The Relationship between Basalts, Trachytes and Phonolites 53

4.7 Evaluation of Mixing Processes 55
4.7.1 Correlation Plots 55
4.7.2 Evaluation of Conservative Mixing 57
4.7.3 Silica-Enthalpy Mixing Model 59

CHAPTER FIVE 60
5.1 Discussion 60
5.2 Conceptual model 62

CHAPTER SIX 65
6.1 Conclusions 65
6.2 Recommendations 65

REFERENCES 67
APPENDIX I 77
APPENDIX II 81
APPENDIX III 82

List of Figures

Figure 1: Map of the Kenya rift showing the location of the Barrier Volcanic Complex 1

Figure 2: Location of hot springs and fumaroles in the study area 5

Figure 3: The potentiometric map between Lake Baringo and Lake Turkana 10

Figure 4: Simplified geological map of the Barrier Volcanic Complex 24

Figure 5: Piper diagram of Logipi hot springs 34

Figure 6: Cl-SO_4-HCO_3 diagram 36

Figure 7: Cl- B - Li Diagram 37

Figure 8: Na-K-Mg diagram 38

Figure 9: CH_4-CO_2-H_2S ternary diagram 41

Figure 10: Quartz and Na/K geothermometers 43

Figure 11: log Na/K vs. log SiO_2 43

Figure 12: Correlation plot of TNa/K vs. Tqtz 43

Figure 13: Na-K against Mg-Ca 45

Figure 14: Comparative K/Mg vs. K/Ca geothermometer plot 45

Figure 15: The log (K^2/Mg) vs. log (SiO_2) plot 47

Figure 16: TH_2S against Temperature 48

Figure 17: Comparison of geothermometers 50

Figure 18: Correlation plot of $\delta\ ^{18}O$ and $\delta\ ^{2}H$ values of waters various water lines 50

Figure 19: $\delta\ ^{18}O$ and $\delta\ ^{2}H$ characteristics of the thermal fluids of the BVC 51

Figure 20: δ 18O and δ 2H characteristics of the cold fluids in the BVC area and Turkana 52

Figure 21: Total Alkali-Silica diagram for BVC rocks 53

Figure 22: Plot of $^{143}Nd/^{144}Nd$ against $^{87}Sr/^{86}Sr$ for lavas in Kakorinya 55

Figure 23: Correlation plot of Na and HCO_3 56

Figure 25: Correlation plot of SO_4 and Cl 57

Figure 26: Correlation plot of HCO_3 against Cl 58

Figure 27: Correlation plot of F against Cl 57

Figure 28: Correlation plot of Na against Cl 58

Figure 29: Correlation plot of Na against F 57

Figure 30: Silica Enthalpy mixing model 59

Figure 31: Cross-section from North to South of the BVC 62

Figure 32: The conceptual model of the BVC geothermal prospect 64

List of Tables

Table 1: Geothermometer equations valid in the range 0-350°C 17

Table 2: Chemistry of the Logipi hot springs 34

Table 3: Fumarole Steam Condensate chemistry 39

Table 4: Fumarole gas chemistry 39

Table 5: Quartz and Na/K geothermometer 42

List of Plates

Plate 1: Geothermal grass (Fimbristylis exilis) in Kakorinya lava dome 7

Plate 2: Eroded Namurinyang tuff cone forming sodic soils 9

Plate 3: Aerial views of the maximum highstand shoreline on Abili Agituk volcano 27

Plate 4: Field sampling of a Fumarole discharge in Kakorinya caldera 29

Plate 5: Field water sampling of Lake Logipi hot spring discharge 30

List of abbreviations and symbols

Mwe	Megawatt electric
AAS	Atomic Absorption Spectrometer
BGS	British Geological Survey
BP	Before Present
BVC	Barrier Volcanic Complex
FAAS	Flame atomic absorption spectroscopy
GDC	Geothermal Development Company
ICP-MS	Inductively Coupled Plasma Mass Spectrometer
IAEA	International Atomic Energy Agency
ISAB	Ionic Strength Adjustment Buffer
ISE	Ion Selective Electrode
IUCN	International Union for Conservation of Nature
KEMFRI	Kenya Marine and Fisheries Research Institute
LCPDP	Least Cost Power Development Plan
MHS	Maximum Highstand Shoreline
MT	Magnetotellurics
NRM	National Resource Management
SGP	Stanford Geothermal Program
TCC	Total Carbonate Carbon
TEM	Transient electromagnetic
UNESCO	United Nations Educational, Scientific and Cultural Organization
UNITAR/UDP	United Nations Training/ Unitary Development Plan
UNU-GTP	United Nations University Geothermal Training Programme
$\delta^{18}O$	Oxygen 18 isotope in delta notation (δ in ‰ = $[(R_{sample} - R_{standard})/R_{standard}]\times 1000$. $R = {}^{18}O/{}^{16}O$; Standard is SMOW (Standard Mean Ocean Water)
$\delta^{2}H$	Deuterium isotope in delta notation. $R = {}^{2}H/{}^{1}H$; Standard is SMOW
TNa/K	Estimated Na/K geothermometer temperature
TK/Mg	Estimated K/Mg geothermometer temperature
$TSiO_2$	Estimated Quartz geothermometer temperature
TNa-K-Ca	Estimated Na-K-Ca geothermometer temperature
TCO_2	Estimated CO_2 geothermometer temperature
TH_2S	Estimated H_2S geothermometer temperature

List of Terms and Definition

Caldera	Large volcanic depressions, more or less circular in form, with a diameter which is many times greater than that of included vents
Cap rock	Impermeable rocks of high resistance overlying a geothermal reservoir
Conceptual model	An illustration showing the components of a geotermal system that are: heat source, production reservoir, sealing cap layer, upflow and outflow zones, and the recharge and discharge zones
Enthalpy	A measure of the total energy of a thermodynamic system that includes the internal energy and is a state function and an extensive quantity
Geothermometer	Geoindicator functions used to compute estimated equilibrium subsurface/ reservoir temperature
Upflow	A zone of a geothermal system characterised by high geothermometry, high chloride without boiling, consistent chemistry, equilibrated benign fluid, thin clay cap associated with hot fluids, extensive vertical permeability associated with intersecting faults and high temperatures and consistent geothermometers in relation to the measured temperature
Outflow	A zone of a geothermal sysytem characterised by an increase in $HCO_{3,}$ inconsistent chemistry, low temperature and inconstitent geothermometers in relation to the measured temperature
Reservoir	A particular subsurface body of rock at elevated temperatures having sufficient porosity and permeability to store and transmit fluids,

CHAPTER ONE

1.1 Introduction

The Barrier Volcanic Complex (BVC) is situated at 2° 20'N, 36° 37'E. It forms an E-W trending whaleback ridge, 20 km in length and 15 km wide, which forms a natural dam across the inner trough separating Lake Turkana from Suguta Valley. The BVC geothermal prospect is located on the floor of the northern sector of the Kenya rift, immediately south of Lake Turkana (Figure 1). The volcanic complex is characterized by four polygenetic volcanic centres namely Kaloleyang, Kakorinya, Likau West and Likaiu East, which are composed of a wide range of lava types including basanite, basalt, hawaiite, mugearite, benmorite, trachyte and phonolite. Reconnaissance surveys by the British Geological Survey (BGS) team found occurrence of strong surface geothermal manifestations, signifying the occurrence of a hydrothermal system. Locations of geothermal activity on the BVC are mainly in three areas, Kakorinya caldera, the flanks and summit area outside the caldera, and Lake Logipi hot springs.

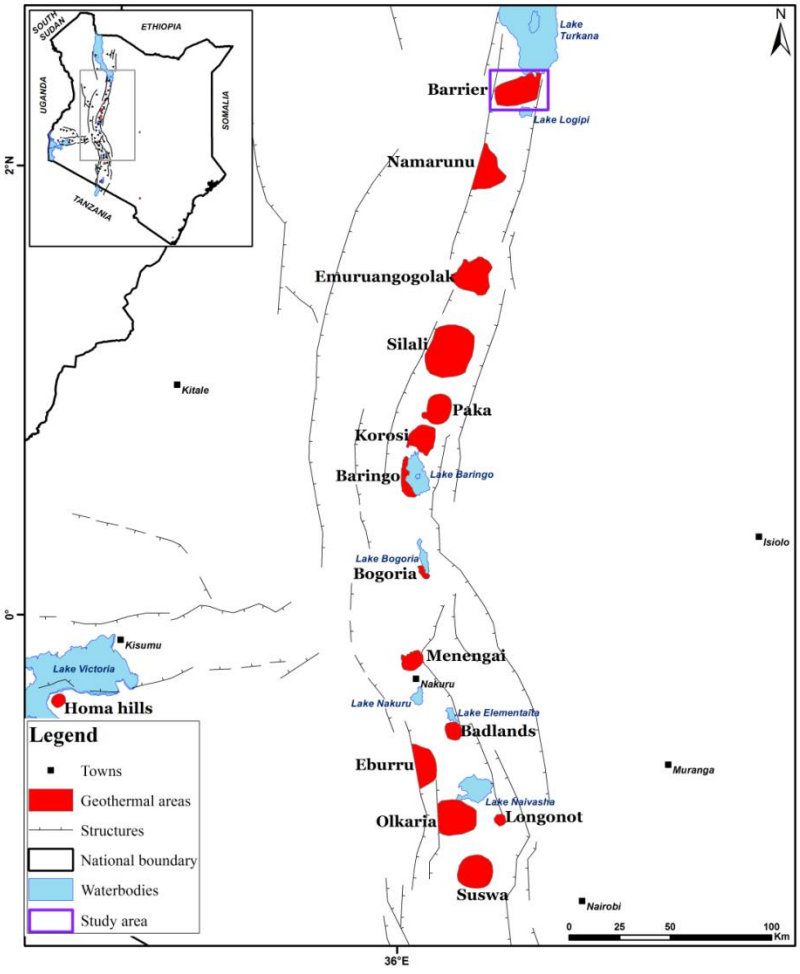

Figure 1: Map of the Kenya rift showing the location of the Barrier Volcanic Complex

At the caldera summit area, there is the hottest and the most vigorous activity that is associated with the ring fractures and trachyte lava domes to the west of caldera. Volcanic geothermal systems are commonly associated with ring structures or calderas; an indication of products of rapid emptying of a shallow magma bodies. High temperature geothermal systems are associated with central volcanoes and in Kenya; these prospects are located at central volcanoes and associated with the development of the Kenya Rift Valley (KRV). Kenya has 14 geothermal prospects of which three (3) – Olkaria, Menengai and Eburru - are proven geothermal fields. Lake Logipi is partly fed by numerous, weak alkaline hot springs and seepages, which issue along the base of the southern flanks of the BVC. Silica veins and sinters indicative of former hot springs activity also occur at a number of sites on the rim and floor of the caldera. Minor occurrences of weak steam seepages occur on Andrews's cone.

Geothermal geochemistry is used to identify the origin of geothermal fluids and to quantify the processes that govern their compositions and the associated chemical and mineralogical transformations of the rocks with which the fluids interact. The subject has a strong applied component: geothermal chemistry constitutes an important tool for the exploration of geothermal resources and in assessing the production characteristics of drilled geothermal reservoirs and their response to production (Malimo, 2012). This project seeks to evaluate the hydrogeochemical characteristics of Lake Logipi hot springs and Kakorinya fumaroles with the interest of developing a geothermal conceptual model of Barrier Volcanic Complex geothermal prospect.

1.2 The Problem Statement

Kenya is grappling with low supply of electrical energy attributed to the over reliance in the hydro-generated electricity that is normally punctuated by erratic rainfall that contributes to the perennial or quasi-perennial power rationing and black outs. Kenya is endowed with viable geothermal prospects that have an estimated resource potential which is greater than 10,000 Mwe, out of this only 215Mwe has been developed and channeled to the national grid. Therefore, exploration of geothermal resources has been given a lot of impetus by the government as one of the solutions to the ever-growing electricity demand pursuant to the Least Cost Power Development Plan (LCPDP) and Vision 2030. The resource area in the BVC as indicated by 25 ohm-m resistivity is about 60 km^2, with estimated output of 750 Mwe (GDC, 2011). This study therefore, will contribute to the generation of the geothermal conceptual model of the BVC that is indeed very important in the incipient exploration and development of geothermal resource towards location of productive exploration drill sites.

1.3 Aim and Objectives

1.3.1 Main Aim

The main aim is to develop a geothermal conceptual model of the Barrier Volcanic Complex based on hydrogeochemical characteristics of Lake Logipi hot springs and Kakorinya fumaroles.

1.3.2 Specific Objectives

1. To establish the chemical characteristics of the Lake Logipi hot springs and Kakorinya fumarole gas chemistry (Na-Cl-HCO_3 facies, CO_2, H_2S, H_2, CH_4, N_2, O_2).
2. To estimate the equilibrium reservoir temperature based on geothermometers in fumarole gas and solute geothermometers of hot springs (TNa/K, TK/Mg, $TSiO_2$, TNa-K-Ca, TCO_2, TH_2S, TH_2S-CO_2, TCH_4/CO_2)
3. To establish the origin of the BVC thermal and ambient waters discharge based on prior stable isotope studies ($\delta^{18}O$ and $\delta^{2}H$) and establish the relationship of various lithologies based on prior radioactive isotope studies ($^{143}Nd/^{144}Nd$ and $^{87}Sr/^{86}Sr$) and rock petrochemistry (Total Alkali Silica)
4. To study both mixing and boiling processes of Logipi thermal waters based on the silica-enthalpy and correlation plots of chemical species (Na vs. HCO_3, Ca vs. SO_4, SO_4 vs. Cl, HCO_3 vs. Cl, F vs. Cl, Na vs. Cl, Na vs. F).
5. Generation of a conceptual model of the BVC.

1.4 Justification and Significance of the Research

The Barrier Volcanic Complex is characterized by various geothermal manifestations that highlight it as a promising geothermal prospect with a productive potential in Kakorinya caldera. Dunkley et al. (1993) in their findings of exploration along the prospects in the rift, ranked the BVC is one of the most viable prospects in the rift but recommended further work to comprehensively understand the potential of the prospect. Mortensen and Axelsson (2013) and Axelsson (2013) discussed that, the key to the successful exploration, development (including drilling), and utilization of any type of geothermal system is a clear definition and understanding of the nature and characteristics of the system in question, based on all available information and data. This is best achieved through the development of a conceptual model of a geothermal system. Geothermal conceptual models are used when making decisions like targeting exploration and siting of production geothermal wells. The conceptual model for locating exploration wells could give an indication of the expected reservoir temperature, depths to the reservoir and in some cases a drilling strategy.

A conceptual model approach is particularly effective when exploring geothermal prospects because it helps in developing strategies of identifying the best drilling targets in pursuit of validating the existence of a geothermal resource. According to Cumming (2009), the

geothermometry isotherms can be used when developing a conceptual model. When no wells are drilled but reliable cation or gas geothermometry data are available, it can be decisive to use this information in order to come up with a model. Ideally besides providing geothermometry, the geochemistry of thermal features can establish origin of thermal waters, characterize the distribution of fluid types around the reservoir, identify boiling scenario, isotherms consistent with a steep thermal gradient can be sketched to outline the reservoir.

Karingithi (2009) elaborated that geothermometers enable the temperature of the reservoir to be estimated using the chemical and isotopic composition of hot springs and fumarole discharges. They are therefore valuable tools in the evaluation of new fields. Chemical and isotope geothermometers constitute an important geochemical tool for the exploration and development of geothermal resources. Commonly used solute/chemical geothermometers are based on solubility of species (silica) and ion exchange reactions (Na/K). The composition of geothermal solutions is commonly, to a large extent, controlled by local and partial chemical equilibria between the fluid and the host rock.

Geothermal waters cool as they rise to the surface and this can occur by conduction, mixing and boiling (Henley et al., 1984). Each of these processes can be traced isotopically. Mixing with cold water before and after boiling is very common in geothermal systems and this can be detected by a change in isotopic composition. Isotopic compositions of mixtures are intermediate between the compositions of the end members. Water ascending from a geothermal reservoir to the surface and emerging in hot springs may cool on the way, by conduction, boiling, or mixing with shallow cold water or by any combination of these three processes. According to Armannsson (1987), fluid geothermometry can provide evidence of the location and mechanism of these processes. Water that ascends relatively rapidly and directly from the reservoir with little conductive cooling is likely to have chemical compositions that reflect rock-water equilibrium at the reservoir temperature (Arkansan and Fridriksson, 2009). The chemical composition of mixed water can be used for temperature estimation applying a mixing model (Fournier and Truesdell, 1973). The model can be applied if there is an independent indication of mixing.

In this regard, the project will focus on evaluating the hydrogeochemical characteristics of Kakorinya fumaroles and Lake Logipi hot springs in pursuit of developing a geothermal conceptual model of BVC. In essence this would be of great value in understanding the geothermal system of the BVC since, high geothermal activity occur mainly in the Kakorinya caldera, the youngest volcanic centre of the BVC that is characterized mainly by fumaroles and hot hydrothermal altered grounds that mostly occur on the upper western and southern flanks of the caldera. Therefore, the findings of this project are invaluable in meeting the aforementioned objectives in pursuit of identifying target drill sites upon the development of the field and the ultimate use of the resource, that will certainly open up the area and community for developments.

1.5 The Study area

1.5.1 General information of the area

The Barrier Volcanic Complex is a composite structure composed of four distinct volcanic centres; Kaloleyang, Kakorinya, Likau West and Likaiu East (Figure 2). Geothermal manifestations occur in the form of fumaroles, hot springs, hydrothermally altered grounds and silica sinters. Previous researchers have proved that geothermal activity is mostly abundant in Kakorinya caldera that is manifested by fumaroles and hot hydrothermally altered grounds. Dunkley et al. (1993) ranked the BVC prospect among the viable geothermal prospects in the Kenyan Rift. The project focused on the chemical characteristics of Kakorinya fumarole and Lake Logipi hot springs discharge. This study concentrated on six fumaroles and seven hot springs as well as Lake Turkana (Figure 2).

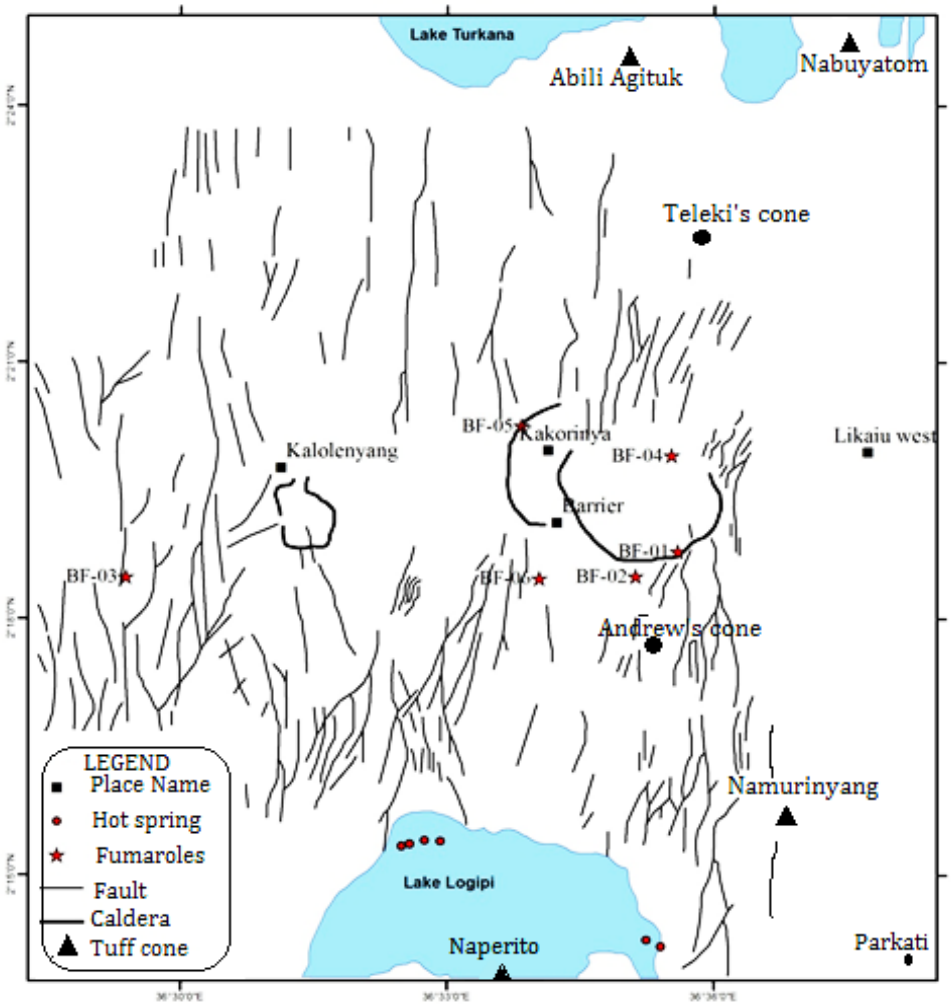

Figure 2: Location of hot springs and fumaroles in the study area

1.5.2 Location and Description

The Barrier Volcanic Complex geothermal prospect lies in Turkana and Samburu counties, Baragoi and Nyiru Divisions, Parkati, Lomunyenakwan/Katilia Locations. Apparently, access to the BVC is indeed challenging. The roads, which lead close to the Barrier prospect terminates approximately 25 km away; the rest of the distance is only motorable with four-wheel drive vehicles. Getting to Kakorinya caldera and surrounding domes, like Teleki's volcano, Namurinyang and Luguruguru, may only be possible by alternative means like using helicopter or walking to such sites by foot through the rugged fresh lava. GDC (2011) reported that, the total population in Parkati village is 380, with pastoralists in surrounding areas making a total of 1288. The locals are mostly nomadic pastoralists, but a few are fishermen. They obtain their water from Lake Turkana and the surrounding seasonal rivers. The Turkana region is classified as one of the poorest regions in Kenya, and investment levels and employment opportunities are very low.

1.5.3 Climate

The area is semi-arid with an annual mean maximum temperature range of 30°C to 34°C and the mean annual rainfall is below 255 mm/year (Survey of Kenya, 1977). Fergusson and Harbott (1982) estimated the average evaporation rate for the surface of Lake Turkana to be 2335± 347mm/yr. There are two rainfall seasons: from March to June, with a peak in April, and from October to December, with a peak in November or December. The mean annual rainfall increases northwards along the shores of the lake, from 166mm at Loyangalani in the South East to 360mm at Todonyang in the North East. On the eastern side of the lake, the mean monthly rainfall variations are different to those of the south of the area. On the eastern side of the lake, the mean monthly rainfall distribution is bimodal with two roughly equal peaks in March-April and November (Fergusson and Harbott, 1982). The occurrence of rainfall is, however, erratic and unpredictable, and it tends to fall in brief, violent storms that result in flash floods (Republic of Kenya, 2002). The area is prone to frequent droughts.

1.5.4 Vegetation

The vegetation of the project area belongs to the Somali-Maasai ecoregion as documented by (White,1983) comprising of deciduous bushland and thicket, semi-desert grassland, bushland and thorny shrubland comprised of *Acacia species; Acacia tortilis, Acacia mellifera* (popularly known as "Ngoja kidogo" by the locals), *Commiphora africana,* and *Balanites aegyptiaca.* Most of these, especially the acacia thorn shrubs, grow around the lake and the volcanic centres of BVC. In the lakes (Logipi and Turkana) the dominant phytoplankton are the blue-green alga *Microcystis ceruginosa* and the green alga *Botryococcus braunii*, while in Ferguson's Gulf *Anabaenopsis arnoldii* (blue-green alga) is dominant (Kallqvist et al., 1988). Hughes and Hughes (1992) discovered that the fairly high alkali content of the lake's waters greatly limits the range species of macrophytic and littoral vegetation. *Fimbristylis exilis* (geothermal grass) is

mainly localized on the hydrothermally altered grounds on the lava domes (Plate 1). Most of the fresh young aa-type and pahoehoe-type lavas in the BVC are unvegetated.

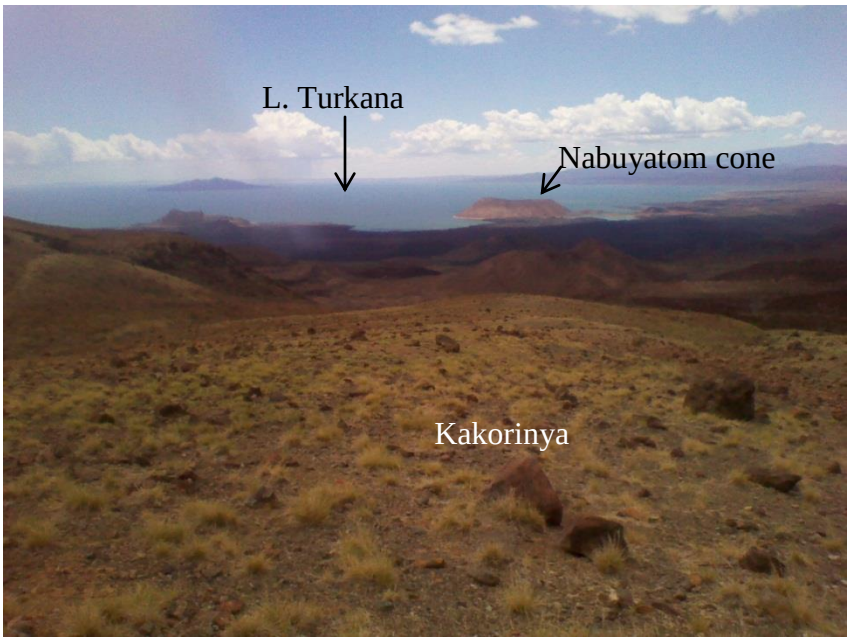

Plate 1: Geothermal grass (Fimbristylis exilis) in Kakorinya lava dome

1.5.5 Land Use and Land Resources

The study area is an arid and semi-arid land (ASAL). Land is mainly used for nomadic and pastoralism; however, a relatively semi-permanent settlement is in the Parkat area. Most of land in this area is trust land and formal land adjudication is not extensive. The trust land is under the Turkana, Samburu and Marsabit County Councils. In the arid areas, land adjudication has not taken root. GOK (2005) reported that, the optimal utilisation of land in the area and its surroundings is greatly hindered by land tenurial issues in the pastoral areas, which revolve around communal use of grazing resources without control over individual actions. Conflict and overgrazing have been the inevitable result.

1.5.6 Physiography

The general topography of the BVC is characterized by numerous residual hills (domes) from the eastern side of Lake Turkana (Loyangalani) towards the south (South Horr) and Suguta Valley. The BVC forms a ridge that separates the Lake Turkana from Lake Logipi or Paleo Lake Suguta. The expansive area of the BVC covers the eastern, southern and south west tip of Lake Turkana and stretches towards Suguta Valley. East to west profiles of the BVC display a more rugged outline of coalescing hills, valleys and craters. Kakorinya forms a low shield rising 666 m above Lake Turkana to reach a maximum height of 1031m on its summit. Kalolenyang volcano rises 828m above Lake Turkana. Likaiu (1193 m) represents the faulted remains of volcanic shield.

The Kakorinya caldera, 3.75km in diameter is partly filled with lavas and pyroclastics that give it a rough topography (Dunkley et al., 1993).

1.5.7 Soils

There are several different types of soils in the project area, each with its own peculiar geological, textural and weathering/erosion-driven properties, as well as anthropogenic footprints such as compaction by grazing animals as reported by Sombroek et al. (1982). Most of the soils in Kakorinya caldera and parts of Logipi area are obscured by a complex lava flow. However, in some parts of the BVC, there are discernible soils types; such as soils from lacustrine plain sediments and soils formed from differential erosion of the volcanic cones. (Abili Agituk, Namurinyang, Andrews's cone etc.). A complex of lacustrine plains and dunes border Lake Turkana basin and form the lakebed sediments. The basin accommodates fluvio-lacustrine and volcanoclastic deposits up to 7 km thick, accumulated between the Late Oligocene-Plio-Pleistocene and the present (Melnick et al., 2012; Dunkelman et al., 1989; Morley et al., 1992). At the foot-slopes of the volcanic features (Plate 2), there are poorly structured soils and alluvial fans that are sodic in nature and have large bare patches with basalt boulders. These soils have sparse vegetation found in natural drains and suffers from overgrazing that contributes to further degrading of the surface soils. When these bare patches are trampled upon by grazing animals', the surface soil is pulverized and is susceptible to windblown erosion. Wind normally cause frequent dust storms of this soil type. Generally at the step-faulted scarps of the rift valley, the soils are well-drained, shallow, dark reddish brown, friable, strongly calcareous, rocky or stony, clay loam; in many places saline (the soil classifies as Lithosols with rock outcrops) (Sombroek et al., 1982).

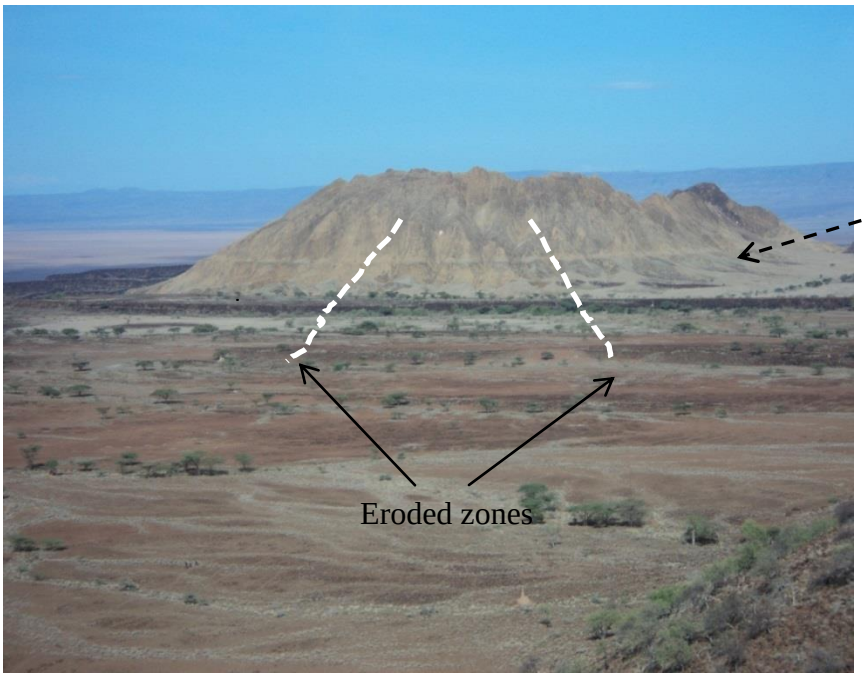

Plate 2: Eroded Namurinyang tuff cone forming sodic soils

1.5. 8 Surface and Groundwater Resources

Surface water resources in the BVC include Lake Turkana and seasonal river channels that drain into Lake Turkana. Lake Turkana is one of Africa's largest lakes, with a length of more than 250 km, a surface area of ~7000 km^2, and a catchment area of 148,000 km^2. Immediately to the south, the Suguta Valley is a smaller basin, partially covered by the shallow ephemeral Lake Logipi (Melnick et al., 2012). Suguta river is the only permanent supply of surface water to the Suguta trough, but Lake Logipi is maintained during dry season by subsurface flow through the alluvium flooring the Suguta trough (Truckle, 1976). Water pans are conspicuously absent in the area.

The potentiometric map established by Dunkley et al. (1993) shows lateral ground water flow from the rift margins and axially from the south for regions around Korosi, Paka, Silali and Namarunu (Figure 3). Lake Turkana lies at an altitude of about 365m and therefore subsurface drainage from the lake is directed southwards towards Lake Logipi passing beneath the BVC. There is also a strong component of the easterly flow from the eastern margin of the rift.

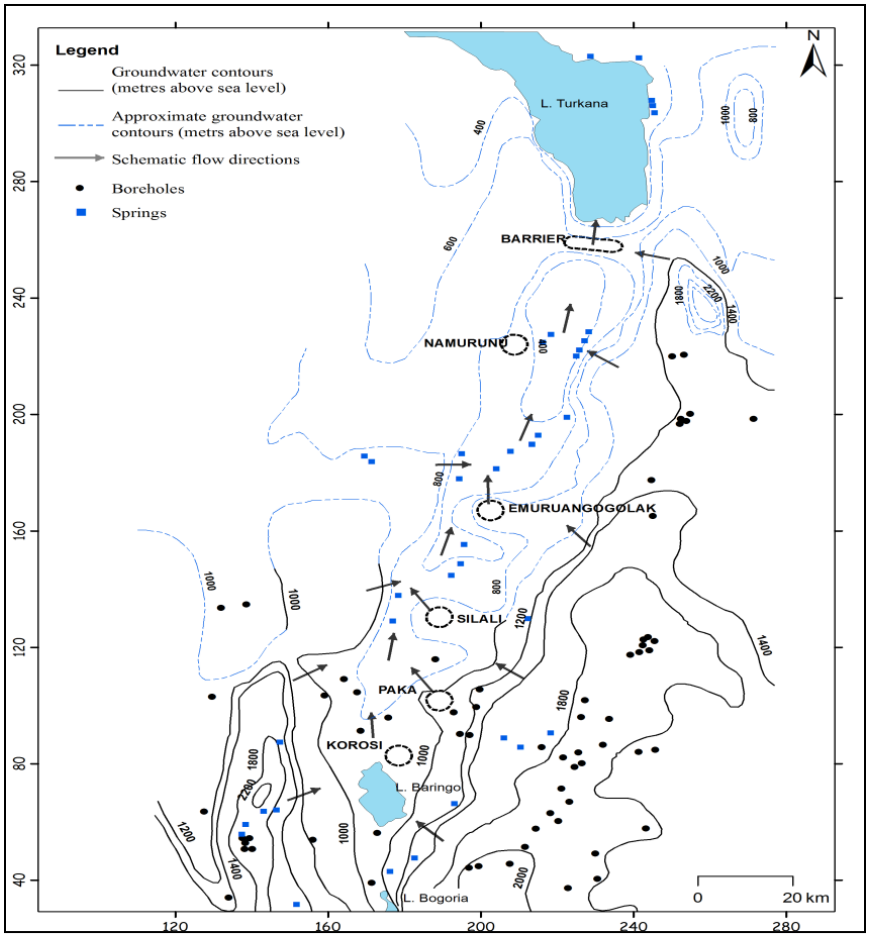

Figure 3: The potentiometric map between Lake Baringo and Lake Turkana (modified from Dunkley et al. 1993).

Garcin et al. (2012) documented a prolonged lake high stand with episodes of fluvial connectivity to the Nile Basin during the early to mid-Holocene, supporting previous regional hydrological reconstructions. Their observations indicated that, the ongoing tectonic segmentation of the Turkana rift-basin has resulted in the vertical displacement of the maximum high stand shoreline (overflow stage) by up to ~20 m, relative to the present-day position of the overflow sill of the Turkana palaeo-lake.

1.6 Literature Review

1.6.1 Previous Work in the BVC

High temperature geothermal systems generally occur in areas of active volcanism where the heat source may be a major magma intrusion, a dyke complex, or a complex of minor intrusions (Arnórsson et al., 2007). Dodson (1963) indicated in his study that the final phases of eruption in Barrier Volcanic Complex were the basalts and basanites, which mantle the lower flanks. Basalts, trachytes and phonolite near Teleki's cone have been described and analysed by Brown

and Carmichael (1971) and Champion (1935). Reconaisance surveys by the British Geological Survey (BGS) team (Dunkley et al., 1993) found occurrence of strong surface manifestations eg. fumaroles, hydrothermally altered zones, hot springs, silica sinters and steaming grounds signifying occurrence of a hydrothermal system (Giggenbach, 1992b). From their findings, they ranked BVC among the best and most viable prospects along the rift. However, the team made recommendations for further detailed investigations to determine the geothermal resource potential of the volcanic complex.

Dunkley et al. (1993) carried out geochemical studies in the Barrier Volcanic Complex, and sampled fumaroles, springs and one borehole, as part of their broad study covering the Kenya Rift between Lake Baringo and Lake Turkana. Their objective was to investigate geothermal activity of the six principal volcanic centres and a number of centres between Lake Baringo and Lake Turkana incorporating the islands and shores of Lake Turkana. In the BVC, a highest temperature of 98.6°C was measured inside the caldera, while outside the caldera the highest recorded value was 97.3°C (Dunkley et al., 1993). The fumaroles and hot grounds on Kakorinya are contained in an area of 20.5 km^2. Near the southern flanks of the Kakorinya caldera, several strong fumaroles exists and the highest temperature recorded for the fumaroles was 96.1°C, while ground temperatures were between 90.3°C and 95.0°C (Dunkley et al., 1993).

Dunkley et al. (1993) found out that the fumaroles tend to be located where N-trending joints or minor faults cut the main NE-trending faults within Kakorinya caldera. The hottest and most vigorous activity is associated with the ring fractures and trachyte lava domes to the west of the caldera. It occurs along the faults, which cut the trachyte lavas, especially near the southern wall of the caldera where several strong fumaroles with temperatures of up to 93.6°C were noted. Lake Logipi is partly fed by numerous hot springs located around its northern shores and around the eroded tuff cone of Naperito. Some of the hot springs are inundated within the lake. Around the northern and eastern shores of Naperito, numerous hot springs and seepages occur on the shores of the lake and are associated with trona deposits and mats of red and dark green algae. A maximum of 70.0°C was recorded from springs located on the northern shores of Lake Logipi from a series of small clear springs. Silica sinters are common at many of the geothermal sites on Kakorinya and indicate former hot spring activity (Dunkley et al., 1993). Silica sinter generally seems to form in situations where hot silica-rich solutions get cooled very quickly. The BVC is punctuated with lava domes on the southern flanks of the caldera which is characterised with *Fimbristylis exilis* 'geothermal grass' that is mainly localized on the hydrothermally altered grounds on the lava domes.

1.6.2 Chemical characteristics

- **Processes Affecting Water Composition**

The chemical processes centre around mineral-fluid reactions, both dissolution and deposition, while the dominant physical process is boiling, although conductive cooling and mixing are also important (Nicholson, 1993).

- **Mineral fluid equilibria**

The rock leaching experiments usually demonstrate that the common dissolved constituents in the deep chloride reservoir fluids fall into two groups based upon their solubility behavior:

Soluble group species: (e.g., B, Br, As, Cs) which readily pass into solution. Often before appreciable alteration of the host rock has occurred. These tend to remain in solution and are considered to be unreactive or conservative species. This is really only true for Cl as the other species can be involved in near-surface reactions, notably with clay minerals.

Common rock-forming: species (e.g., SiO_2, Na, K, Ca, Mg etc) whose solubilities are controlled by temperature dependent mineral-fluid equilibria and only enter the solution after alteration of the host minerals.

Mineral-fluid equilibria therefore play a fundamental role in determining the chemistry of the discharge fluids. The reactions, which take place, are a function of the temperature, pressure, salinity and host rocks of the geothermal system. There are two types of mineral-fluid reactions, which need to be considered: dissolution-precipitation or solubility equilibria (e.g., quartz, calcite) and ion-exchange equilibria (e.g., Na and K between feldspars and micas). The product of mineral-fluid reactions is an assemblage of secondary alteration minerals.

- **Solubility reactions**

These determine how much of a particular species can enter and remain in solution before precipitation occurs. Examples of mineral solubilities, which plays major role in determining geothermal fluid composition, include quartz, calcite and anhydrite. Temperature is the dominant control on mineral solubility in geothermal systems, but changes in pH, pressure or salinity can also have an effect. In most geothermal systems, the solubility of minerals follows one of the three behavior patterns (Nicholson, 1993):

1) Mineral solubility increases with increasing temperature (e.g., alkali metal chlorides)
2) Mineral solubility decreases with increasing temperature; known as retrograde solubility (eg. gypsum. anhydrite. calcite)
3) Mineral solubility increases with increasing temperature but only to a maximum value and then decreases with further temperature rises (e.g., silica).

Silica and calcite equilibria are particularly important in geothermal systems as they govern the amount of SiO_2 and Ca in solution, and are the two main causes of scaling in wells.

Silica: The solubility of any silica mineral (quartz, chalcedony etc.) can be written as

$$SiO_2(s) + 2H_2O\ (1) = H_4SiO_4\ (aq) = H_3SiO_4\ (aq) + H^+\ (aq) \quad (1)$$

and the solubility constant is given by

$$K._{SiO2} = aH_4SiO_{4s} \quad (2)$$

Silicic acid is a weak acid and dissociates to yield hydrogen ions. If the pH of the solution is increased (ie. becomes more alkaline) then the solubility of silica will also increase as the hydrogen ions are consumed by reactions such as

$$HCO_3\ (aq) + H^+(aq) = H_2CO_3(aq) = H_2O(l) + CO_2(g) \quad (3)$$

The BVC analytical results were evaluated in a series of graphic plots pioneered by Giggenbach (1988, 1991) to infer the origin of the fluids relative to the potential chemical equilibrium in an active geothermal reservoir. The ubiquitous Cl-SO_4-HCO_3 ternary diagram is used to classify geothermal fluids based on the major anion concentrations (Giggenbach, 1988). The diagram indicates several types of thermal fluids such as immature waters, peripheral waters, volcanic, and steam heated waters. It helps to distinguish immature unstable waters and gives an initial indication of mixing relationships or geographic groupings. The position of a data point in this plot is obtained by first calculating the sum, Σ, of the concentrations, C (mg/kg) of all the species involved:

$$\Sigma anion = C.Cl + C.SO_4 + C.HCO_3 \quad (4)$$

The next step is to obtain the percent (%) of every constituent using the following equation:

$$\%Cl = 100\ C.Cl\ /\ \Sigma_{anion}\ ;\ \%SO_4 = 100\ C.SO_4\ /\ \Sigma_{anion}\ ;\ \%\ HCO_3 = 100\ \boldsymbol{C.}HCO_3\ /\ \Sigma_{anion} \quad (5)$$

This plot indicates the compositional ranges for the different kinds of waters typically found in geothermal areas, such as: mature NaCl waters of neutral pH, which are rich in Cl and plot near the Cl vertex; and Na-HCO_3 waters, which are indicated as peripheral waters. Volcanic and steam heated waters (SO_4 enriched waters) are generated through the absorption of either high temperature HCl-bearing volcanic gases or lower-temperature H_2S-bearing geothermal steam into the groundwater respectively.

Giggenbach (1988) suggested that a triangular diagram with Na/1000, K/100 and %Mg at the apices could be used to classify waters according to their state of equilibrium at given

temperatures. He adopted the Na/K and slightly modified K/Mg geothermometer equations. The use of the triangular diagram is based on the temperature dependence of three reactions:

$$Albite + Na^{+} = K\text{-}feldspar + K^{+} \quad (6)$$

$$0.8muscovite + 0.2clinochlore + 5.4silica + 2Na^{+} = 2albite + 0.8K\text{-}feldspar + 1.6water + Mg^{2+} \quad (7)$$

$$0.8muscovite + 0.2clinochlore + 5.4silica + 2K^{+} = 2albite + 2.8K\text{-}feldspar + 1.6water + Mg^{2+} \quad (8)$$

The Na-K-Mg triangular diagram shows attainment of the water-rock equilibrium if the data point plots on the full equilibrium line, or suggests a field of immature water below the "immature water curve" which indicates an initial dissolution of minerals before equilibrium reaction sets in. No geoindicators can be used in the latter case (Giggenbach, 1988). The field of partial equilibrium lies between the curves, and suggests that either a mineral dissolved, equilibrium reactions have set in but equilibrium has not been reached, or a mixture of a water that has reached equilibrium (e.g. a geothermal water) with a dilute unequilibrated water (e.g. cold groundwater) has occurred. Geothermometer temperatures may often be deduced from such a position.

The coordinates of a point on the diagram are calculated by

$$S = C.\ Na^{+} / 1000 + C.K+ / 100 + \%C.\ Mg \quad (9)$$

$$\%Na = C_{Na}/10S\ ;\ \%K = C_K / S\ ;\ \%Mg = \%C_{Mg} / S \quad (10)$$

Where S and C stands for sum and concentration respectively.

The pH of surface geothermal waters is principally determined by the loss of carbon dioxide on boiling which causes the solution to become progressively more alkaline. However, pH is also influenced by the fluid salinity and temperature and by mineral buffers. The most common type of fluid found at depth in high-temperature geothermal systems is of near neutral pH with chloride as the dominant anion. Other waters encountered within the profile of a geothermal field are commonly derived from this deep fluid as a consequence of chemical or physical processes (Nicholson, 1993). The sulphate concentration is usually low in deep geotherermal fluids (50 mg/kg), but increases with increasing oxidation of the hydrogen sulphide (Nicholson, 1993).

- **Chemistry of geothermal gases**

Geothermal gases are conveniently divided into two groups like the water soluble constutuents (Nicholson, 1993):

- reactive gases (eg. H_2O, CO_2, H_2S, NH_3, H_2, N_2, CH_4) which take part in chemical

equilibria and provide information on the subsurface conditions such as temperature

- inert or conservative gases (eg. the Noble gases, hydrocarbons other than methane) which act in an analogous manner to chloride in that they do not lake part in chemical reactions. They can he used to provide information on the source of the gases.

The two main geothermal gas equilibria are the methane breakdown or Fischer-Tropsch reaction,

$$CH_4 + 2H_2O = CO_2 + 4H_2 \quad (11)$$

and the ammonia breakdown reaction

$$2NH_3 = N_2 + 3H_2 \quad (12)$$

All constituents are in the gaseous phase, and the equations are written to favour the products at higher temperatures. The solubility of a gas in the liquid phase of a geothermal fluid governs the extent to which it fractionates into the vapour phase on steam formation. For the common geothermal gases, the solubility order is (most soluble) NH_3> H_2S > CO_2 >CH_4 >H_2 > O_2 > N_2 (least soluble) (Giggenbach, 1980; Nicholson, 1993).

- **Carbon dioxide (CO_2)**

This is the most abundant gas in geothermal systems, often representing over 85% by both volume and weight of the total gas content of a discharge (Mahon et al., 1980). The gas can be produced by thermal alteration of carbonate rocks and minerals from the degradation of organic matter within sedimentary rocks at depth or in near-surface reactions, and from solutes in meteoric waters (notably the conversion of HCO_3(aq) to CO_2(g) on boiling) or it can be in part, of a magmatic origin. The influence of carbon dioxide on the overall chemistry and hydrology of a geothermal system should not be under-estimated. Water chemistry, density and pH, boiling point-depth relationships, rock alteration and the deposition of secondary minerals and scale are an controlled to some degree by the concentration of carbon dioxide (Mahon et al., 1980). The pH of geothermal fluids is buffered by CO_2/HCO_3 equilibria, and loss of CO_2 through boiling causes a change in the solution pH to more alkaline values (Ellis, 1962).

The partial pressure of carbon dioxide increases with increasing temperature (Amorsson et al., 1982). The value of P_{CO2}, at the point of gas equilibrium can he calculated by the expression derived by (Chiodini and Cioni, 1989):

$$\log P_{CO2} = 3.573 - 4/T - \log(X_{H2}/X_{CO2}) \quad (13)$$

Where P stands for partial pressure and X stands for gas concentrations.

This model, which is almost independent of temperature, assumes that P_{H20} is fixed by the presence of liquid water and can be applied both to fumaroles and well discharges (Chiodini and Cioni, 1989).

- **Hydrogen sulphide (H_2S)**

This common gas may be produced by alteration of the reservoir rocks or from a magmatic source. It is reactive and is removed on reaction with wall rocks to form iron sulphides. Although this appears to be a slow process, the gas is lost through such reactions over time, increasing the CO_2/H_2S ratio with increased migration. Hydrogen sulphide is 2-3 times more soluble than carbon dioxide (Ellis, 1962; Nicholson, 1993).

- **Hydrogen (H_2)**

A highly reactive gas, hydrogen is readily removed on reaction with wall rocks. It is commonly lost over time and with increased migration (Arnorsson and Gunnlaugsson, 1985), and this enables the hydrogen and H_2/CO_2 content of discharges to be used to recognize flow directions and upflow zones (Nicholson, 1993).

- **Methane (CH_4)**

Of all the hydrocarbon gases, methane is the one most commonly encountered. High concentrations of methane can he produced by the alteration of sedimentary rocks at depth, particularly of organic rich, and it is not unusual for methane to be a principal constituent in gas discharges from sedimentary-hosted low-temperature systems (Nicholson, 1993).

- **Ammonia (NH_3)**

This is the most soluble of the geothermal gases. High concentrations of ammonia can be the result of alteration of organic matter in sedimentary rocks at depth, or in the near-surface environment. On migration to the surface, the gas may be removed as a consequence of reaction with wall rocks, by adsorption onto clay alteration products or by solution into steam condensate. Although relatively soluble, ammonia increasingly partitions into the steam phase as temperature decreases; therefore as the geothermal water cools, more ammonia will be evolved (Nicholson, 1993).

- **Nitrogen (N_2) and Oxygen (O_2)**

As the principal atmospheric gas, most nitrogen in geothermal systems is derived from that dissolved in the meteoric recharge waters, although it can also be of magmatic origin. However, the original source of nitrogen in magmatic discharges is uncertain. It may be derived from the degradation of organic matter in the crust when it comes into contact with the magma. Nitrogen tends to assume greater proportions in low-temperature systems where it can be the major gaseous component. The presence of oxygen in a gas sample often indicates contamination either by soil air or during the sampling procedure (Nicholson, 1993).

1.6.3 Geothermomometry

According to Oyuntsetseg (2009), geochemical methods are relatively inexpensive and can provide valuable information on the temperature conditions in a geothermal reservoir and the

source of the geothermal fluid. The use of geochemistry in geothermal exploration has a profound importance in inferring subsurface conditions by studying the chemistry of surface manifestations or discharge fluids that carry the signature of the deep geothermal system. (Arnórsson, 2000a) described geothermometers as geoindicators that can be used to estimate subsurface reservoir temperature. When geothermometers are applied to estimate the subsurface or aquifer temperature, a basic assumption is always made, namely that temperature dependent chemical or isotopic equilibria prevail in the source aquifer (Arnórsson, 2000a). The equations used for calculation of the estimated equilibrium reservoir temperature are as indicated in (Table 1).

Table 1: Geothermometer equations valid in the range 0-350°C

Geothermometer	**Equation (T^oC)**	
$T_{qtz}{}^{a}$	$-42.2+0.28831\times S-3.6686\times10^{-4}\times S^2+3.1665\times10^{-7}\times S^3+77.034\times\log(S)$	(14)
$T_{qtz}{}^{b}$	$-55.3+0.3659\times S-5.3954\times10^{-4}\times S^2+5.5132\times10^{-7}\times S^3+74.36\times \log(S)$	(15)
$T_{qtz}{}^{c}$	$-54.8+0.3729\times S-5.602\times10^{-4}\times S^2+5.1719\times10^{-7}\times S^3+73.917\times\log(S)$	(16)
$T_{qtz}{}^{d}$	$1522/5.75-\log S-273.15$	(17)
$T_{Chal}{}^{e}$	$1112/4.91-\log S-273.15$	(18)
$T_{Na/K}{}^{f}$	$1217/1.438+\log Na/K-273.15$	(19)
$T_{Na/K}{}^{g}$	$733.6-770.551\times Y+378.189\times \log Y^2-95.753\times Y^3+9.544\times Y^4$	(20)
$T_{Na/K}{}^{h}$	$1390/1.75+\log Na/K-273.15$	(21)
$T_{Na\text{-}K\text{-}Ca}{}^{i}$	$1647/\log(Na/K)+\beta\log(Ca^{0.5}/Na)+2.24-273.15$	(22)
$T_{K\text{-}Mg}{}^{j}$	$4410/14+\log(K^2/Mg)-273.15$	(23)
T_{CO_2}k	$-44.1+269.25Q-76.88Q^2+9.52Q^3$	(24)
$T_{H2S}{}^{k}$	$246.7+44.8Q$	(25)
$T_{H2S}{}^{k}$	$173.2+65.04Q$	(26)
$T_{H2S}{}^{l}$	$4.811Q^2+66.152Q+177.6$	(27)
$T_{H2S\text{-}CO2}{}^{m}$	$194.3+56.44(\log H_2S+1/6\log CO_2)+1.53(\log H_2S+1/6\log CO_2)^2$	(28)
$T_{CH_4/CO_2}{}^{n}$	$4625/10.4+\log CH4/CO2-273.15$	(29)

a :*Fournier and Potter (1982)*
b: Arnórsson et al.(1988),
c: Gunnarsson & Arnórsson (2000),
d: Fournier 1977,
e: Arnórsson et al.(1983b),
f: Fournier (1979)
g: Arnórsson et al. (1998),
h: Giggenbach et al.(1988),
i: Fournier and Truesdell (1973),
j: Giggenbach.(1988),
k: Arnórsson and Gunnlaugsson (1985),
l: Arnórsson et al. (1998)
m: Nehring and D'Amore (1984),
n: Giggenbach (1991)

Where the symbols stands for:

S: Represents silica concentration as SiO_2 in mg/kg

Y: Designates the logarithm of the molal ratio of Na/K

β: 4/3 for t < 100^{o}C and 1/3 for t >100^{o}C and for log ($Ca^{0.5}$/Na) <0

Q: Designates the logarithm of the respective gas concentrations or gas ratio, gas concentrations in mmol/kg

1.6.4 Stable and radioactive isotope chemistry

Oyuntsetseg (2009) suggested that knowledge of the origin of geothermal waters is very important in geothermal studies because it helps in discriminating the chemical properties of the thermal waters and also their sources of recharge. Studies of stable isotopes play an important role in hydrogeological investigations of both thermal and non-thermal waters because the isotopes carry imprints of the origin of the waters. Isotopes have become an essential part of major geothermal developments. Their use and interpretation are strengthened if complemented and combined with chemical techniques. Craig (1963) established the isotopic characteristics (^{2}H and ^{18}O) of precipitation relating to latitude and altitude as well as continental effects. Ellis and Mahon (1964, 1967) and Mahon (1967) demonstrated that all the solutes in the geothermal fluids could be derived from reactions between the meteoric groundwater and the host lithologies.

This report seeks to establish the origin and recharge of the thermal discharges towards the construction of geothermal conceptual model. Geothermal fluids originate mainly from meteoric water and sea water (Craig, 1963). The determination of the recharge to geothermal systems is an important aspect of geothermal investigations. This is done by measuring the hydrogen and oxygen isotope composition of the steam and water of a geothermal field; the isotopic ratio is the number of atoms of a given isotope divided by the number of atoms of the most abundant isotope of that element. Correlation plot of the available δ^{2}H and δ^{18}O values for the groundwater samples from the study area (data from Dunkley et al. (1993) and Clarke et al. (1990).

(i) the worldwide meteoric water line, which is defined by the relation (Craig, 1961):

$$\delta^{2}H = 8\,\delta^{18}O + 10 \qquad (30)$$

(ii) the meteoric water line of the whole Kenyan Rift Valley (from Lake Magadi in the south to Lake Turkana, in the north), corresponding to the relation from Clarke et al. (1990).

$$\delta^{2}H = 5.56\,\delta^{18}O + 2.04 \qquad (31)$$

Kenya Rift Valley Evaporation Line (KRVEL) from Ármannsson (1994) is also described

$$\delta D = 5.49\,\delta^{18}O + 0.08 \quad (32)$$

And Continental African Rain Line (CARL), Ármannsson (1994).

$$\delta D = 7\,\delta^{18}O + 11 \quad (33)$$

This project report will describe the analytical results of samples collected from different features (including rocks, fumaroles, pools, hot springs, warm springs, cold springs, and shallow wells, both excavated and drilled) after the geochemical surveys carried out by Dunkley et al. (1993) and GDC (2011). Dunkley et al. (1993) stable and radioactive isotope findings are used in this project. This project employs various proved classical geochemical methods of interpretation of surface manifestation data during exploration and exploitation in pursuit of developing the geothermal conceptual model of the BVC.

The expression (equation 34, 35 and 36) adopted from (Brownlow, 1979; Depaolo, 1981) for the isotopic abundance ratio of $^{143}Nd/^{144}Nd$ and $^{87}Sr/^{86}Sr$ that were used in this project is;

$$\left(\frac{^{143}_{0}\mathrm{Nd}}{^{144}_{0}\mathrm{Nd}}\right)_{\mathrm{Measured}} = \left(\frac{^{143}_{0}\mathrm{Nd}}{^{144}_{0}\mathrm{Nd}}\right)_{\mathrm{Initial}} + \frac{^{147}_{0}\mathrm{Sm}}{^{144}_{0}\mathrm{Nd}}\left(e^{\lambda t} - 1\right) \quad (34)$$

The $^{143}Nd/^{144}Nd$ ratio of samples is invariably expressed relative to the CHUR (Chondritic Uniform Reservoir) line. Thus the ϵ_{Nd} represents, in units of parts in 10^4, the deviation of the $^{143}Nd/^{144}Nd$ value of a sample from that of the CHUR line at the same time t.

$$\epsilon_{\mathrm{Nd}} = \left[\frac{\left(^{143}_{0}\mathrm{Nd}/^{144}_{0}\mathrm{Nd}\right)^{t}_{\mathrm{sample}}}{\left(^{143}_{0}\mathrm{Nd}/^{144}_{0}\mathrm{Nd}\right)^{t}_{\mathrm{CHUR}}} - 1\right] \times 10^4 \quad (35)$$

$$\left(\frac{^{87}_{0}\mathrm{Sr}}{^{86}_{0}\mathrm{Sr}}\right)_{\mathrm{Measured}} = \left(\frac{^{87}_{0}\mathrm{Sr}}{^{86}_{0}\mathrm{Sr}}\right)_{\mathrm{Initial}} + \frac{^{87}_{0}\mathrm{Rb}}{^{86}_{0}\mathrm{Sr}}\left(e^{\lambda t} - 1\right) \quad (36)$$

Where Nd and Sr stand for Neodymium and Strontium respectively. Dunkley et al. (1993) did the isotopic composition of Nd and Sr in the BVC rocks.

1.6.5 Evaluation of mixing and boiling processes

Nicholson (1993) established the critieria of recognising mixed fluids as; plots of conservative elements for a group of springs show a near-linear relationship (eg. CI vs B) and variations in

major cation concentrations (especially K) due to leaching and/or adsorption after mixing. (Can be significant where mixing prevents boiling resulting in CO_2(aq) being converted to HCO_3). Arnórsson (2000a) established that mixing of geothermal water with cold water may occur after a variable amount of conductive cooling of the hot water and before, during or after boiling. Mixing is most prone to occur where there is a change in permeability. Drillings have indicated that the pressure potential in the upflow of many geothermal systems is lower than in the enveloping cold ground water body. Mixing, such as conductive cooling and boiling, can upset chemical equilibrium between water and rock minerals, thus causing a tendency for the water to change composition after mixing with respect to reactive chemical components. Arnórsson (2000a) suggested that water ascending from a geothermal reservoir to the surface and emerging in hot springs may cool on the way, by conduction, boiling, or mixing with shallow cold water or by any combination of these three processes. Fluid geothermometry can provide evidence of the location and mechanism of these processes (Fournier and Truesdell, 1974). Water that ascends relatively rapidly and directly from the reservoir with little conductive cooling is likely to have chemical compositions that reflect rock-water equilibrium at the reservoir temperature. Other thermal water has ascended from deep reservoirs so slowly that much of their initial chemistry has been altered by equilibration at lower temperatures. Where the aquifer is at temperatures above the boiling point at atmospheric conditions the water will cool by boiling on its way to the surface whereas waters from reservoirs at temperatures below atmospheric boiling can reach the surface at about the temperature of the aquifer. The chemical composition of mixed water can be used for temperature estimation applying a mixing model (Fournier and Truesdell, 1973). The model can be applied if there is an independent indication of mixing.

Mixing can upset chemical equilibria between water and rock minerals causing a tendency for the water to change composition after mixing with respect to reactive chemical components. Geothermal waters may boil in the upflow of geothermal systems if reservoir temperatures exceed 100^{o}C. The boiling causes the concentrations of aqueous solutes to increase in proportion to the steam formation. It also causes the pH of the water to increase because the weak acids dissolve in the water as, CO_2 and H_2S are transferred into steam phase. Isoenthalpic mixing of equilibrated waters of equal salinity causes the Na/K geothermometry temperature to become higher than the actual temperature of the mixed water (Arnosson, 2000a; Arnórsson, 1985), the difference increasing with increasing temperature difference between the end-member components in the mixture and reaching as much as 30^{o}C. Mixing of waters of equal salinity in the range 100-250^{o}C does not lead to significant discrepancy between the quartz and the Na/K geothermometry temperatures and particularly so, if the hot water component is <200^{o}C. Isoenthalpic mixing of two or more water components, which are at equilibrium with quartz, does not cause the quartz equilibrium temperature to depart significantly (less than about 5^{o}C) from the actual temperature of the mixed water, if the temperatures of the components in the mixture lie within 150^{o}C and 300^{o}C (Arnosson, 2000a). It is in this regard that Arnórsson (2000b) described the mixing of equilibrated geothermal waters of different temperatures to be

the reason that leads to discrepancy between quartz and Na/K geothermometry temperatures, the discrepancy increases with increasing temperature difference between the end-member components in the mixture. The main sources of discrepancy include: 1) equilibrium between the respective minerals and solution is not closely approached for one or both of the geothermometry reactions; 2) the discharge is a mixture of two or more components of quite different temperature, 3) partial re-equilibration occurs during cooling in the up flow zones. In this report, the silica-enthalpy mixing model is used. This mixing model is invariably used to study both mixing and boiling processes. Arnórsson (2000a) pointed out that water ascending from a geothermal reservoir to the surface and emerging in hot springs may cool on the way, by conduction, boiling, or mixing with shallow cold water or by any combination of these three processes. Mixing models have been developed to allow estimation of the hot water component in mixed waters emerging in springs or discharged from shallow wells. There are essentially three kinds of mixing models: 1) the chloride-enthalpy mixing mode (Truesdell and Fournier, 1977); 2) the silica-enthalpy warm spring mixing model (Fournier, 1977); 3) the silica-carbonate mixing model (Arnórsson, 2000a). The method is based on heat and silica balance and its successful application is dependent upon three basic assumptions (Fournier and Truesdell, 1974; Truesdell and Fournier, 1977):

- there is no loss of heat after mixing
- the solubility of quartz controls the silica content of the reservoir fluid
- there is no deposition or dissolution of silica once the geothermal fluid has left the deep reservoir, ie. before or after mixing.

1.6.6 Conceptual Model Approach

Cumming (2009) stated that, a conceptual model approach to geothermal resource assessment addresses the weaknesses of anomaly hunting and anomaly stacking by integrating data sets across all disciplines in the context of a physical model. A successful study that was carried out in Mongolia by Oyuntsetseg (2009) indicated that geothermal conceptual models are used when making decisions like targeting exploration and production geothermal wells. The conceptual model for locating exploration wells give an indication of the expected reservoir temperature, depths to the reservoir and other features of the geothermal system. The main components in a conceptual model are: heat source, production reservoir, sealing cap layer, upflow and outflow zones, and the recharge and discharge zones. Geothermometer isotherms were used to construct iso-contours that would define the geothermal system.

The conceptual model aims at highlighting the distribution of temperature, pressure, permeability and fluid chemistry within the geothermal reservoir in order to delineate the direction of fluid flow and circulation (e.g., hot upflow, outflow and colder recharge) symbolized with arrows (Mortensen and Axelsson, 2013).

Geochemical techniques used during the various stages of exploration and evaluation of geothermal resources, as well as monitoring studies, are particularly important because of the information they provide are at relatively low cost. Delineated hydrogeochemical model of the geothermal system shows as far as possible the distribution of the subsurface temperatures and directions of ground water flow. In many geothermal areas fumaroles characterize the geothermal manifestations on high ground but hot springs do the same thing on low grounds. The hot springs discharge boiled water that has flowed laterally from an upflow as determined by hydraulic gradient. This distribution of thermal manifestations is a characteristic feature of many geothermal systems associated with andesitic volcanoes such as Amatitlàn in Guetamala, Alauchapàn and Berlin in El Savador as well as other geothermal areas in the Phillipines. Rising geothermal steam may condense partly or complete in surface waters. When this occurs, steam heated springs form. If a limited amount of water is available, the surface water may be heated to the boiling point. Boiling of this water and the associated alteration of the soil and rock into clay leads to the development of the mud pools, mud pots and mud volcanoes (Arnosson et al., 2000).

CHAPTER TWO

2.1 Geological and Structural setting

The BVC polygenetic structure is composed of four distinct volcanic centres from west to east. These centres are; Kolalolenyang, Kakorinya, Likaiu West and Likaiu East. Kakorinya is the youngest of all the four centres. They are composed of a wide spectrum of lava types including basanite, basalt, hawaiitte, mugearite, benmorite, trachyte and phonolite. Trachytic and pyroclastic deposits cover much of the western slopes of Kakorinya and the summit area of Likaiu West. The latest eruption in the area is historic and occurred in 1921 (Dunkley et al., 1993). A brief summary of geological units (Figure 4) is outlined below.

The Pliocene foundation rocks of the BVC dated at about 4.53 ma are well exposed in the adjacent rift margins (Dunkley et al., 1993). They cover most of the East of the BVC and are called the Parkati Basalts. They are the oldest lavas of the BVC and occur in the faulted ground far east of Lake Logipi. The oldest lavas on the west are Lorikipi Basalts dated to be between 4.0-1.86 ma. Dodson (1963) established that the Lorikipi Basalts are intercalated with Loriu trachytes, rhyolites and Precambrian Basement rocks composed of biotite gneiss. The youngest basaltic lava flows are dated at about 1000 years (Dunkley et al., 1993) and are exposed to the north and south of Kakorinya in the inner trough of the main rift. These recent basalts are oriented in the NE-SW direction, in the north it touches the margin of Lake Turkana while on the south it touches the margins of Lake Logipi. The flow direction of lavas postulated from surface texture is to the NE. North of Kakorinya, recent basalts border the upper basalts including the mugearites and are dated at 0.01 ma in the west and Latarr Basalts are dated at 1.37 ma in the east (Dunkley et al., 1993). The Latarr Basalt borders younger basalt lavas of between 0.7- 0.23 ma to its south. Minor basalts of phreatic origin dot the area to the north and south of Kakorinya.

Dunkley et al. (1993) found out that the early phases of trachytic volcanism constructed the centres of Kalolenyang and Likaiu East, and major trachytes lavas are exposed within the inner trough. The youngest trachytes form the domes to the west of Kakorinya caldera around the caldera rim and these trachytes are dated to be about 0.05 ma. Upper trachytes of 0.09 ma are exposed in the east of the caldera running in a N-S direction, with a minor outcrop of this formation being noted in the north west with a strip in the south west. Older trachytes are exposed closer to the flanks in the east and are dated to be about 1.37 ma. An older trachyte formation but younger than the east formation is exposed at Kalolenyang. Minor exposures of Lower Tracyhte Formation are exposed in the north west and south east.

The phonolites are older than the recent basalts and are exposed within Kakorinya caldera (Dunkley et al., 1993). The source is most likely the conduits within the rim caldera. The texture indicate that the flows might have flowed to the south east, with a small component flow

to the north east indicating that there were several episodes of the eruption. The rock is very young and is about 1000 years.

Pyrocalstics cover most parts of the western side of Kakorinya while pockets of alluvial sediments are within this area. Some alluvials are found on top of cones suggesting that the lake levels were much higher than present. The youngest pyroclastic deposits on Kakorinya are airfall pumice lapilli and are best exposed in a thick wedge, which infills the western dipping slope between the caldera rim and the outer ring fractures. These deposits bank against and mantle the ring fracture escarpments and the pre-caldera domes. They are cut by the caldera wall in the west and bury the northern wall. This relationship indicate that the eruption of these trachytic tuff was broadly contemporaneous with the caldera collapse. Lacustrine sediments provide evidence of the existence of former Lake Suguta, which infilled the inner trough northwards from Emuruangogolak (Dunkley et al., 1993).

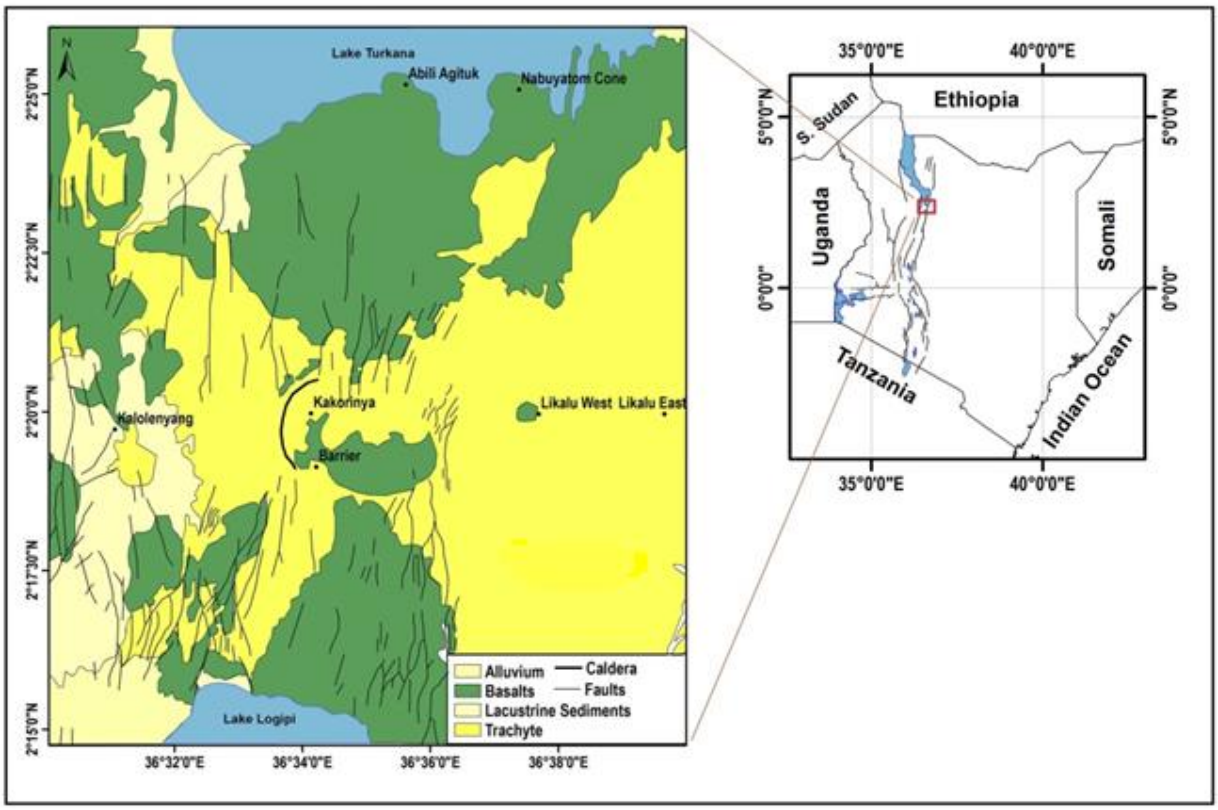

Figure 4: Simplified geological map of the Barrier Volcanic Complex (modified after Dunkley et al. 1993)

Most of the prospects located in the rift are characterised by phonolites lava which also occur in the BVC. The most voluminous and best preserved phonolites are the young domes found around the Kakorinya caldera and on its northern flanks. In the BVC the trachytes of Kalolenyang are over saturated with comenditic lavas (Dunkley et al.1993). Mugearites are relatively common in the BVC,they closely resemble basalts in appearance.

2.2 Structures

Geothermal that invariably occurs in extensional and transtensional tectonic environments have long been the major targets in the exploration of geothermal resources. The interactions between normal faults and strike-slip faults, acting either as strain relay zones have attracted significant interest in geothermal exploration as they commonly result in fault-controlled dilational corners with enhanced fracture permeability and thus have the potential to host blind geothermal prospects (Stockli, 2013). The geothermal fluids in the BVC appear to be controlled by major faults, caldera ring structures and subsidiary faults. The fumaroles tend to be located where N-trending joints or minor faults cut the main NE-trending faults within Kakorinya caldera. The most active being located along the ring structures of the caldera (Dunkley et al., 1993). As the faults lose displacement, it breaks into multiple splays (or horsetails). The higher density of faults and greater number of fault intersections generates a broad zone of highly fractured and therefore highly permeable rock, which facilitates the ascent of geothermal fluids.

Seismic reflection profiles at the southern Lake Turkana have imaged an east-dipping master fault controlling a half graben (Dunkelman et al., 1988). Melnick et al. (2012) observed and proposed that this east-dipping master fault and half graben extends, continuously southward and defines the structural setting of the entire Suguta Valley. This interpretation is based on (1) the similar asymmetric topography in all swath profiles, characterized by steep western flanks with footwall back tilt and gently sloping eastern flanks with a broad, antithetically faulted monocline. (2) the remarkably linear morphology of the western rift flank and of fault traces over a distance exceeding 120 km, which contrast both with the morphology and fault geometries along the eastern flank. These structures are exposed along the southern margin of Lake Turkana, where they offset late Pleistocene – Holocene lava flows, monogenetic cones, and Quaternary alluvium. The EARS in the Lake Turkana region is characterized by marked variations in geometry and structure (Melnick et al., 2012). The BVC is transected by a complex pattern of NNE-striking faults parallel to the rift trend (Figure 4).

Faulting and eruptions have occurred throughout the BVC and have migrated toward the axis of the with time. Dunkley et al. (1993) unraveled that, the main phase of *en échelon* faulting appears to have been closely associated with the start of the collapse of the summit area of Kakorinya and the formation of the outer ring. Adjacent to the rift margins N-trending faults produce tilted escarpments and affect Likaiu East and Kalolenyang. The central part of BVC is transacted by a series of curvilinear N to NE trending normal faults which produced tilted escarpments and also affect Likiau East and Kalolenyang. The central part of the BVC is transected by a series of curviliner N to NE trending normal faults which extend in an *en échelon* right- stepping fashion across the volcano from the south-western flanks of Kakorinya to the nothern flanks of Likaiu West. Dunkelman et al. (1988) established that the faults are associated with geothermal manifestations indicating that the major fault systems in the area are conduits for vertical recharge. The faults run NS and NE-SW; other structures are the caldera and

volcanic centres. The faulting that accompanied rifting occurred in several stages starting with faulting on the western side accompanied by basaltic and phonolitic volcanism on the crust uplift (Baker et al., 1987). Other structures in BVC include several pyroclastic cones, a caldera and sympathetic curvilinear structures. The slightly elongate N75°W oriented Kakorinya caldera covers an area of 8.25 km^2, is slightly elipsoidal in plan, having a long axis of 3.75 km and a short axis of 3.0 km. The caldera wall reaches a maximum height of 100 m in the west, and progressively declines in height via a series of normal faults to about 10 m in the south (Dunkley et al., 1993). The location of the fumaroles in Kakorinya caldera mimic the ring strucutres of the caldera. Kakorinya has two outer ring fractures located approximately 1 and 1.3km west of the main caldera. The fractures are manifested by prominent east-facing scarps that can be traced through about 40^o of arc, and they have their largest apparent displacements in the middle of the arc where the scarps are at their highest (Dunkley et al., 1993).

2.3 Hydrogeology

The deep ground water in the region occurs in weathered and fractured zones in volcanic and volcaniclastic rocks and in sediments inter-bedded between volcanic rocks. Shallow ground water is mostly found at the banks of the seasonal rivers that traverse the area such as Parkati well, which is for both domestic and livestock use. The ground waters are recharged from the surrounding rift flanks. The groundwater is sensitive to rainfall fluctuations and during dry seasons, the water levels in the well fall rapidly. The project area has several hot springs along Lake Logipi; due to the high salinity of the discharge, the locals never use the water for any purpose.

Based on the stable isotope of $\delta^{18}O$ and $\delta^{2}H$ studies, the recharge of the BVC geothermal system is mainly from meteoric origin from the rift flanks and partly from Lake Turkana, the borehole water also have an input of the Lake Turkana water recharge (Dunkley et al., 1993). During the mid-Holocene (~5270±300 cal. yr BP), however, the lake water-level fell by ~50 m, coeval with major episodes of aridity on the African continent (Garcin et al., 2012). This must have had an impact into the local groundwater recharge, assuming that the local BVC surroundings show unconfined aquifer characteristics.

Hydrologic isolation of the Suguta and Turkana basins was established at ~0.2 Myr as a result of growth of The Barrier complex that today separates both basins (Dunkley et al., 1993; Champion, 1935; Truckle, 1976). The palaeo-shoreline record of Lake Turkana form a staircase morphology of successive former lake water-levels, well exposed over a vertical range of ~100m, from the present-day lake water-level at ~360 m to a maximum elevation of ~455m. At this Holocene time Lake Turkana and the palaeo Lake Suguta were connected as also marked by the Maximum highstand shoreline in Namurinyang cone next to Lake Logipi (Plate 2) and Abili Agituk (Plate 3) at the shores of Lake Turkana (Melnick et al., 2012). Abili Agituk is an eroded complex of overlapping and nested craters cut by N-trending faults. A prominent wave-cut notch

on the side of the cone occurs at an elevation of 440m and correlates with the last maximum highstand shoreline of Lake Turkana around 10Ka. Phreatomagmatic activity is indicated by the eroded and faulted remnants of the tuff cone (Dunkley et al., 1993). The Suguta trough was first initiated less than 3.0 Myr ago, and was subsequently filled in by younger volcanic products. The reforming of this trough, less than 0.75Myr ago led to the eventual development of Lake Suguta. Various studies have established the occurrence of sediments flooring the trough and of wave-cut platforms on the southern side of the BVC, and it is concluded that Lakes Suguta and Lake Turkana were continuous before they became separated by growth of the Barrier. Once separation was complete, Lake Suguta disappeared because of insufficient water supply from the Suguta river relative to the evaporation rate (Truckle, 1976).

The mid-Holocene fall in the lake's water-level (Plate 3) together with the ^{18}O-enrichment (+4‰) of the $\delta^{18}O$ values of lacustrine carbonates from the early Holocene to the present-day, suggests that Lake Turkana experienced a major decrease in the local hydrological balance (lower precipitation/higher evaporation) as well as possible changes in the air-mass source areas, which affected the isotopic composition of water input into the lake from both rivers and precipitation (Levin et al., 2009). Studies of the Suguta sediments and preliminary determinations of strand line altitudes, indicate that around 9,600 yr BP Lakes Suguta and Lake Turkana occupied apparently separate basins. The difference in altitude between the Lake Suguta and Lake Turkana strand lines suggest that from the Suguta sediments, the BVC was sufficiently well developed to prevent the two lakes from coalescing (Truckle, 1976). A comparison between palaeo-hydrological and archaeological data from the Turkana Basin suggests that the mid-Holocene climatic transition was associated with fundamental changes in prehistoric cultures, highlighting the significance of natural climate variability and associated periods of protracted drought as major environmental stress factors affecting human occupation in the East African Rift System (Garcin et al., 2012).

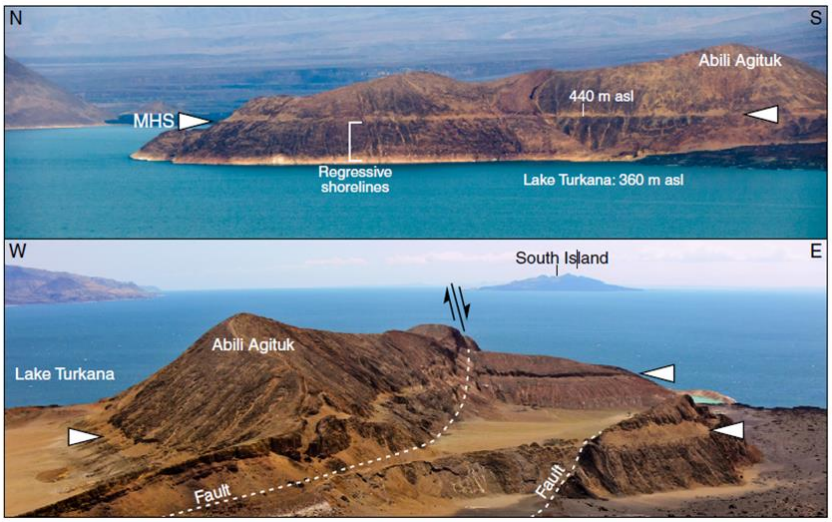

Plate 3: Aerial views of the maximum highstand shoreline on Abili Agituk volcano (MHS: white arrows) (Garcin et al., 2012)

CHAPTER THREE

3.1 Materials and Methods

The methods used in this study were holistically aimed at developing a geothermal conceptual model of the BVC. This will be achieved by delineating the direction of fluid flow and circulation (e.g. hot upflow and colder recharge) symbolized with arrows, and based on the computed equilibrium geothermometry temperatures from the chemistry of the thermal fluids, delineate the reservoir using the isotherms as well to characterize the chemistry of the fluids in the upflow and the outflow of the BVC system. In this regard, the methods used include desktop studies, fieldwork sampling and analysis, laboratory analysis, data analysis and interpretation. The methods and the materials used in pursuit of achieving the set objectives of this research are as elaborated below.

3.2 Desk Top Studies

- Study of previous work done in the Barrier Volcanic Complex surface geology, structures and geochemistry of the thermal fluids
- Literature review mainly on fluid geochemistry and isotope chemistry and obtain prior isotope data of the project area.
- Review of mixing models and conceptual modelling of geothermal systems from other geothermal field in the world.

3.3 Field Work

A preliminary surface exploration fieldwork was carried out by Geothermal Development Company on the 23rd-29th May 2011 to determine the potential of the BVC prospect. The geochemical fieldwork entailed fumarole and hot spring sampling. The sampling procedures are those described by Arnórsson et al. (2006)**.** The fumarole discharge was trapped using a plastic funnel whose contact points with the ground were sealed with mud to prevent any contamination with atmospheric air (Appendix I; Plate 4). The condensed steam was then delivered into a sampling bulb through butyl tubing via a stainless steel cooling coil immersed in cold water to trap the steam condensate.

Plate 4: Field sampling of a Fumarole discharge in Kakorinya caldera

The fumarole gases were sampled by directing the steam into an evacuated Giggenbach gas flask containing 50 ml of 40% NaOH solution with cold water continuously pouring on top of the flask to cool it. The acidic gases (CO_2 and H_2S) are absorbed into the NaOH solution giving room in the evacuated flask for the minor none condensable gases usually found in thermal fluids to concentrate to measureable levels. The gas sample was used for analysis of hydrogen (H_2), methane (CH_4), nitrogen (N_2) and oxygen (O_2) by gas chromatography at the KenGen, Olkaria Geochemistry Laboratory while the condensate sample was used for the analysis of volatiles (Cl, B, SO_4, CO_2, SiO_2 etc.) that on boiling partition into the steam phase.

A portion of the condensate collected was set aside for immediate analysis and measurements of pH, conductivity, total dissolved solids (TDS), hydrogen sulphide gas (H_2S) and carbon dioxide (CO_2). A measured quantity of zinc acetate (CH_3COO_2Zn) was added to another portion of the condensate for fixation of SO_4. Another untreated portion was reserved for Cl^- and F^- analysis. A different sample was also collected and preserved with concentrated HNO_3 for later analysis of metal ions. A portion for SiO_2 analysis in the water sample was diluted ten times to avoid polymerization of monomeric silica using deionized water. The hot springs were sampled (Plate 5) in accordance to the procedures of Arnórsson et al. (2006). The hot springs discharges sampled were divided into different portions for onsite, immediate analysis and for preservation for later laboratory analysis just like the fumarole condensate.

Plate 5: Field water sampling of Lake Logipi hot spring discharge

3.4 Laboratory Analyses

- Fumarole Steam samples were analysed for CO_2, H_2S, CH_4, H_2, N_2 and O_2. Analysis of CO_2 and H_2S will done titrimetrically using 0.1M HCl and 0.001M mercuric acetate respectively (Ármannsson and Ólafsson, 2006; 2007; Arnórsson et al., 2000). Non-condensable gases (CH_4, H_2, N_2 and O_2) were analysed by gas chromatograph of shimadzu model. Analysis of H_2S in the spring water samples was done on site in the same way as in steam samples.

- Measurements of pH, TDS and conductivity together with Total Carbonate Carbon (TCC) analysis from the water samples were carried out in the field laboratory at room temperature a few hours after sampling using pH meter, conductivity meter and pH controlled titration from (8.3-3.8) using HCl. Correction for interferences from SiO_2, B and H_2S in the analysis of total carbonates was also done.

- Water sample analysis of B, SiO_2 and SO_4 was done spectrophotometrically using UV/Vis. Where B, SiO_2 and SO_4 were analysed using reagents such as curcumin, ammonium molybdate and turbidimetrically using Barium Chloride respectively. The major aqueous cations (Na, K, Ca, Mg, Al, Fe) were determined using AAS. Chloride analysis were done titrimetrically using argentometric Mohr's method using silver nitrate reagent while fluoride were analysed using ISE.

- The $\delta^{18}O$ and $\delta^{2}H$ stable isotopes adopted from Dunkley et al. (1993) could have been analysed using the conventional inductively coupled plasma mass spectroscopy while the petrochemical data, was analysed using an X-ray fluorescence machine.

3. 5 Analytical Equipment

Sample analysis was done at different stages such as onsite analysis, immediate analysis and later laboratory analysis with the following important analytical equipment used.

3.5.1 Atomic Absorption Spectrometer

Atomic absorption spectroscopy (AAS) is one of the most common instrumental methods for analyzing for metals and some metalloids (arsenic, selenium, and tellurium). It is based on the same principle as the flame test used in qualitative analysis. When an alkali metal salt or a calcium, strontium or barium salt is heated strongly in the Bunsen flame, a characteristic a colour of the flame is used to distinguish the corresponding metal (Erxleben, 2009). The BVC water samples were analysed using an Aurora manufactured Flame atomic absorption spectroscopy (FAAS) which has a nebulizer that sucks up liquid sample (aspiration), a hollow cathode lamp (HCL) that uses a cathode made of the element of interest with a low internal pressure of an inert gas. The technique of FAAS requires a liquid sample to be aspirated, aerosolized, and mixed with combustible gases, such as acetylene and air or acetylene and nitrous oxide. The mixture is ignited in a flame whose temperature ranges from 2100 to 2800^{o}C. During combustion, atoms of the element of interest in the sample are reduced to free, unexcited ground state atoms, which absorb light at characteristic wavelengths. The characteristic wavelengths are element specific and accurate to 0.01-0.1nm (Erxleben, 2009; Chasteen, 2000). Liquid samples were manually put in cuvettes for analysis of metals (Na, Mg, Ca, Fe, Li, K, and Al) with the respective cathode lamps of the elements placed during the analysis.

3.5.2 UV-Visible Spectrophotometer

The ultraviolet-visible (UV-Vis) spectrophotometer is an instrument commonly used in the laboratory that analyzes compounds in the ultraviolet (UV) and visible (Vis) regions of the electromagnetic spectrum. It allows one to determine the wavelength and maximum absorbance of compounds. From the absorbance information and using a relationship known as Beer's Law ($A = \varepsilon bc$, where A = absorbance, ε = molar extinction coefficient, b = path length, and c = concentration), one is able to determine either the concentration of a sample if the molar extinction coefficient is known, or the molar absorptivity, if the concentration is known (Settle, 1997). Shimadzu UV-1800 spectrophotometer with a spectral band of 1nm was used to analyse for SO_4, B, and SiO_2 in the BVC liquid samples.

3.5.3 Ion Selective Electrode

An ion selective electrode generates a difference in electrical potential between itself and a reference electrode. The output potential is proportional to the amount or concentration of the

selected ion in solution. The number of effective ions is called the activity of the solution. It is therefore reasonable to assume that the electrode will measure the activity rather than the finite concentration of the ions. In dilute solutions though, the ionic activity and concentration are practically identical but in solutions containing many ions, activity and concentration may differ. This is why dilute samples are preferred for measurement with ISE's. It is possible to 'fix' the solution so that activity and concentration are equal. This can be done by adding a constant concentration of an inert electrolyte to the solutions under test. This is called an Ionic Strength Adjustment Buffer (I.S.A.B.). Thus, the ion selective electrode will measure concentration directly. The most common ISE is the glass-bodied pH combination electrode (Settle, 1997). It is used Br^-, F^-, Cl^-, I^-, etc. The ELIT 9801-ISE was used for the analysis of the analysis of Cl^- and F^- of the BVC samples.

3.5.4 Gas Chromatograph

A gas chromatograph (GC) is an analytical instrument that measures the content of various components in a sample. Principle of gas chromatography: the sample solution injected into the instrument enters a gas stream, which transports the sample into a separation tube known as the column with helium or nitrogen or argon are used as the carrier gas. The various components are separated inside the column. The detector measures the quantity of the components that exit the column (Settle, 1997). It measures various gas species such as, CH_4, He, H_2, N_2, O_2 with a separation on a 4.0m (1/8 inch outside diameter) column packed with molecular sieve 5A (50-80 mesh) at 30^oC with argon as carrier gas at a flow rate of 20ml/min. A thermal conductivity detector gives high sensitivity for He and H_2 with lower sensitivity for the other gases. Ar, CH_4, CO, N_2 with a separation on a 15m molecular sieve 5A column at 80^oC with subsequent conversion of O_2 to water in 0.5m MS5A column al 220^oC with hydrogen, as the carrier gas at a rate of 20ml/min. Separation of Ar and O_2 is not necessary in this scheme. A thermal conductivity detector yields high sensitivity for these gases (Nicholson, 1993). Shimadzu's versatile GC-2014 gas chromatograph was used in the analysis of CH_4, H_2, N_2, O_2 of Kakorinya fumaroles gas samples.

3.6 Data Handling, Interpretation and Reporting

It is common practice to check on the quality of analytical results before processing available data for aqueous solutions, therefore, an initial check on the quality of Logipi springs water analytical results was done by means of equation 37 used for calculating the charge balance for water analysis. For first class analysis, the difference in the sum of cations charges should be within 5% of the sum of the anion charges. However, 10% difference is generally regarded as satisfactory, for very saline and extremely dilute water, where acceptable errors are larger than for more common salinities, a charge balance of more than 10% may be acceptable. Charge balance is of course only of value to check on the results of the major ions in solution (Arnosson et al., 2000).

$$\%_{\mathrm{Dev}} = \frac{\sum_{cations} - \sum_{Anions}1}{\sum_{Cations} + \sum_{Anions}1} \times 100 \qquad (37)$$

The project entailed production of maps, analytical results and interpretation of data using computer softwares and programs, these include:

- ArcGIS 10.1 For generation of Maps
- Grapher 9 For drawing most of the graphs and correlation plots
- Powell Spread sheet For drawing the ternary diagrams (Na-K-Mg, Cl-SO_4-HCO_3 and Cl-Li-B diagrams)
- Aquachem Ploting Piper and Scatter Diagrams
- Canvas Drawing the conceptual model

CHAPTER FOUR

4.1 Results

4.2 Chemical Characteristics of the Hot Spring Fluids

The analytical results of Logipi hot springs show that the spring discharge chemistry is dominantly a Na-Cl-HCO_3 facies with regards to the dominant cation and anion as illustrated in Table 2. The pH of the springs ranges from 9.0 to 9.3. The pH of surface geothermal waters is principally determined by the loss of carbon dioxide on boiling which causes the solution to become progressively more alkaline. However, pH is also influenced by the fluid salinity and temperature and by mineral buffers (Nicholson, 1993). This implies that the spring waters have experienced a lot of CO_2 degassing. The springs display a low concentration in silica. The findings of the chemical composition of the hot springs are consistent with the findings of Dunkley et al. (1993).

Table 2: Chemistry of the Logipi hot springs

Hot springs	g Temp (^{0}C)	Cond (µΩ/cm)	TDS (ppm)	pH/20°C	Concentration (ppm)													
					B	SO_4	Cl	CO_2	F	H_2S	SiO_2	Al	Ca	Li	Na	K	Mg	Fe
BS-1	63	14730	7400	9.35	0.1338	488	3567	4035	132	0.068	58.1	0.035	1.364	0.028	2420	61	0	0.02
BS-2	65	18300	9150	9.35	0.1673	585	3976	3408	131	0.204	46.3	0.066	1.42	0.026	2321	55	0	0.02
BS-3	54	33540	16780	9.36	0.1338	586	4046	4070	131	0.204	48.9	0.108	1.796	0.042	2682	71	0.01	0.03
BS-4	70	19780	9900	9.4	0.167	603	4455	3714	141	0.272	77.5	0.068	1.45	0.052	2619	74	0	0.02
BS-5	54	15500	7710	9	0.1673	429	3215	2882	62	0.17	70.5	0.064	1.75	0.046	1476	32	0.03	0.02
BS-6	70	26390	13250	9.05	0.268	730	5701	1806	104	0.238	88.4	0	0	0	2928	69	0	0
BS-7	61	30020	15010	9.05	0.3011	781	7448	4572	116	0.238	111.6	0.07	2.452	0.13	4712	128	0.02	0.04

4.2.1 Piper Diagram of the Logipi springs

The piper diagram (Figure 5) shows the hydrogeochemical characteristics with concentrations of Na, Ca, Mg, HCO_3, Cl and SO_4 in milliequivalent per litre. The diagram confirms that the BVC waters are of Na-Cl-HCO_3 type. Sodium is apparently the most dominant cation.

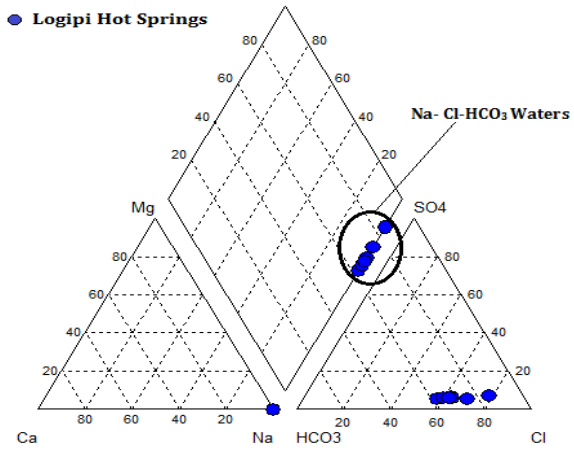

Figure 5: Piper diagram of Logipi hot springs

It is worth noting that, both HCO_3^- and SO_4^{2-} decline relative to Cl^- within the Suguta valley around the Logipi area. It is anticipated that during passage northwards to the sump area of Lake Logipi, evaporating waters would tend to precipitate bicarbonates and sulphates first, which may explain why chloride is increases relative to bicarbonate (Dunkley et al., 1993). Reactions between the dissolved carbon dioxide and the host rocks form HCO_3, the concentration of whieh is therefore influenced by permeability and lateral flow.

As a consequence, boiling springs fed directly from the reservoir tend to have the lowest HCO_3 concentrations. This enables the HCO_3/SO_4 ratio to be used as an indicator of flow direction. The flow of a fluid away from the upflow yields greater opportunity for rock-water reaction and therefore increased production of HCO_3. This, combined with the loss of H_2S by rock-water reactions with increased lateral flow, leads to an increase in the HCO_3/SO_4 ratio away from the upflow zone (Nicholson, 1993). In this regard, the BVC springs show a considerable consistency of ratio of HCO_3/SO_4 in order of 6-8, implying a similar source of fluids flowing laterally away from the upflow zone.

The concentration of magnesium in the BVC springs is in the order of 0.02-0.03 ppm. Calcium concentrations are controlled by minerals of retrograde solubility ($CaCO_3$. eg. calcite; $CaSO_4$, eg. anhydrite; CaF_2, fluorite) and to a lesser extent by Ca-rich aluminosilicates. Factors, which affect the solubility of these minerals, will also influence the level of Ca in the geothermal fluid (Nicholson, 1993). Calcium in the BVC springs is in the order of 0-2.452 ppm.

4.2.2 $Cl\text{-}SO_4\text{-}HCO_3$ Diagram

The ubiquitous Giggenbach (1991), $Cl\text{-}SO_4\text{-}HCO_3$ ternary diagram (Figure 6) was used in the classification of waters based on the major anions. The BVC hot springs plot along the $Cl\text{-}HCO_3$ line at the centre suggesting a $Na\text{-}Cl\text{-}HCO_3$ chemical facies and peripheral waters. This observation is also consistent with the piper diagram (Figure 5) indicating the hydrogeochemical facies.

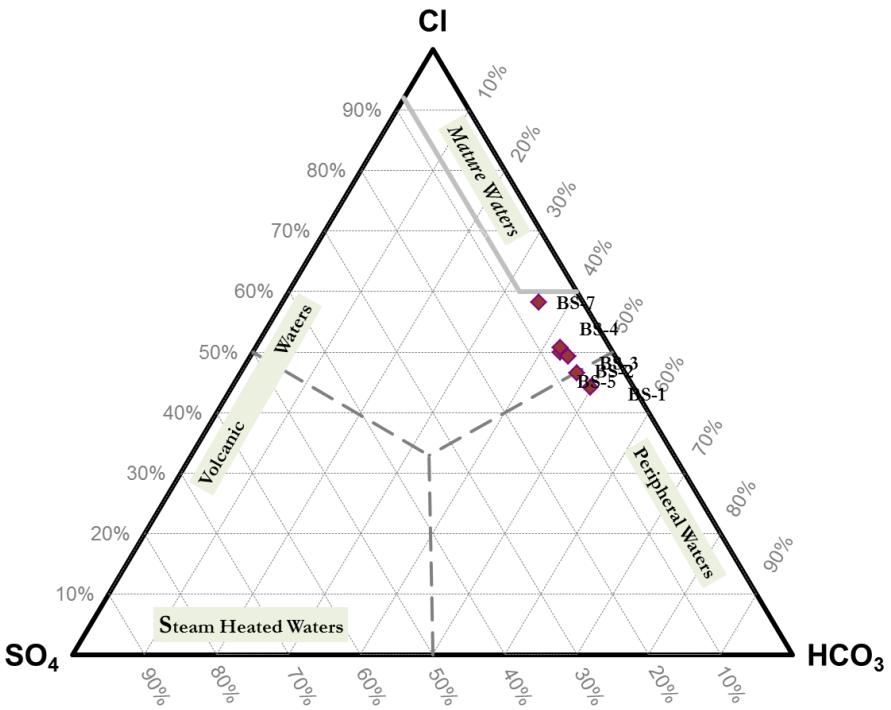

Figure 6: Cl-SO_4-HCO_3 diagram

4.2.3 Relative Cl-Li-B Ternary Diagram

The ternary diagram of chloride, lithium and boron in the form presented in Giggenbach (1991) is used to distinguish fluids from different sources, to reveal fractionation associated with boiling or mixing with fluids that have boiled, or fluids generated by different sources of high temperature steam. In Powell et al. (2001), for example, it was used to distinguish geothermal waters influenced by absorption of high temperature steam from differing sources. The Cl-Li-B ternary diagram shows the variations of the conservative elements Cl, Li and B in geothermal waters. The alkali Li is the least affected by secondary processes and may therefore be used as a 'tracer' for the initial deep rock dissolution process and as a reference to evaluate the possible origin of Cl and B. The B content of thermal fluids is to some degree likely to reflect the maturity of a geothermal system. Boron is volatile and is easily expelled during the early heating up stages. In such a case, fluids from older hydrothermal systems can be expected to be depleted in B while the inverse holds for younger hydrothermal systems. Both Cl and B are added to the Li containing solutions in proportions close to those in crustal rocks (Giroud, 2008).

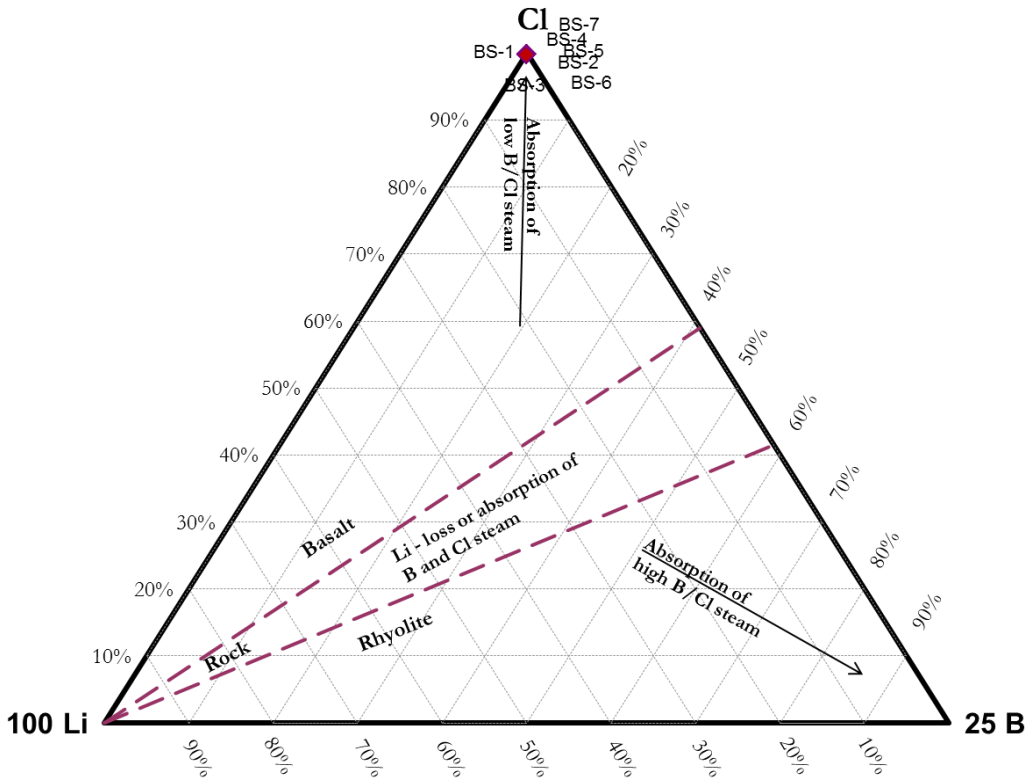

Figure 7: Cl- B - Li Diagram

The water discharged from Logipi springs plot at the region of chloride apex (Figure 7). The waters are depleted in boron in relation to either chloride or lithium suggesting the possibility that a dilution of the deep geothermal reservoir waters by waters from aquifers of relatively lower temperatures or by preferential uptake of boron by clays and other minerals. Another possible reason, could be the fluids are tapping from an old BVC hydrothermal system given that old hydrothermal systems are relatively depleted in boron probably attributed to the Holocene recharge of the Lake Turkana and Palaeo Lake Suguta.

4.2.4 Relative Na-K-Mg

The Giggenbach (1988) Na-K-Mg graphical method involving the simultaneous use of a Na/K and $K/Mg^{0.5}$ ratio was used to establish the equilibrium between the fluids and hydrothermal minerals and ultimately determine the suitability of the waters in the estimation of the equilibrium reservoir temperature. From (Figure 8), the Logipi springs water samples plot above the fully equilibrated line. This could be indicative that waters have attained equilibrium with minerals in the host lithologies and an effect of boiling processes and subsequent steam loss is eminent due to the long residence time of interaction with the host lithologies. The estimated Na/K equilibrium temperatures range between 160-180°C.

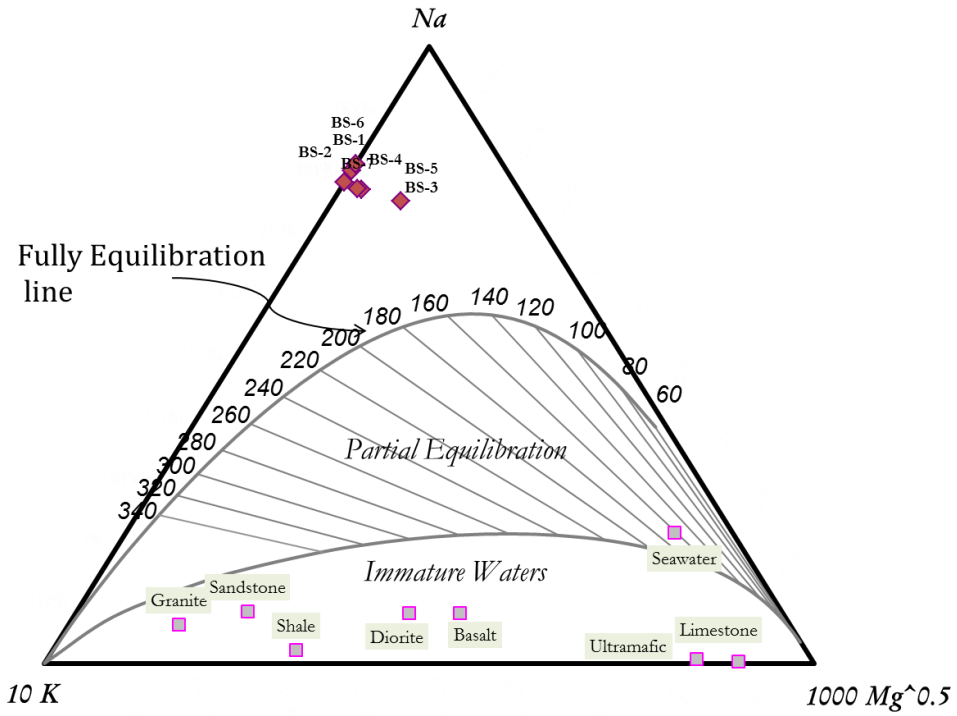

Figure 8: Na-K-Mg diagram

The concentration of sodium and potassium is controlled by temperature dependent mineral-fluid equilibria, which form the basis of the Na/K geothermometer. Lower Na/K ratios (~ <15) tend to occur in waters which have reached the surface rapidly and are therefore associated with upflow structures or more permeable zones. Higher ratios are indicative of lateral flow, near-surface reactions and conductive cooling (Nicholson, 1993). The Logipi springs Na/K values range between 35-46 and 52-53 from the Dunkley et al. (1993) spring data. This implies a lateral flow of thermal waters to the Logipi springs

4.3 Fumarole Discharge chemistry

4.3.1 Fumarole Steam Condensate Chemistry

It is invariably common that most chemical analysis of fumarole discharge, usually have low concentrations of the partitioning chemical parameters analysed as exemplified by the Kakorinya fumaroles steam condensate (Table 3). In some instances, the reaction of the fumarole steam with the wall rock during its ascent to the surface may perturb the chemistry of the fumaroles steam. The pH of the sampled Kakorinya fumaroles ranges from acidic to slightly neutral that translates to 5.26 to 7.48, with a TDS of 4 to 34ppm. It is generally assumed that lower pH and solute content of steam condensates indicates less interference by shallow ground waters. This relationship is an indication of the strength of the steam flows, with weaker fumaroles being more susceptible to dilution and condensation. With reference to the TDS of the Kakorinya

fumaroles steam condensate, the order from low to highest concentration is, BF-04, BF-01, BF-06, BF-02, BF-03 and BF-05 this implies that BF-03 and BF-05 are the weakest fumaroles while BF-04 and BF-01 are the strongest discharging fumaroles.

Table 3: Fumarole Steam Condensate chemistry

	Sampling	Cond	TDS		Concentration (ppm)													
Fumaroles	Temp°C	(µΩ/cm	(ppm)	Ph/20°C	B	SO_4	Cl	CO_2	F	H_2S	SiO_2	Al	Ca	Li	Na	K	Mg	Fe
BF01	96.4	14	7	5.26	0.033	2.6	3.2	480	0.4	0.14	0.03	0.03	0.48	0.01	0	0	0	10
BF02	93.6	30	15	6.65	0.067	3.8	2.6	526	0.2	0.14	0.05	0.04	0.41	0.01	0.5	0	1	17
BF03	93.6	50	25	6.76	0.034	4.9	3.8	515	0.1	0.2	0.05	0.03	0.44	0.01	1.5	0	0	3
BF04	93.3	8	4	5.44	0.034	4.4	5.3	620	0.1	0.14	0.03	0.03	0.44	0.01	0	0	0	0
BF05	93.2	69	34	7.48	0.134	5.4	9.8	519	0.2	0.17	0.03	0.03	0.44	0.01	0	0	0	0
BF06	93.1	16	8	6.81	0.067	3.8	5.8	568	0.1	0.17	0.03	0.04	0.37	0	0	0	0	3

4.3.2 Fumarole Gas Chemistry

The concentrations of reactive gases are also useful in estimating the temperatures of the reservoir fluids. Therefore, concentrations of major reactive gases (CO_2, H_2S, H_2 and CH_4) together with N_2 and O_2 were analysed. The results (Table 4) of the fumarole gas chemistry indicate an high atmospheric contamination, propelled by the interconnectivity of the various fissures, fractures and minor faults in the caldera or from dissolved air in shallow aquifers that might consequently upset the chemistry of the weaker fumaroles.

Table 4: Fumarole gas chemistry

				Gas concentration in mmole/kg					
Fumaroles	**Temp°C**	**Eastings**	**Northings**	**CO_2**	**H_2S**	**CH_4**	**H_2**	**O_2**	**N_2**
BF-01	96.4	232332	255904	25072	2.9	21.5	0	1444	3024
BF-02	93.6	231450	255368	2496	66.4	0	0	344474	71386
BF-03	93.6	220822	255374	18871	6.8	0	0	55457	114698
BF-04	93.3	232198	257973	29074	2.1	28.8	0	6243	13434
BF-05	93.2	229074	258615	49937	14.3	0	0	12113	25128
BF-06	93.1	229440	255323	5902	1	0	0	174412	360939

A clear indication of atmospheric contamination of gases sampled is, when N_2 and O_2 gases are highly detected. Gases are often major solutes in fluids of most volcanic geothermal systems, in particular CO_2, H_2S and H_2, but in some systems, CH_4 may also be present in abundance (Arnorsson et al., 2010). CO_2 shows a considerable concentration in the range of 1% to 85% in relation to the total gases depending on degree of atmospheric contamination and entrainment. Ideally, hydrogen and methane are indicators of proximity to or strength of hydrothermal up

flows. Due to the atmospheric incursion in most of the fumarole discharge, hydrogen was not detected; however, BF-01 and BF-04 show a considerable concentration of 0.06 and 0.04% of methane, implying that they could be closer to the upflow zone of the system.

The concentrations of CO_2, H_2S and H_2 in the aquifer fluids are greatly affected by physical properties such as enhanced boiling and recharge, but are generally believed to be kept in close equilibrium with specific hydrothermal mineral assemblages. (Arnorsson et al., 1983b; D´Amore and Truesdell,1985; Arnorsson and Gunnlaugsson, 1985; Karingithi et al., 2010). This indicates that the activity of dissolved gases such as CO_2 is controlled by a close approach to equilibrium with specific mineral buffers, at least prior to utilization. At temperatures above 230°C, epidote + prehnite + calcite + quartz hydrothermal mineral assemblages are considered to buffer CO_2.

The equilibrium reaction is:

$$2Ca_2Al_3Si_3O_{12}(OH) + 2\,CaCO_3 + 3SiO_2 + 2\,H_2O \leftrightarrow 3\,Ca_2Al_2Si_3O_{10}(OH)_2 + 2CO_2, aq \quad (33)$$

The mineral assemblage pyrite–pyrrhotite–magnetite controls aquifer water H_2S and H_2 concentrations.

Steam discharge chemistry can thus be used to deduce which fumarole is closest to the upflow zone and to select suitable drilling sites. Gas is lost from the deep fluid on boiling; the more the fluid migrates, the greater the amount of near-surface boiling and hence the lower the gas content of the steam. Further, ammonia, hydrogen and hydrogen sulphide are removed from steam by such processes as wall rock reactions and solution into steam condensate. The further steam travels from the reservoir, the lower the absolute gas concentrations and the greater the CO_2/H_2S, CO_2/NH_3 and CO_2/H_2 ratios. These are likely to be closest to the underlying hot water source (Nicholson, 1993). The low CO_2/H_2S of Kakorinya fumaroles BF-01 and BF-04 indicate that the two fumaroles are closer to an upflow than the other fumaroles.

4.3.3 CH_4-CO_2-H_2S Ternary Diagram

The CH_4-CO_2-H_2S ternary diagram (Figure 9) is useful for examining the process of degassing of a shallow thermal aquifer. The left side of the ternary shows a CO_2-CH_4 geothermometer grid, assuming a R_H (redox potential) expressed as (log fugacity (H_2)/fugacity (H_2O)) for the system (Powell and Cumming, 2010; Powell 2000; Giggenbach, 1991b). A specific redox potential (-2.8) of a hot spring/fumarole environment, has been proposed by Giggenbach and Goguel (1989) as representative of most volcanic-hosted geothermal systems, and was applied to the BVC. The BVC fumaroles (BF-01 and BF-04) plot on the left side on the CO_2-CH_4 geothermometer grid along which coincides with equilibrium reservoir temperature that is >350^{o}C based on Powell (2000) gas geothermometer, this indeed is consistent with the computed gas geothermometers of TCO_2 and TCH_4/CO_2 from Arnórsson and Gunnlaugsson (1985) and Giggenbach (1991b) functions respectively (Tables 1 and 6).

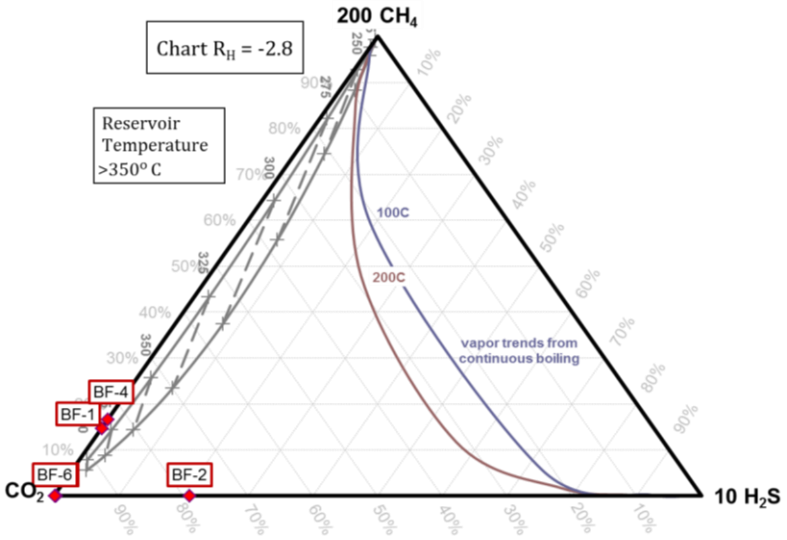

Figure 9: CH_4-CO_2-H_2S ternary diagram

4.4 Geothermometry

Many chemical and isotopic geothermometers are used to estimate the aquifer temperatures beyond the zone of secondary processes like boiling, cooling and mixing on the basic assumptions that the sampled fluids are representative of the undisturbed aquifers where local equilibrium conditions are achieved. In this project, both solute and gas geothermometers have been used to evaluate the BVC reservoir temperatures.

The geothermometer functions of Fournier and Truesdell (1973), Fournier (1977), Fournier (1979), Fournier and Potter (1982), Arnórsson et al. (1983b), Nehring and D'Amore (1984), Arnórsson and Gunnlaugsson (1985), Giggenbach et al. (1988) , Giggenbach (1988), Arnórsson et al.(1988), Giggenbach (1991), Arnórsson et al. (1998), and Gunnarsson & Arnórsson (2000), were used to compute equilibrium temperatures (Table 1). The temperatures derived from these functions were subsequently used to construct isotherm for the conceptual model as discussed by Oyuntsetseg (2009).

4.4.1 Solute Geothermometers

The quartz geothermometer is dependent on the experimentally determined solubility of different silica species in water as a function of temperature.

The basic reaction for the dissolution of silica mineral is shown in the equation below:

$$SiO_{2,\,s} + 2H_2O_l \rightarrow H_4SiO_{4,\,aq} \qquad (34)$$

The Na/K ratio is based on temperature dependent cation equilibrium reactions between Na – feldspar (albite) and K - feldspars (microcline). This forms the basis of the sodium potassium geothermometer.

$$K^+ + \text{Na-feldspar} = \text{K-feldspar} + Na^+ \quad (35)$$

Table 5: Quartz and Na/K geothermometer

Barrier Logipi Springs	Samp. Temp (°C)	Tqtz[a]	Tqt$_z$[b]	Tqtz[c]	Tqtz[d]	TChal[e]	TNa/K[f]	TNa/K[g]	TNa/K[h]	TNa-K-Ca[i]	TK/Mg[j]
BF-1	63	109	95	95	109	80	128	110	142	178	
BF-2	65	99	84	84	100	70	124	107	139	174	
BF-3	54	101	87	87	102	72	130	113	145	180	262
BF-4	70	124	111	111	121	95	134	116	148	185	
BF-5	54	119	105	106	117	90	119	103	134	160	195
BF-6	70	131	118	118	127	102	124	107	138		
BF-7	61	144	132	132	138	115	132	114	146	189	276
	Average	**118**	**105**	**105**	**116**	**89**	**127**	**110**	**142**	**178**	**244**

The solute geothermometer results (Table 5) show the computed average quartz equilibrium temperatures range between 109-118°C while computed average Na/K equilibrium temperatures range between 127-142°C while chalcedony, K/Mg and Na-K-Ca computed average equilibrium temperature of 89, 178 and 244°C respectively. Calculated Na/K geothermometers temperatures are slightly higher than the quartz geothermometers.

Apparently, it is worth noting that, the poor performance of the Na-K geothermometer functions with the Cl-rich liquids from the Menengai geothermal system, like BVC geothermal system could be explained assuming that these aqueous solutions attain equilibrium with Na- and K-bearing secondary solid phases other than feldspars. Possible candidates are hydrothermal micas (e.g., Fournier, 1991), i.e., muscovite [$KAl_3Si_3O_{10}(OH)_2$] and paragonite [$NaAl_3Si_3O_{10(}OH)_2$]. If so, the exchange reaction controlling the Na/K ratio would be (ELC, 2013):

$$\text{Paragonite} + K^+ = \text{Muscovite} + Na^+. \quad (36)$$

Generally, the solute geothermometers indicate, that the fluids are derived from the shallow aquifer of the reservoir, which has temperature in the order of 90-240°C.

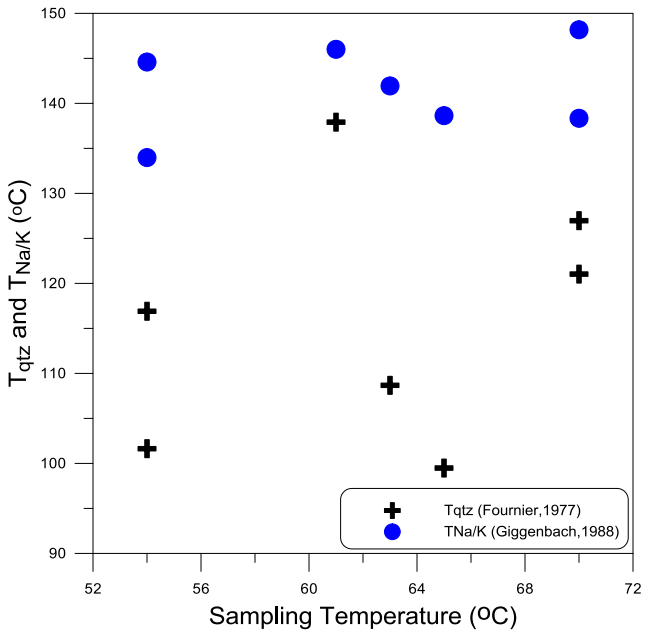

Figure 10: Quartz and Na/K geothermometers

The correlation between the Na/K and quartz geothermometers is invariably representative when considering errors, including contribution of fluids from two or more aquifers, which could be the case for the BVC fluids.

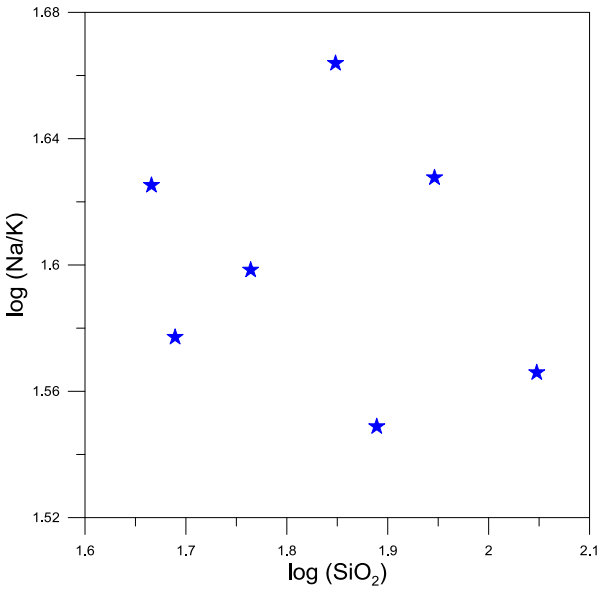

Figure 11: log Na/K vs. log SiO_2

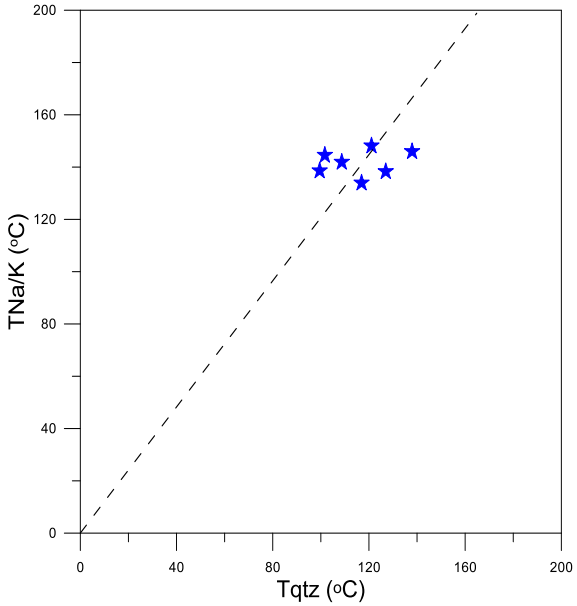

Figure 12: Correlation plot of TNa/K vs. Tqtz

The BVC samples are either not enriched or no magnesium was detected or measured in the samples, Dunkley et al. (1993) also reported magnesium concentrations from the springs in the order of magnitude of <0.1mg/l. However, in order to contain the problem caused by the lack of Mg data

for most BVC samples a comparison the Na-K geothermometer with the silica (quartz) geothermometer through the plot of log (Na/K) vs. log (SiO_2) and the TNa/K vs. TQtz was done (Figure 11 and 12) respectively. The greater spread of points in the (Figure 11), is due to variations in silica concentrations and this is registered in the wide range in the subsequent computed quartz temperatures.

4.4.2 Na-K/Mg-Ca and K/Mg vs. K/Ca Diagram

The Giggenbach and Goguel (1989) Na-K/Mg-Ca diagram (Figure 13) is a geoindicator plot that is viewed as an elaboration of the Na-K-Mg plot (Figure 8). It juxtaposes the Na-K geothermometer with equilibration of the system Mg-Ca. Its most widespread application is the determination of the influence of shallow, low temperature processes, which have particular influence on the apparent Mg-Ca equilibrium (EGS, 2010; Powell and Cumming, 2010). The K/Na ratio of Logipi thermal springs show a consistency of 0.02 and 0.03. The Na-K/Mg-Ca for BVC hot springs illustrates that, by vertical projection on the diagram's equilibrium line, the springs were exposed to temperatures in the range of 140-160°C which indeed coincides with Na-K-Mg diagram (Figure 8). A comparative K/Mg vs. K/Ca plot (Figure 14) confirms that the BVC Na-Cl-HCO_3 hot springs are mature, since they plot above the mature line and also coincides with the Na-K-Mg. This K/Mg vs. K/Ca plot juxtaposes the potassium-magnesium geothermometer with a measure of the partial pressure of CO_2 based upon equilibrium between K-feldspar, calcite and K-mica on one side and dissolved Ca^{2+} and K^+ on the other. The purpose of this K/Mg vs. K/Ca plot is to determine the partial pressure of CO_2 at the last temperature of the water equilibration with rock, as determined by the K-Mg geothermometer. In that, values of the CO_2 partial pressure (PCO_2) assume equilibrium between calcite and the other mineral phases, PCO_2 of analyses plotting outside the "calcite formation" field can only be interpreted qualitatively. This being the case, this plot is probably limited to assessments of whether the sampled fluid is likely to be in equilibrium with calcite in the subsurface (Powell and Cumming, 2010) of which is the case for the BVC thermal fluids, that are in equilibrium with calcite or limestone. Calcite formation in the subsurface is likely to occur since this is confirmed by the low concentration of Ca in the fluids, which is likely to be used up in the formation of calcite in the subsurface, calcite formation can be adequately addressed with the mineral saturation indices. Calcium concentrations are controlled by minerals of retrograde solubility ($CaCO_3$. eg calcite; $CaSO_4$, eg.anhydrite; CaF2, fluorite) and to a lesser extent by Ca-rich aluminosilicates. Factors which affect the soluhility of these minerals will also influence the level of Ca in the geothermal fluid (Nicholson, 1993).

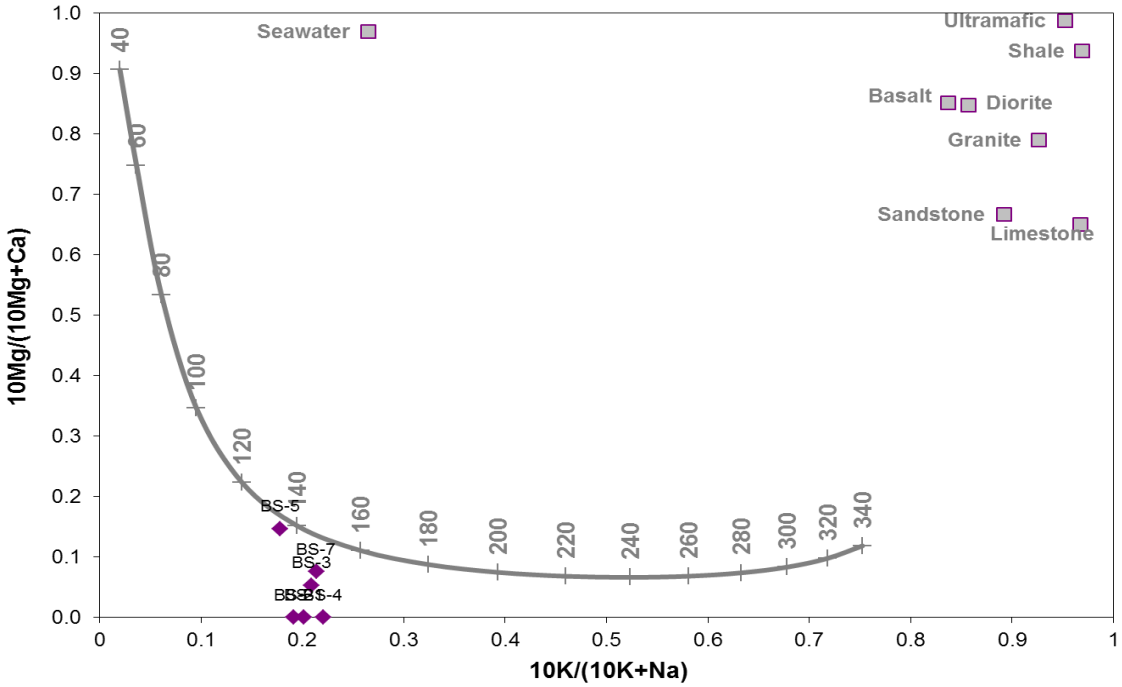

Figure 13: Na-K against Mg-Ca

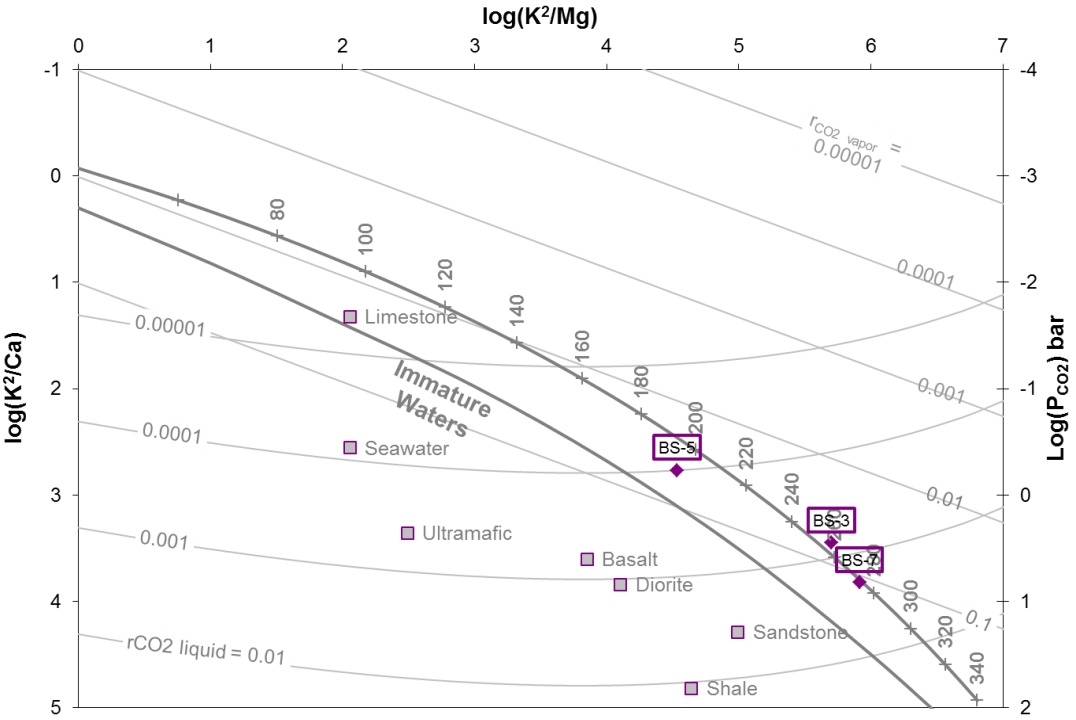

Figure 14: Comparative K/Mg vs. K/Ca geothermometer plot

PCO_2, is particularly important in this respect, and calcite often precipitates in response to a loss of CO_2 on boiling. Calcium concentrations are usually at low levels in high-temperature fluids (<50mg/kg), but increase with both acidity and salinity. The Na/Ca ratio can be used in a similar

way to the Na/K ratio, to indicate upflow zones, with the highest values indicating a more direct feed from the reservoir (Nicholson, 1993).

4.4.3 The log (K^2/Mg) vs. log (SiO_2) Plot

This cross-plot of the K-Mg geothermometer and the quartz (conductive) geothermometer (Figure 15) is from Giggenbach and Goguel (1989). This plot uses the chalcedony geothermometer, which is often more appropriate to use than quartz for water from a lower temperature source. By comparing two low temperature geothermometers, it increases confidence in both if they agree. Disagreement between these two geothermometers might be due to dilution, equilibration with amorphous silica, or perhaps some residual effect of an acid zone that invalidates the geothermometry even though the water has been neutralized (Powell and Cumming, 2010).

From the diagram of log (K_2/Mg) vs. log (SiO_2), the few BVC hot springs samples plot above the quartz solubility curve reflecting a partially equilibrated silica temperature between chalcedony and amorphous silica (EGS, 2010) . Ideally, waters that plot between the chalcedony and quartz curves suggest equilibrium with SiO_2. Quartz and chalcedony geothermometers gives temperature in the range of 105 -118 °C and average of 89 °C respectively.

However, the discrepancy in the geothermometer of Na/K, K/Mg and SiO_2 is likely to be due to:

- Incorporation of Mg in the probable precipitating calcite at the subsurface;
- The unavailability and or low concentrations of Mg
- Possible absence of K-feldspar (that would be replaced by K-mica) in some zones of the BVC geothermal reservoir which contrast with the presence of K-feldspar in the hydrothermal assemblage controlling the K-Mg geothermometer (Giggenbach, 1988)

It is pertinent to note that, the K-Mg geothermometer (Giggenbach, 1988) provides temperatures ranging from 195 and 276°C for the reservoir hot spring liquids in the BVC-Logipi. These temperature values are indeed higher than those estimated by means of silica and Na-K geothermometers (Table 5).

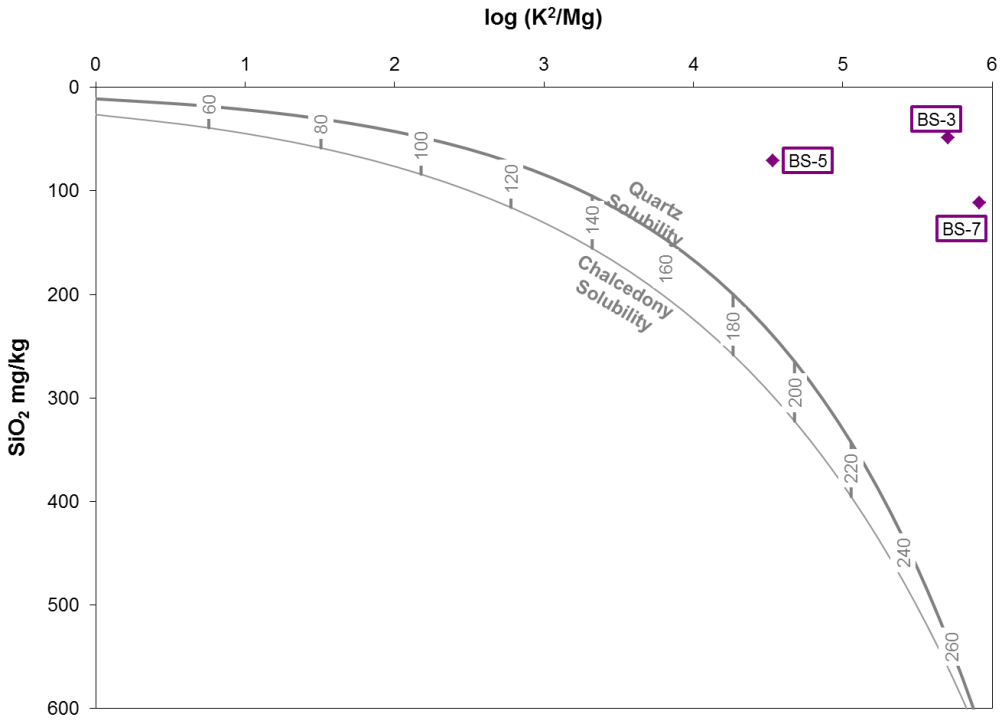

Figure 15: The log (K^2/Mg) vs. log (SiO_2) plot

4.4.4 Gas Geothermometer

Studies in many high-temperature geothermal fields (>200°C) indicate that the concentrations (or ratios) of gases like CO_2, H_2S, H_2, N_2, NH_3 and CH_4 are controlled by temperature dependent gas-gas and/or mineral-gas equilibria (Arnórsson et al., 2000; Giggenbach, 1993). On this basis, data from chemical analyses of these gases have been used to develop relationships between the relative gas concentrations and reservoir temperatures. Such relationships are known as gas or steam geothermometers.

For each chemical equilibrium considered, a thermodynamic equilibrium constant may be expressed in terms of temperature, in which case the concentration of each gas species is often represented by its partial pressure in the vapor phase (Giggenbach, 1993). Arnosson (1986) developed a method of correcting for the effect of steam condensation in the upflow below fumaroles on the results of those gas geothermometers that are based on gas concentrations in steam. Geothermometers based on gas ratios are not affected by steam condensation. For this reason it is advantageous to use gas ratios.

Table 6: Gas geothermometers

Kakorinya Fumaroles	Samp. Temp (°C)	TCO_2^k	TH_2S^k	TH_2S^k	TH_2S^l	$TH_2S\text{-}CO_2^m$	TCH_4/CO_2^n
BF-1	96.4	>350	267	-	209	264	>350
BF-2	93.6	>350	328	292	314	338	-
BF-3	93.6	>350	284	227	236	285	-
BF-4	93.3	>350	261	-	-	256	>350
BF-5	93.2	>350	298	248	260	309	-
BF-6	93.1	>350	247	-	-	230	-
	Average	**>350**	**281**	**256**	**255**	**280**	**>350**

k*: Arnórsson and Gunnlaugsson (1985),*
l: Arnórsson et al. (1998)
m: Nehring and D'Amore (1984),
n: Giggenbach (1991)

The computed average geothermometer temperatures of TCO_2, TH_2S, TH_2S, TH_2S, $TH_2S\text{-}CO_2$ and $TCH_4\text{-}CO_2$ displayed in Table 6 are >350°C , 281°C, 256°C, 255°C, 280°C and >350°C respectively. From (Figure 17), it is indeed evident that there is a discrepancy in the high gas geothermometer temperature *vis-à-vis* the computed solute geothermometer temperatures, and indicates that two or more feed zones of significantly different temperatures feed the springs.

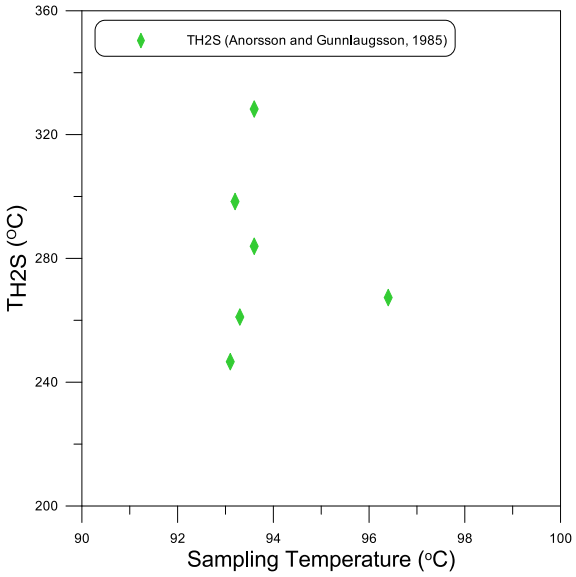

Figure 16: TH_2S against Temperature

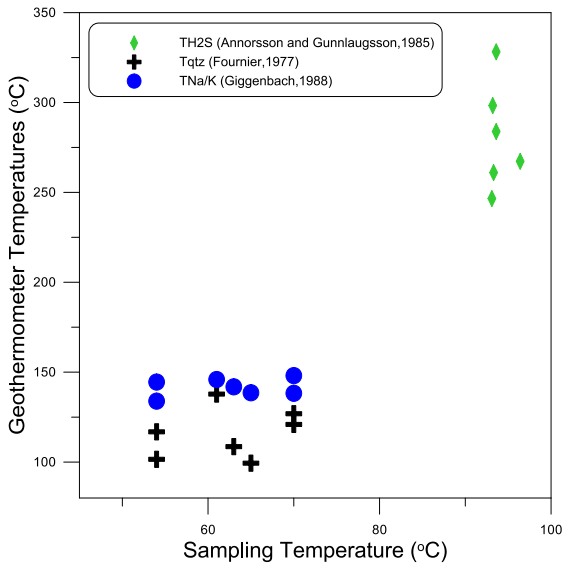

Figure 17: Comparison of the geothermometers

Apparently the gas geothermometer temperatures from the springs calculated by Dunkley et al. (1993) is in the order of magnitude of 285°C with respect to TCO_2/H_2 from the function of

Arnórsson and Gunnlaugsson (1985). Dunkley et al. (1993) computed geothermometers for Logipi hot springs is 107, 72, 61 and 285°C for TNa/K, TQtz, TChal and TCO_2/H_2 respectively. While the fumarole TCO_2 gas geothermometers give temperatures in excess of 300°C. These calculations do relate pretty well with the computed equilibrium reservoir temperatures of this project study.

4.5 Stable Isotope Characteristics

The plot of stable isotopes of oxygen ($\delta\ ^{18}O$) and hydrogen (deuterium or D, $\delta\ ^{2}H$) in relation to World Meteoric Water Line (Craig, 1961), Kenya Rift Valley Meteoric Water Line (Allen and Darling, 1987), Continental African Rain Line (Ármannsson, 1994), and Kenya Rift Valley Evaporation Line (Ármannsson, 1994) suggest the origin of the BVC hot springs waters is essentially a mixture of meteoric waters from the rift flank and Lake Turkana waters (Figure 20). Local annual means for precipitation have been established and (Craig, 1961) showed that a meteoric line describing the relationship between δ^2H and $\delta^{18}O$ applies all over the world although deviations are known and local lines have been described. However, geothermal water values suggest its origin but mixing, water-rock interaction, condensation and age may have to be accounted for (Ármannsson, 2011; Giggenbach, 1992a; Giggenbach, 1997). Oxygen and hydrogen isotopes are widely used in geothermal studies. They are extensively applied to determine the origin and history of geothermal fluids and most often serve as natural tracers for the provenance of geothermal water An important aspect of geothermal investigations is to determine the recharge to the geothermal systems that is essentially from meteoric recharge (Sekento, 2012). The $\delta\ ^{18}O$ and $\delta\ ^{2}H$ values of meteoric waters are linearly related and can be presented by equations listed in chapter one section 1.6.4 and illustrated in Figure 18.

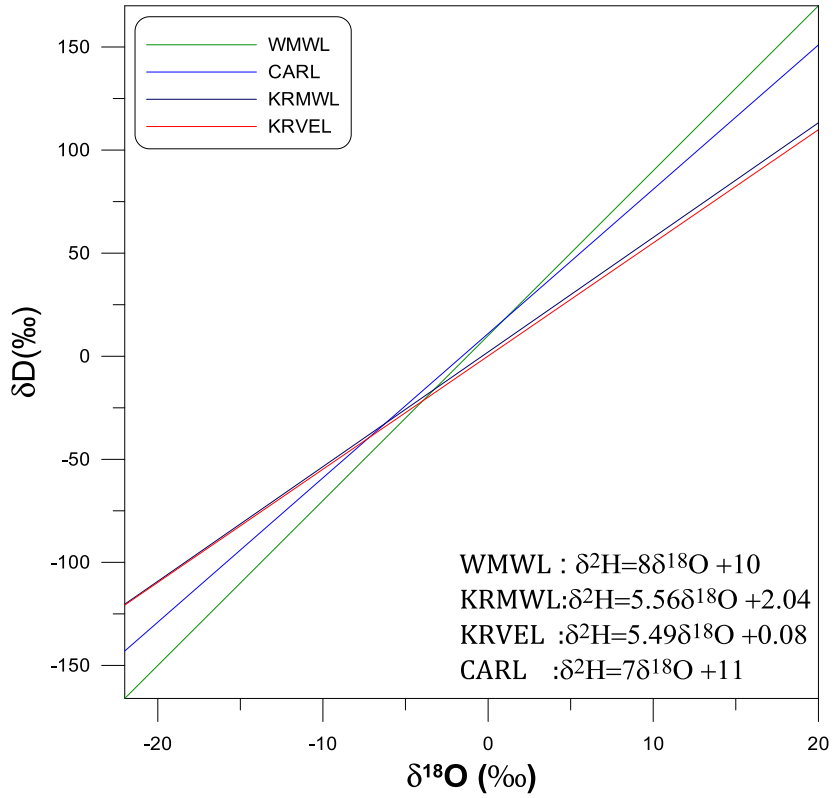

Figure 18: Correlation plot of δ ^{18}O and δ ^{2}H values of waters various water lines

4.5.1 Isotopic Analysis of Hot Thermal Waters and Lake Turkana

Isotopic analysis of Lake Turkana is highly enriched in heavy stable isotopes just like Lake Baringo waters for the purposes of comparison of the Lake waters (Figure 19). However, the Lake waters show that, they have suffered a considerable isotopic fractionation due to evaporation. According to Clarke et al. (1990), the typical rift wall water has a composition of -28‰ δ ^{2}H and -4.8‰ δ ^{18}O. The hot spring water samples range from – 1.3 to – 3.6‰ in δ^{18}O and from -5 to -18 ‰ in δ ^{2}H.

Lake Turkana and Lake Logipi waters are highly enriched with heavy stable isotopes in contrast to the spring waters owing to the great potential for evaporation (Appendix III). Isotopic analysis of the Logipi hot springs show that there is an input from the Lake Turkana and meteoric waters. The ephemeral Lake Logipi has been maintained despite the ample shrinkage experienced during periods of drought; this suggests a probable subsurface outflow from Lake Turkana beneath the Kakorinya. Ideally, from Figure 19, the Logipi springs plot along the KRMWL showing a mixture of the meteoric water and Lake Turkana waters.

Dunkley et al. (1993) isotopically computed the proportions of Lake Turkana waters in Logipi springs to be 70%, however, this may be masked by evaporative effects during recycling. While the Kakorinya fumaroles discharge have a lake water input of about 40%, this is a more likely

figure for the actual contribution. The large fractionation attributed to the steam condensation factors and experienced in weak fumaroles usually coincides with their proximity to their upflow (Darling and Armannsson, 1989, 1990).

The isotopic composition of the fumaroles indicate that the Kakorinya fumaroles discharge originate as a mixture of ground water from Lake Turkana waters and water from the rift flanks. The fumaroles that are highly depleted in the isotopes could indicate groundwater-lake water mixing and subsurface steam condensation factors. Dunkley et al. (1993) noted that, the most isotopically enriched steam is found towards the centre of Kakorinya, where the hydrothermal plume is likely to be strongest.

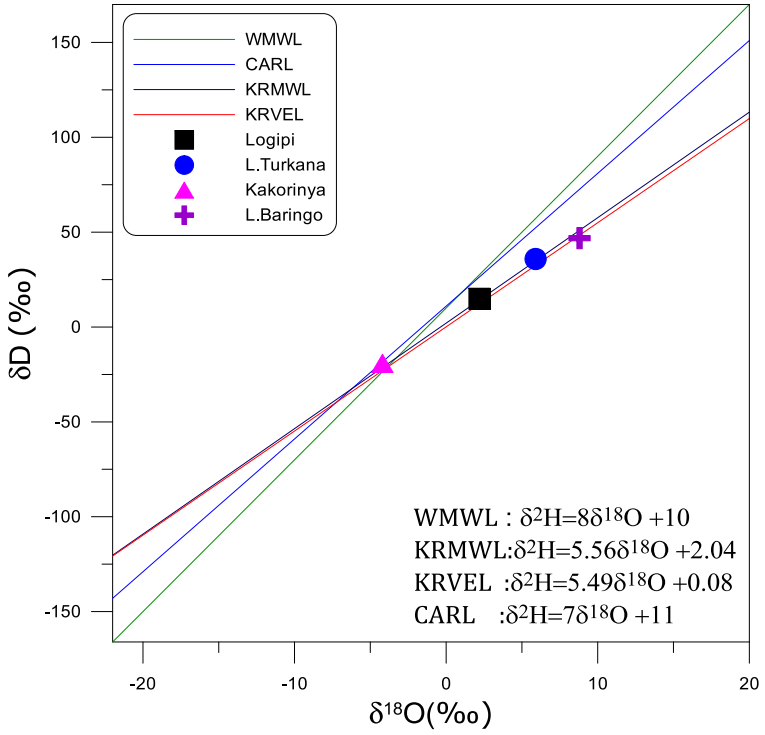

Figure 19: δ ^{18}O and δ ^{2}H characteristics of the thermal fluids of the BVC (Modified after Dunkley et al., 1993)

4.5.2 Isotopic Analysis of Ambient Waters in the Turkana

Stable isotope analysis show that the springs at Loyangalani on the south east shores of Lake Turkana, derive their water at least partly from a higher-than-local altitude, but not exclusively from Mt. Kulal, which rises to 3500m. On the other hand, the springs on the west side of the lake at Eliye springs must be derived from lower altitudes because they are relatively enriched. The well at Parkati situated at the base of the rift escarpment adjacent to the eastern end of the BVC

has a stable isotope composition that is compatible with the local recharge (Figure 20). Tum is located south of Parkati to the south of the BVC prospect. Parkati and Tum show a composition in isotope of – 3.9 and – 5.2 ‰ in $\delta^{18}O$ and -22 and -25 ‰ in $\delta^{2}H$.

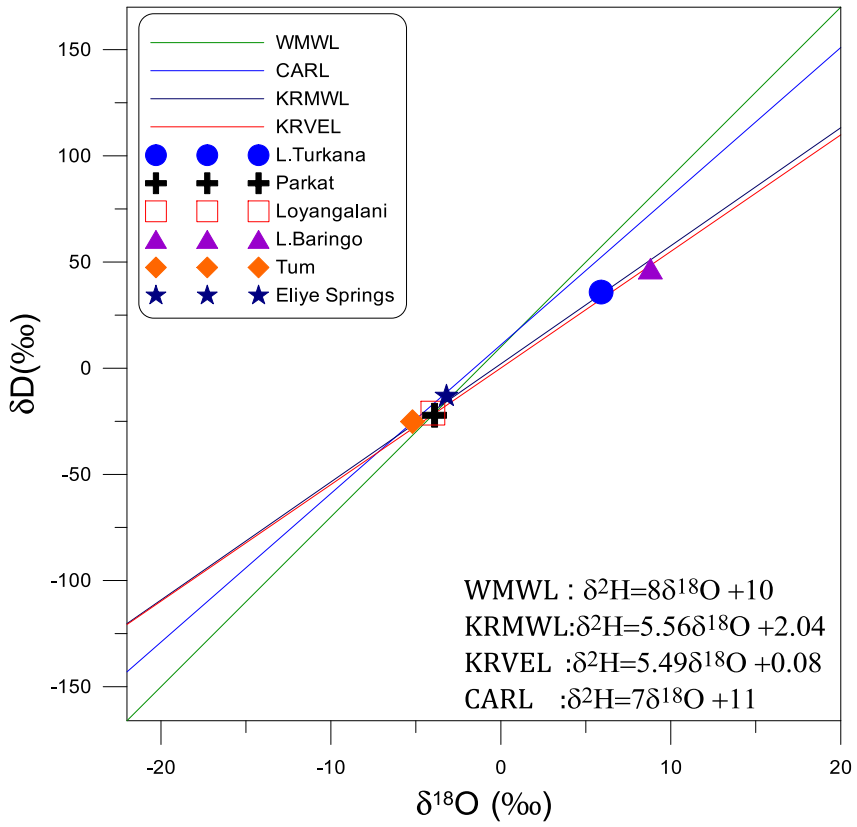

Figure 20: $\delta^{18}O$ and $\delta^{2}H$ characteristics of the cold fluids in the BVC area and Turkana (Modified after Dunkley et al., 1993)

4.6 Petrochemistry

4.6.1 Total Alkali-Silica Diagram

The analysis of whole rocks for major and trace elements is often very important in understanding the conditions under which the rocks formed, as well as their economic potential. This plot, which is useful for the classification of volcanic rocks, is also useful for distinguishing between two types of parental magmas (or of magmatic rock series or trends): alkalic and tholeiitic. Alkalic magmas are produced by partial melting at considerable depths and differentiate into a specific group of rocks, with the most differentiated ones rarely, if ever, becoming SiO_2 oversaturated. Tholeiitic magmas form at shallower depths and may differentiate to the SiO_2 oversaturated rhyolites.

Samples were classified using Le Bas et al. (1986). TAS diagram (Figure 5) illustrate the bimodal composition of the BVC rocks, which is predominantly basalts, trachytes and phonolites. The trachyte lavas of the Kakorinya and Likaiu volcanic centres define trends of increasing undersaturation towards phonolitic compositions, whereas those of Kalolenyang show a contrasting trend towards strongly silica oversaturated trachytes. On the BVC most of the basalts are porphyritic, some being strongly so, and aphyric types are uncommon. Phenocryts assemblages include plagioclase, olivine, clinopyroxene, titanomagnetite and magnetite. They are normally zoned, although reverse zoning is common, and mostly fall in the compositional range from bytownite to sodic labradorite (Dunkley et al., 1993).

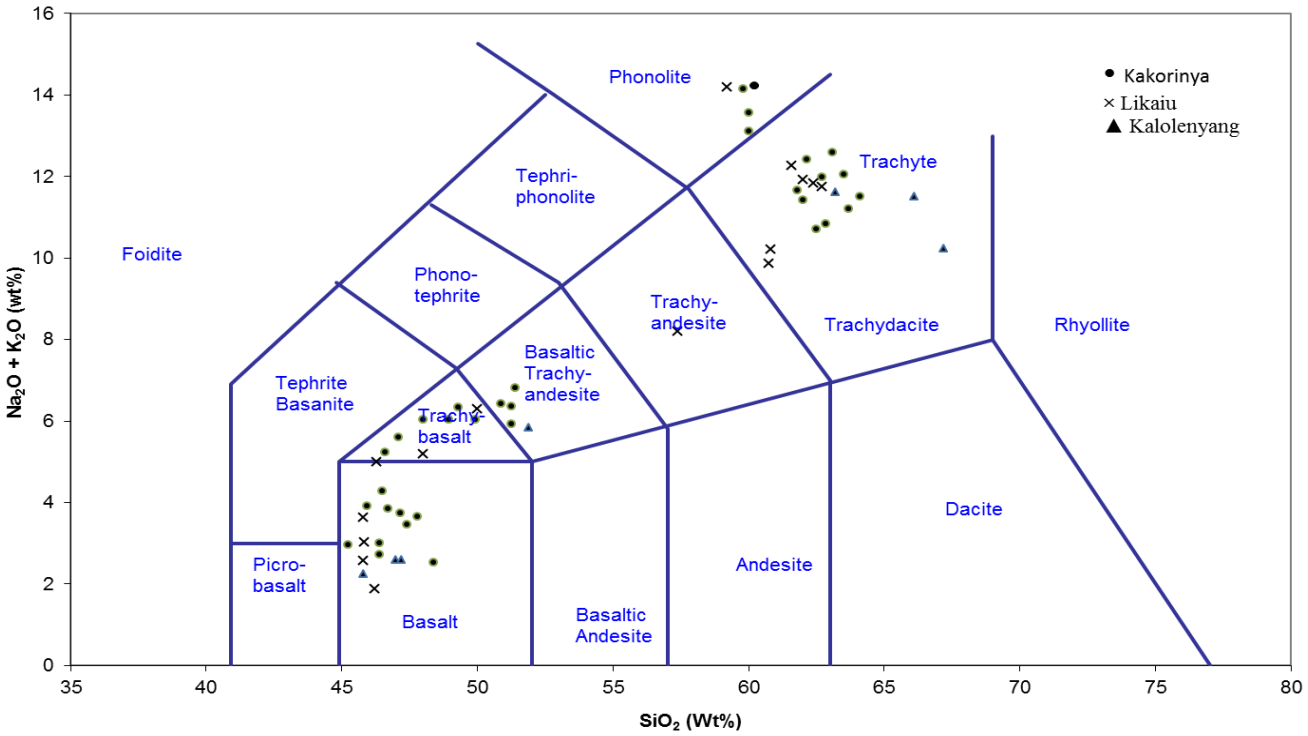

Figure 21: Total Alkali-Silica diagram for BVC rocks (modified after Le Bas et al., 1986; Dunkley et al., 1993)

4.6.2 The Relationship between Basalts, Trachytes and Phonolites

In terms of the relationship between the mixing process and the petrogenesis, the possibilities can be separated into three overlapping categories: 1) Mixing of source materials prior to the melting events that produced the basaltic magmas, e.g. interlaying of mantle-derived volcanic rocks with sedimentary rocks; (2) Contamination of mantle derived magmas by crustal materials as the magmas rise through the crust; and (3) Mixing of magmas derived from the end member sources (DePaolo, 1981; DePaolo and Wasserburg,1977).

An understanding of the relationship between basalts and trachytes is of fundamental importance, as this gives an insight into the nature of the magmatic plumbing systems within the volcanic centres of the region (Dunkley et al., 1993). Magmas in most volcanic geothermal systems are invariably believed to be the source of the heat, water and solutes of geothermal systems (Nicholson, 1993).

Linear correlations between pairs of incompatible trace elements (ITE), such as Zr and Nb, in the basalt–trachyte sequences of the rift's volcanic centres have been widely cited as evidence for derivation of the trachyte from basaltic magmas by fractional crystallization (Sceal and Weaver, 1971; Weaver et al., 1972; Weaver, 1977; Baker et al., 1977; Baker, 1987).

The rubidium-strontium (Rb-Sr) method is used to determine ages of geologic events, and it serves as a tracer of geochemical processes. Isotopic analysis provides useful information bearing on the relationship between basalts and trachytes (Norry et al., 1980). The basalts and trachytes have similar Pb and Nd isotopic compositions, which are consistent with derivation from a common source, but the trachytes have significantly higher $^{87}Sr/^{86}Sr$ than the related basalt (Figure 22). Norry et al. (1980) believed that the trachytes were derived by fractional crystallization of the basalts, but interpreted the higher Sr isotope ratios as an indication of crustal contamination within the trachytes. From Figure 22, based on the $^{87}Sr/^{86}Sr$ the Kakorinya trachytes show evidence of crustal contamination relative to the basalts, but the phonolite show no sign of contamination and have virtually identical Sr, Pb and Nd isotopic compositions to the basalts (Dunkley et al., 1993). The phonolites of Kakorinya post-date the trachytes and with respect to trace element composition are generally more fractionated (Dunkley et al., 1993). Form the petrochemisty of the rocks in the BVC, Dunkley et al. (1993) noted that high-level trachyte bodies could have formed *in-situ* by fractionation of basaltic magmas, or by the migration of trachyte from the deeper source. In either case, the high-level trachytes became crustally contaminated. In such a model, it is envisaged that phonolitic magmas from such a deeper source would have been prevented from reaching the surface because of the presence of the high-level trachyte magma bodies, which would have intercepted them.

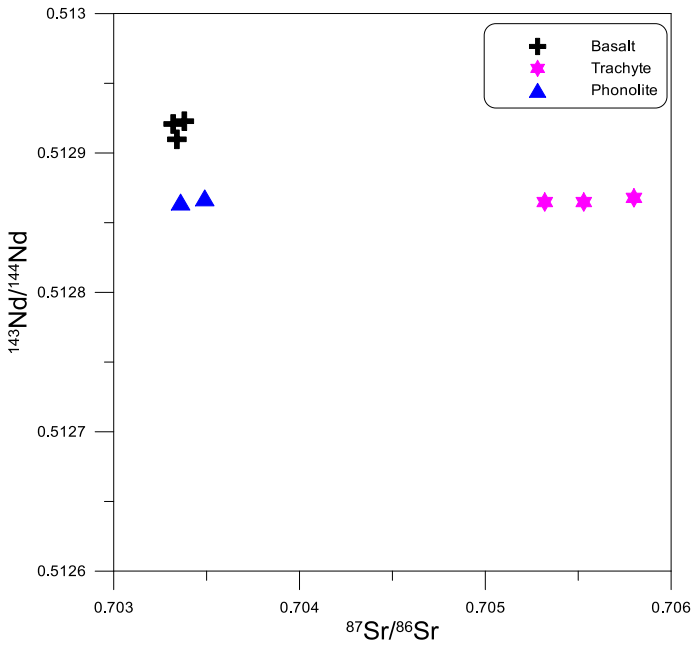

Figure 22: Plot of $^{143}Nd/^{144}Nd$ against $^{87}Sr/^{86}Sr$ for lavas in Kakorinya

Only at a late stage in the evolution of Kakorinya, after the caldera collapse and evacuation (or solidification) of the high-level trachyte chamber, was it possible for unconsolidated phonolites and basalts to rise from the deeper levels and erupt on the upper parts of the volcano (Dunkley et al., 1993).

4.7 Evaluation of Mixing Processes

4.7.1 Correlation Plots

Ideally mixing can upset the chemical equilibria between water and rock minerals causing a tendency for the water to change composition after mixing with respect to reactive chemical components. In principle, chloride plots and other binary diagrams between dissolved chemical constituents can be used to investigate the occurrence of mixing between geothermal liquids and shallow ground waters (ELC, 2013). In the correlation plot for Na vs. HCO_3 (Figure 23) Logipi spring waters, Lake Turkana waters, and local ground waters of Parkati well show a linear correlation with an exception of one sample from the Logipi springs. This is probably due to various reasons: (i) progressive acquisition of Na and HCO_3 through water rock interaction, (ii) dilution of geothermal reservoir liquids, and (iii) mixing between ground waters and lake waters.

The Lake Turkana water is slightly enriched in Na in relation to the Logipi springs (Appendix II) which is highly endowed in Na, the ground water of Parkati is considerably slightly enriched in sodium considering that it is used for drinking. The concentration of Na in Turkana waters is in the order of magnitude of 909-985mg/kg for waters adjacent to the BVC, while Logipi springs, Na is in the range of 1476 - 4712mg/kg. Where N designates, number of data points and

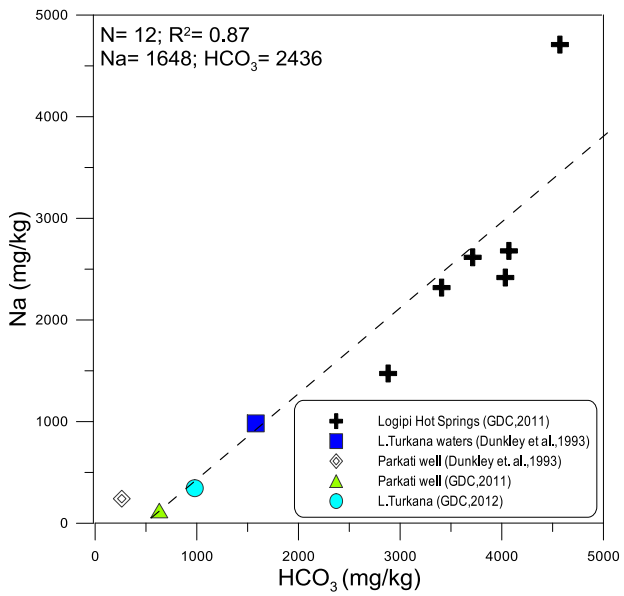

Figure 23: Correlation plot of Na and HCO_3

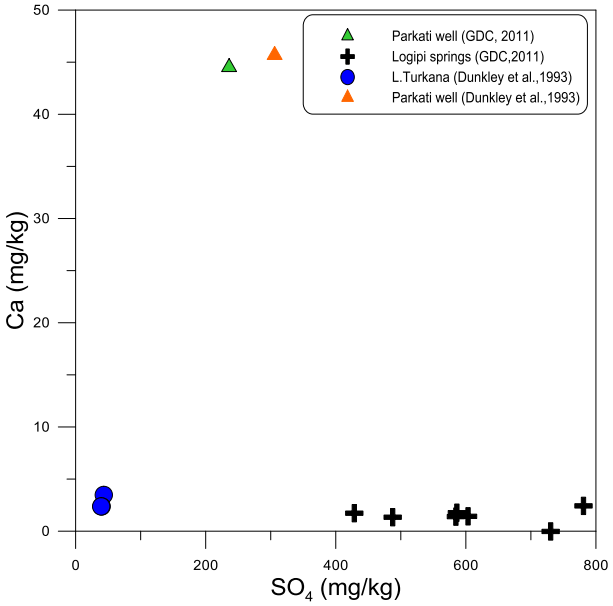

Figure 24: Correlation Plot of Ca and SO_4

R^2 designates coefficient of determination. The general enrichment of Na in the Logipi hot springs can be attributed to one of the following reasons (ELC, 2013):

a. Leaching of soluble sodium carbonates, such as Natron [$Na_2(CO_3)\cdot 10(H_2O)$], Thermonatrite [$Na_2(CO_3)\cdot(H_2O)$], Trona [$Na_3(HCO_3)(CO_3)\cdot 2(H_2O)$], and Nahcolite [$NaHCO_3$]. These typically form through evaporation of lacustrine waters in dry arid regions; this could be evidenced by the presence of "crunchy" surface along the shores the Lake Logipi due to the deposits the white Trona deposits.
b. Mixing of either ground waters or geothermal fluids with Lake Turkana waters;
c. Preferential dissolution of Na-bearing silicate and Al-silicate minerals of volcanic rocks;
d. Non-stoichiometric dissolution of Na-bearing silicate glasses (and possibly crystalline minerals) of volcanic rocks, with preferential release of Na. This seems to be the most likely one, based on the dissolution mechanism of basaltic glass (e.g., Oelkers, 2001), which comprises a sequence of metal-proton exchange reactions, involving monovalent cations first and divalent cations afterwards. These exchange reactions are followed by the partial removal of trivalent cations, whereas the liberation of partially detached Si atoms represents the final step of the dissolution process.

The correlation plot of Ca-SO_4 (Figure 24) shows the enrichment of sulphate with a slight decrease in sulphate in relation to the Lake Turkana waters. This is probably due to oxidation of H_2S to SO_4 and subsequent dissolution. The ambient temperature in Parkati well indicate the enrichment of SO_4 and a considerable concentrations of Calcium, this is most likely due to dissolution of gypsum or anhydrite by the ground waters. Since sulphate concentrations do have

an inverse relationship with temperature, then mixing of Lake Logipi hot springs waters with Lake Turkana waters and ground water is likely.

4.7.2 Evaluation of Conservative Mixing

Conservative mixing of two components requires linear relationships for every pair of species (Renaut et al., 1986; Jones and Deocampo, 2003; Deocampo, 2004a, b). Chloride, which is a conservative ion in geothermal fluids, does not take part in reactions with rocks after it has dissolved; it does not precipitate after it has dissolved and its concentration is independent of the mineral equilibria that control the concentrations of rock-forming constituents. Thus, chloride is used as a tracer in geothermal investigations. Where N designates, number of data points and R^2 designates coefficient of determination.

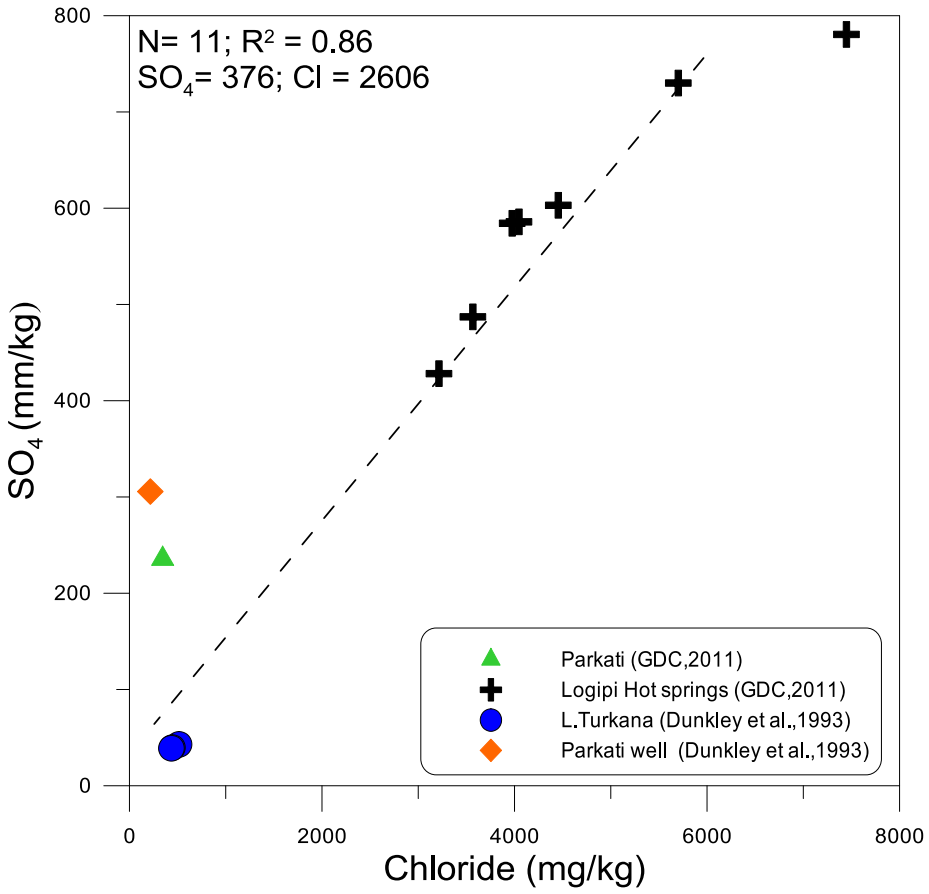

Figure 25: Correlation plot of SO_4 and Cl

Figure 25: Correlation Plot of SO_4 and Cl

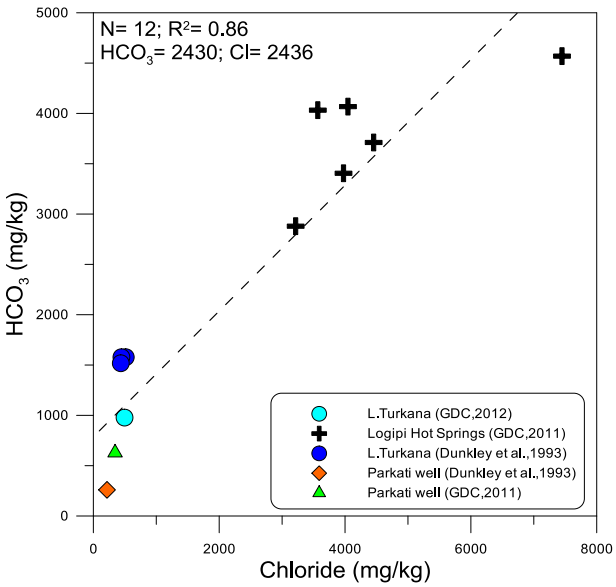

Figure 26: Correlation plot of HCO_3 against Cl

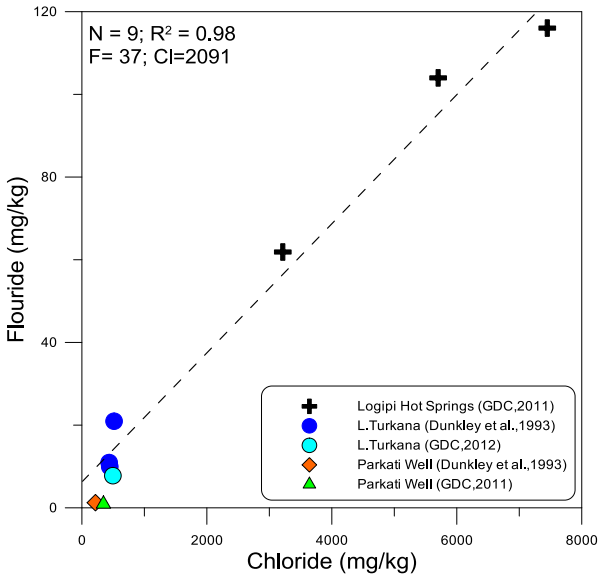

Figure 27: Correlation plot of F against Cl

Correlation plots of SO_4 against Cl, HCO_3 against Cl, and F against Cl (Figure.25, 26 and 27) show a linear correlation of the chemical species in ground water, Parkati well, Lake Turkana and Logipi hot springs. This indeed confirms a common origin of waters, where the Logipi springs show a considerable enrichment in HCO_3, SO_4 and F because of mixing of the Lake Turkana waters with geothermal fluids.

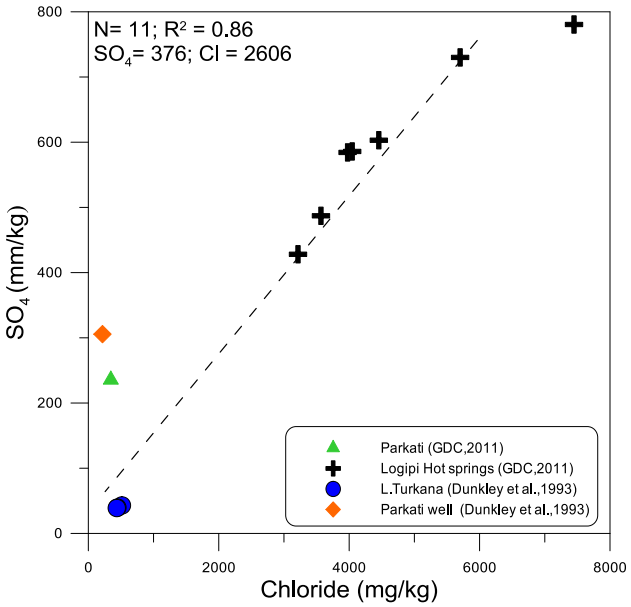

Figure 28: Correlation plot of Na against Cl

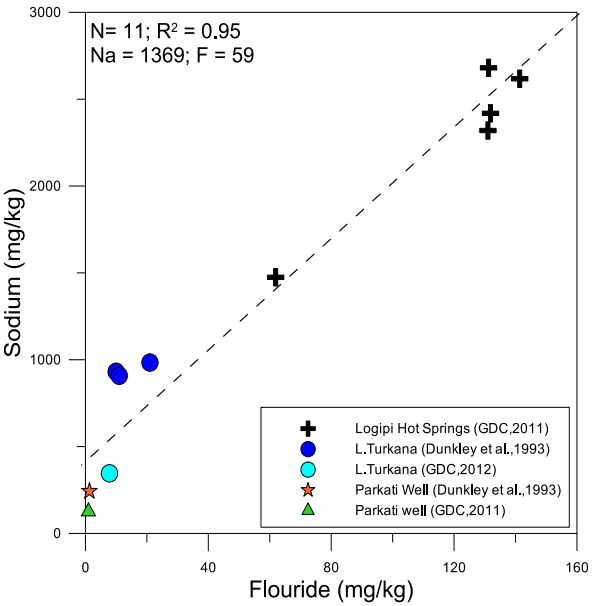

Figure 29: Correlation plot of Na against F

The correlation plots of F and Cl Na, shows a linear trend implying that F and Cl are conservative and the elements (Na, Cl and F) have a common origin, which may be dissolution and/or rock weathering, and that both accumulate predominantly in the liquid phase (Tarits et al.,

2006). It is worth noting that Na total cation concentration (Figure 28 and 29), a correlation of Na against conservative constituents, such as Cl and F display a linear relationship suggesting a common origin of the Lake Turkana waters, Parkati ground water well and Logipi hot springs. High F concentrations are often associated with low Ca levels. Unusually high F levels can be produced by the condensation of volcanic gases (HF) into meteoric waters, in this case it is invariably accompanied by very high Cl and SO_4 levels (Nicholson, 1993).

4.7.3 Silica-Enthalpy Mixing Model

The silica-enthalpy mixing model was also used to detect possible mixing trends. Truesdell and Fournier (1977) proposed a plot of dissolved silica versus enthalpy of natural waters to estimate temperatures of the deep hot water component. This mixing model handles boiled and non-boiled waters separately in that it distinguishes the waters that have boiled before mixing where the boiled waters have low gas and relatively high pH (>8), while the non-boiled waters are gaseous and have relatively low pH (<7-8) (Arnórsson et al, 2000; Oyuntsetseg, 2009). This indicates mixing of boiled water with non-boiled waters therefore removal of silica from solution giving low temperatures (indicated by the low enthalpy). Conductive cooling of the water before or after mixing might also lead to the low enthalpies reflecting low temperatures. From the silica-enthalpy plot (Figure 11), if mixing occurs after boiling and as considered for the BVC, then extrapolating the best-fit lines through the hot spring samples indicates enthalpy of approximately 600kJ/kg for the hot water component. This translates to temperatures of 142.5°C.

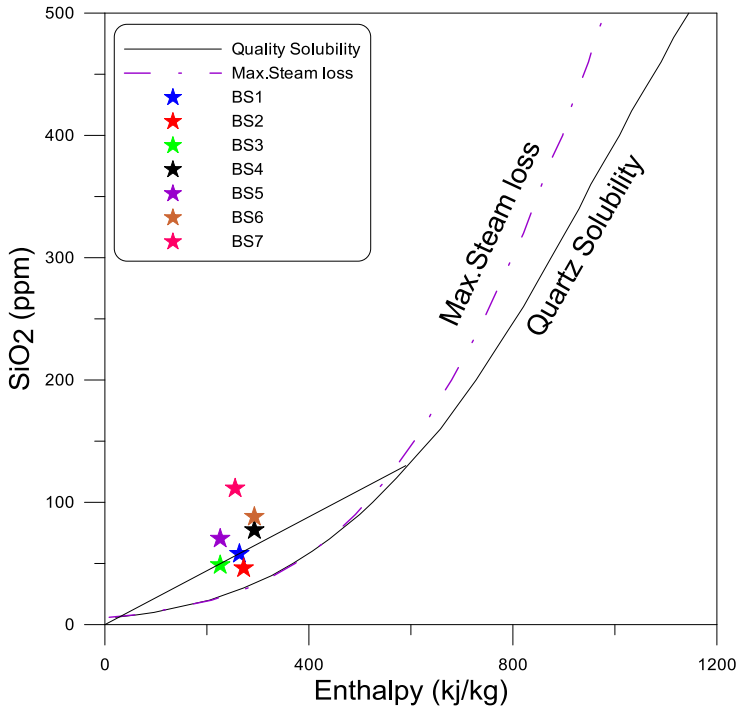

Figure 30: Silica Enthalpy Mixing Model

CHAPTER FIVE

5.1 **Discussion**

The Logipi thermal springs discharge waters of Na-Cl-HCO_3 facies suggesting peripheral waters. According to Giggenbach (1991), the Cl-rich waters are found near the upflow zones of geothermal systems. A hot spring with significant chloride, moderate bicarbonate and minimal sulfate is consistent with outflow from a geothermal reservoir. Based on the Na-K-Mg plot, the waters are fully equilibrated and have attained equilibrium with minerals and are ultimately suitable for ionic solute geothermometry.

It is generally assumed that lower pH and solute content of fumarole steam condensates indicates less interference by shallow ground waters. This relationship is indeed an indication of the strength of the steam flows, with weaker fumaroles being more susceptible to dilution and condensation. It is usually common that most chemical analysis of fumarole discharge, usually have low concentrations of the partitioning chemical parameters analysed as exemplified by the Kakorinya fumaroles steam condensate. However, with reference to the TDS for the Kakorinya fumaroles, the order from low to highest concentration is, BF-04, BF-01, BF-06, BF-02, BF-03 and BF-05 this implies that BF-03 and BF-05 are the weakest fumaroles while BF-04 and BF-01 are the strongest discharging fumaroles. The fumarole gas chemistry indicate an immense atmospheric contamination, propelled by the interconnectivity of the various fissures, fractures and minor faults in the caldera or from dissolved air in shallow aquifers, that might consequently upset the chemistry of the weaker fumaroles. Ideally, hydrogen and methane are indicators of proximity to or strength of hydrothermal up flows. Due to the atmospheric incursion in most of the fumarole discharge, hydrogen was not detected; however, BF-01 and BF-04 show a considerable concentration of 0.06 and 0.04% of methane, implying that they could be closer to the upflow zone of the system. CO_2 show a considerable concentration in the range of 1% to 85% depending on degree of atmospheric contamination and entrainment.

The gas geothemometer functions of TCO_2, TH_2S^a, TH_2S^b, TH_2S-CO_2 and TCH_4-CO_2 estimated average equilibrium reservoir temperatures of >350°C , 281°C, 256°C, 280°C and >350°C respectively. The computed average reservoir temperatures are 127-142°C, 178°C, 244°C for Na/K, K/Mg, Na-K-Ca respectively, while quartz and chalcedony give average temperatures of 109-118°C and 89°C. Gas geothermometers of the hot springs computed by Dunkley et al. (1993) estimated the reservoir temperature to be 285°C. It is indeed evident that there is a discrepancy between the high gas geothermometer temperature vis-à-vis the computed solute or water geothermometer temperatures indicating that the springs are fed by more than one aquifer of significantly different temperatures.

Lake Turkana and Lake Logipi waters are highly enriched in heavy stable isotopes of $\delta^{18}O$ and $\delta^{2}H$ in contrast to the spring waters owing to the great potential for evaporation. Isotopic analysis of the Logipi hot springs show that there is a major derivative recharge from the Lake waters and

ample contribution from rift margin meteoric waters. On the other hand, the of $\delta^{18}O$ and $\delta^{2}H$ composition of the fumaroles indicate that the Kakorinya fumaroles discharge originate as an mixture of ground water from Lake Turkana waters and water from the rift flanks. The fumaroles are highly depleted in the heavy isotopes indicative of groundwater-lake water mixing and subsurface steam condensation factors.

The major lithofacies in the BVC include trachytes, basalts and phonolites based on the modal composition according to the TAS diagram (Figure 22), however, there are pockets of basanite, hawaiite, mugearite and benmorite, which are fractionated forms of basalt. The occurrence of the Kakorinya caldera and various volcanic centres implies that there is a magmatic heat source in the BVC. The BVC radiometric isotopic data of Nd and Sr as well as ITE indicate that the young resurgent phonolites and basaltic rocks in the caldera must have fractionated in a separate magma chamber from the trachytes and erupted episodically after the caldera collapse presumably after the trachyte had solidified (Dunkley et al., 1993). As far as the geometry of the heat source is concerned, Gichira et al. (2011) reported from the resistivity structure of the BVC that, the reservoir zone of the BVC in a NS direction marked by intermediate resistivity in the central part of the profile, starting from 1000 mbsl to 3000 mbsl due to hydrothermal activity. The heat source occurs at depths starting from 4000mbsl indicated by the highly conductive body.

The silica-enthalpy mixing model handles non-boiled and boiled mixed waters separately with mixing occurring after boiling. The figure denotes that the BVC springs mixed after boiling with enthalpy of 600kJ/kg for the hot water component, which translates, to 142.5°C. Conductive cooling of the water before or after mixing might be the reason for the low enthalpies reflecting low temperatures.

In principle, conservative mixing of two components requires linear relationships for every pair of species. Chloride, Fluoride plots and other binary diagrams between dissolved chemical constituents can be used to investigate the occurrence of mixing between geothermal liquids and shallow ground water and other water bodies. The correlation plots of F and Cl, Na, shows a linear trend implying that F and Cl are conservative and the elements (Na, Cl and F) have a common origin, which may be dissolution and/or rock weathering, and that both accumulate predominantly in the liquid phase. The correlation plots Na-F, F-Cl, Na-Cl display a liner relationship between Logipi thermal springs, ground water of Parkati well and Lake Turkana waters. Na vs. HCO_3 correlation plot of the Parkati well, Lake Turkana, Logipi thermal springs also show a linear relationship, which implies a possible mixing of these water facies. The correlation could also be attributed to leaching of soluble sodium carbonates, such as natron [$Na_2(CO_3)\cdot 10(H_2O)$], thermonatrite [$Na_2(CO_3)\cdot(H_2O)$], trona [$Na_3(HCO_3)(CO_3)\cdot 2(H_2O)$], and nahcolite [$NaHCO_3$]. These typically form through evaporation of lacustrine waters in dry arid regions, which is characteristically discernible along the shores of Lake Logipi where the springs are located.

This study has mainly focused on evaluation of the hydrogeochemical facies of the thermal fluids in the BVC with the interest of developing a conceptual model. It is invariably inherent to develop a conceptual model with an aim of clearly defining, and understanding the nature and characteristics of the geothermal system towards a successful exploration, development, utilization and optimization of geothermal resource. In essence, this project objectively elucidates the classical geochemical characteristics of the fluids in order to delineate the direction of fluid flow and circulation (e.g. hot upflow, outflow and colder recharge) symbolized with arrows. The conceptual model reservoir was delineated using the isotherms based on the computed equilibrium reservoir temperatures from the temperature dependent chemical species of the thermal fluids, as well as defining the direction of the fluids in the upflow and the outflow, and evaluating the origin and mixing of the water facies in the BVC**.**

The three main areas exhibiting geothermal activity in the BVC are mainly, Kakorinya caldera, the flanks and summit area outside the caldera, and Lake Logipi hot springs. Ideally geothermal manifestation in the BVC occur in the form of fumaroles, hot springs and argillic alteration with deposition of alunite, kaolinite, and other clay minerals that affects the hydrothermally altered rocks outcropping in and nearby the area of fumarolic activity in the caldera and its summit. A past existence of thermal springs is confirmed by the presence of silica sinters in the caldera. All these surface manifestations strongly suggest that a long-established geothermal system is present in the BVC and most potentially in the Kakorinya caldera.

5.2 Conceptual model

The presence of a possible heat source, reservoir and a cap rock is an indication that there is a viable geothermal resource in the BVC. A cross-section from the north around Lake Turkana towards Lake Logipi to the south and cutting across the Kakorinya (Figure 31) was used to define the conceptual model of the BVC based on the fluids analysed in the respective areas (Figure 32). The heat source is mainly magmatic. The gases released from the degassing magma batch enter the overlying hydrothermal aquifer from below, thus supplying both heat and chemical substances to it, including H_2O, CO_2, SO_2, H_2S, HCl, HF, etc. The magmatic contribution decreases further and the lake water contribution increases correspondingly moving towards the peripheral parts of the hydrothermal caldera area. Essentially hydrogeochemical characteristics indicate that there is an upflow to the Kakorinya caldera as indicated in the chemistry of the fumaroles. Generally, high temperature condensed geothermal fluids that had boiled at depth and enriched in H_2S, H_2O and CO_2 flow upwards below Kakorinya caldera, the summit and its flanks although suffering atmospheric incursion during the ascent and eventually starts boiling at depth. Below the Kakorinya caldera area, these deep hydrothermal liquids rise up towards the surface, along fractures and faults, experience heat loss through conduction. The ascending deep fluids boil and the vapours discharge at the surface after experiencing either negligible condensation or significant condensation (as in the case of Kakorinya fumaroles).

There is lateral outflow of fluids towards Logipi springs, which is essentially Na-Cl-HCO_3 facies that is diluted and neutralized by ground water. Temperatures towards the outflow is likely to be low due to mixing and cooling from cold groundwater along open fractures within a probable fissure swarm that is channeling the lateral flow. The study of the stable isotopes of $\delta^{18}O$ and $\delta^{2}H$ indicate that thermal waters in the BVC show a derivative recharge from Lake Turkana and meteoric waters from the rift flanks.

Gas geothermometry indicate equilibrium reservoir temperatures in excess of 300°C and some give an average of 250°C outlined by the isotherms as a probable indication of a vapour-dominated aquifer. On the other hand, water geothermometry estimate equilibrium reservoir temperature of atmost 200°C as also outlined by the isotherm this is deemed to probably indicate a water dominated aquifer. Therefore a well drilled in the BVC geothermal system will likely to be fed by multiple aquifers of varying temperatures.

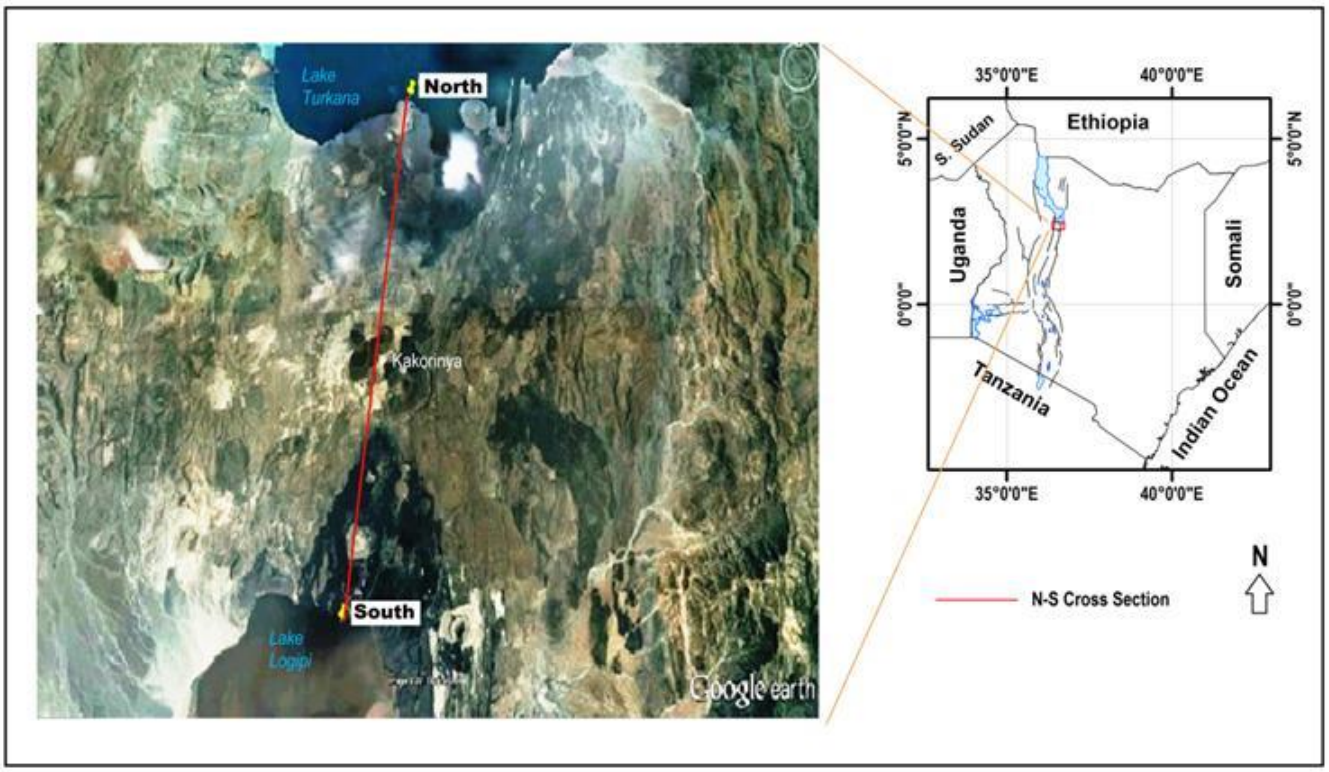

Figure 31: Cross-section from North to South of the BVC

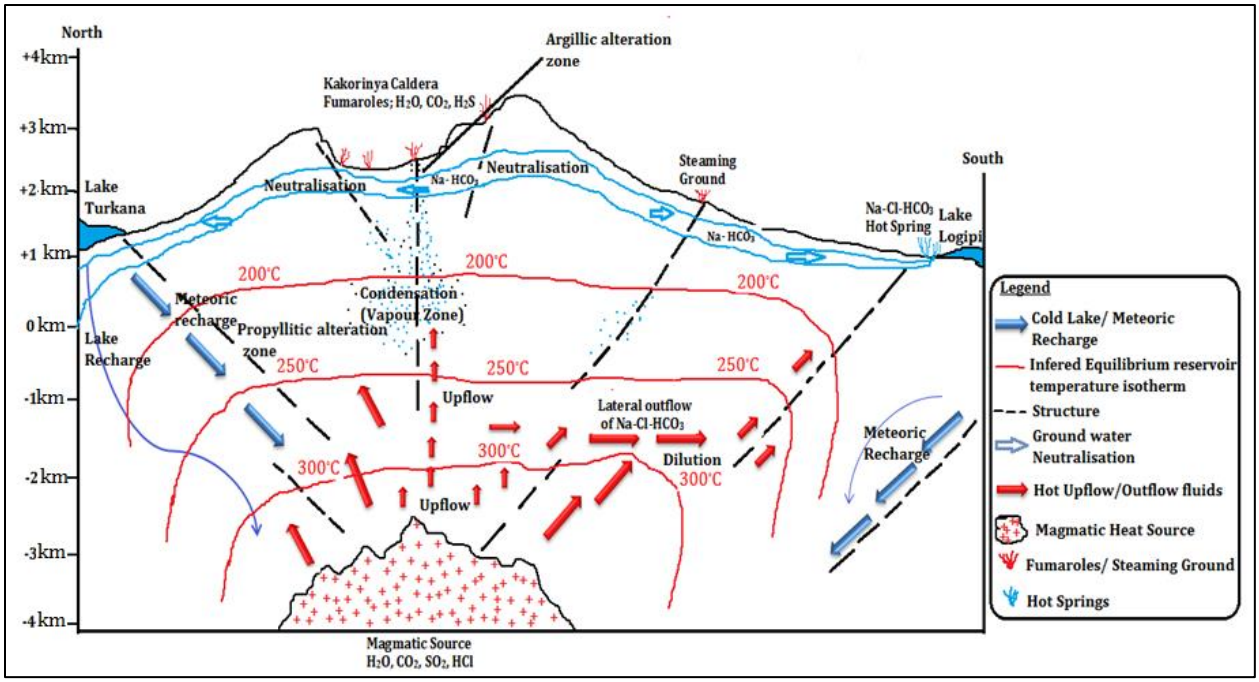

Figure 32: The conceptual model of the BVC geothermal prospect

There occurs an argillic hydrothermal alteration with deposition of alunite, kaolinite, and other clay minerals (stable at temperature range of 50-120°C; Barrios et al., 2013) that affects the hydrothermally altered rocks outcropping in and nearby the areas of fumarolic activity in the caldera and its summit. The propyllitic alteration zone at depth is expected to be the zone of hydrothermal minerals that are stable at temperatures above 250°C such as; epidote, illite, quartz, prehnite, wairakite, chlorite, anhydrite, sphene, actinolite, scapolite, brucite, stilpnomelane, pyrite, arsenopyrite e.t.c (Reyes, 1990; Barrios et al., 2013; Ambrosio et al., 2010).

CHAPTER SIX

6.1 Conclusions

- The Logipi springs discharge waters of Na-Cl-HCO_3 facies. The fumaroles discharge steam whose condensate TDS suggest that BF-01 and BF-04 are the strongest and could suggest a proximity to the upflow zone, which is also confirmed by the gas chemistry.

- The computed equilibrium reservoir temperature of the BVC based on gas geothermometer indicates temperatures above 280^{o}C but this could be representing the vapour-dominated aquifer at greater depths of the reservoir. An average of the water geothermometer of TNa-K-Ca and TK/Mg gives temperatures in the order of 200^{o}C, this could be representing the water dominated incipient part of the reservoir.

- The study of composition of the stable isotopes of $\delta^{18}O$ and $\delta^{2}H$ in the BVC thermal fluids indicate an meteoric origin with a mixture from Lake Turkana waters. The ephemeral Lake Logipi has been maintained despite the ample shrinkage experienced during periods of drought; this suggests a probable subsurface outflow from Lake Turkana beneath the Kakorinya.

- The BVC radiometric isotopic data of Nd and Sr as well as ITE indicate that the young resurgent phonolites and basaltic rocks in the caldera must have fractionated in a separate magma chamber from the trachytes and erupted episodically after the caldera collapse presumably right after the trachyte had solidified. Based on the $^{87}Sr/^{86}Sr$ the Kakorinya trachytes show evidence of crustal contamination relative to the basalts, but the phonolite show no sign of contamination.

- The correlation plots of the conservative constituents and Na-HCO_3 correlation plot display a linear relationship hence confirming mixing between Lake Turkana waters, Lake Logipi thermal springs waters and ground water of Parkati well. On the other hand, the silica-enthalpy mixing model, which handles non-boiled and boiled mixed waters separately, indicates mixing after boiling in the Logipi springs, with an enthalpy of 600 kJ/kg for the hot water component that translates to 142.5°C.

- A high temperature and viable geothermal resource exists in the BVC with an estimated equilibrium reservoir temperature of above 280°C.

6.2 Recommendations

- It is pertinent to carry out further geochemical work involving soils gas diffuse measurements (e.g., Radon, Carbon dioxide, helium) in order to demarcate areas of permeability with the aim of understanding the characteristics of the geothermal system, thus refining the model.

- Geophysical survey that includes gravity and magnetics should be carried out with an aim of clearly defining the geometry of the heat source and the reservoir.

- Resistivity (MT and TEM) sounding of the BVC with a minimal spacing should be carried out in order to mirror the resistivity structure of the prospect and ultimately demarcate the most viable areas and subsequently the geometry of the cap rock, heat source and the reservoir

- Drilling should be done in Kakorinya caldera, preferably areas around the fumarole BF-01 and BF-04, that is likely to be viable, in order to validate the model and prove the existence of the resource.

- Mineral saturation indices in the BVC fluids should be determined, in order to confirm the calcite saturation, hence proper measures (e.g., use of antiscalants and calcite inhibitor, work over drilling, acidification e.t.c.,) should be taken to mitigate the calcite scaling that is likely to cause problems during production.

REFERENCES

Allen, D.J., and Darling, W.G., 1987: *Kenya Rift Valley geothermal project: Interpretation of fluid sample analyses from Magadi-Silali area.* British Geological Survey, Wallingford, U.K., 26 pp.

Ambrosio, M., Doveri, M., Fagioli, M. T., Marini, L., Principe, C., Raco, B., 2010*: Water–rock interaction in the magmatic-hydrothermal system of Nisyros Island (Greece)*, J. Volcanol. Geotherm. Res. doi:10.1016/j.jvolgeores.2010.02.005

Arkansan, H, and Fridriksson, T., 2009:.*Application of geochemical methods in geochemical exploration,* Short course on surface exploration for geothermal resources, UNU-GTP and LaGeo, El Salvador 17-30

Ármannsson, H. and Ólafsson, M. 2006: *Collection of geothermal fluids for chemical analysis.* ÍSOR,Reykjavík, report ÍSOR-2006/016, 17 pp.

Ármannsson, H. and Ólafsson, M. 2007: *Geothermal sampling and analysis. Presented at the Short Course II on "Surface Exploration for Geothermal Resources",* organized by UNU-GTP and KenGen, at Lake Naivasha, Kenya, 2-17 November.

Ármannsson, H., 1987: *Studies of the geochemistry of steam in the Suswa and Longonot areas and the water in the Lake Magadi, Kedong Valley and Lake Turkana areas, Rift Valley ,Kenya.* Final Technical Report. Project KEN/82/002.United Nations Department of Technical cooperation for development.

Ármannsson, H., 2011: *Application of geochemical methods in geothermal exploration.* Paper presented at "Short Course VI on Surface Exploration for Geothermal Resources", organized by UNU-GTP, GDC and KenGen, at Lake Naivasha, Kenya, 8 pp.

Ármannsson, H., 1994: *Geothermal studies on three geothermal areas in West and Southwest Uganda.* UNDESD, UNDP project UGA/92/002, report, 85 pp.

Arnórsson, S. and Gunnlaugsson, E 1985: *New gas geothermometers for geothermal exploration–calibration and application*. Geochim. Cosmochim. Acta, 47, 567 – 577pp.

Arnórsson, S., 1985: *The use of mixing models and chemical geothermometers for estimating underground temperature in geothermal systems*. J. Volc. & Geotherm. Res.,23, 299-335.

Arnórsson, S., 2000a: *Mixing processes in upflow zones and mixing models. In:* Arnórsson, S. (ed.), *Isotopic and chemical techniques in geothermal exploration, development and use. Sampling methods data handling, interpretation*. IAEA, Vienna, 200-202.

Arnórsson, S., 2000b: *The quartz and Na/K geothermometers. II. Results and applications for monitoring studies*, proceedings of world geothermal congress, Kyushu Japan, pp 935-946.

Arnórsson, S., 1986: *Chemistry of gases associated with geothermal activity and volcanism in Iceland.* A review. *J. Geophys. Res., 91,* 12261-12268.

Arnórsson, S., Andrésdottir, A., Gunnarsson, I., and Stefánsson, A. 1998: *New calibration for the quartz and Na/K geothermometers – valid in the range 0-350°C, Proceedings,* Geoscience Society of Iceland Annual Meeting, 42-43.

Arnórsson, S., Bjarnason, J.Ö., Giroud, N., Gunnarsson, I., and Stefánsson, A., 2006: *Sampling and analysis of geothermal fluids*. Geofluids, 6, 203-216

Arnórsson, S., Gunnlaugsson, E., and Svavarsson, H., 1983a: *The chemistry of geothermal waters in Iceland III. Chemical geothermometry in geothermal investigations.* Geochim. Cosmochim. Acta, 47, 567-577.

Arnórsson, S., Gunnlaugsson, E., and Svavarsson, H., 1983b: *The chemistry of geothermal waters in Iceland II. Mineral equilibria and independent variables controlling water compositions*. Geochim. Cosmochim. Acta, 47, 547-566.

Arnórsson, S., Sigurdsson, S. and Svavarsson, H., 1982: *The chemistry of geothermal waters in Iceland I. Calculation of aqueous speciation from 0°C to 370°C*. Geochim. Cosmochim. Acta, 46, 1513-1532.

Arnorsson, S., Stefansson, A. and Bjarnason, J.Ö. 2007: *"Fluid-fluid interaction in geothermal systems*," Reviews in Mineralogy & Geochemistry, 65, 229-312.

Axelsson, G., 2013: *Dynamic modelling of geothermal systems. Proceedings of the "Short Course on Conceptual Modelling of Geothermal Systems",* organized by UNU-GTP and LaGeo, Santa Tecla, El Salvador, 21 pp.

Barrios, L., Henríquez, E and Quezada, A., *Stratigraphic, Tectonic and thermal mapping through geological well logging in El Salvador,* Proceedings of the "Short Course on Conceptual Modelling of Geothermal Systems", organized by UNU-GTP and LaGeo, Santa Tecla, El Salvador,16 pp.

Baker, B. H., 1987: *Outline of the petrology of the Kenya rift alkaline province.293-211 in alkaline igneous rocks*. Fitton,J.G and Upton B.G.J (editors) Geological society special publication.No.30.

Baker, B. H., Goles, G., Leeman, W. P., and Lindstrom, M. M., 1977: *Geochemistry and petrogenesis of basalt benmoreite-trachyte suite from the southern part of the Gregory Rift,Kenya. Contributions to mineralogy and petrology*, vol 64,303-332.

Brown, F.H., Carmichael, I.S.E., 1971: *Quaternary volcanoes of the Lake Rudolf region: II. The lavas of North Island, South Island and the Barrier*. Lithos 4, 305–323.

Brownlow, A. H., 1979: *Geochemistry*, .Boston University, Pretince Hall inc - USA 2nd edition 52-89 pp

Champion, A. M., 1935: *Teleki's volcano and the lava fields at the southern end of Lake Rudolf,* Geographical Journal, vol 85, 323-341

Chasteen, T. G., 2000: *Hydride Generation Atomic Absorption Spectroscopy*. Department of Chemistry, Sam Houston State University, Huntsville, Texas 77341

Chiodini, G. and Cioni, R., 1989: *Gas geobarometry for hydrothermal systems and its application to some Italian geothermal areas*. Appl. Geochem., 4, 465-472.

Clarke, M.C.G., Woodhall, D.G., Allen d., Darling, G., 1990: *Geological, volcanological and hydrogeological controls on the occurrence of geothermal activity in the area surrounding Lake Naivasha, Kenya*. British Geological Survey Report for the Ministry of Energy, Republic of Kenya.

Craig, H., 1961 - *Isotopic variations in meteoric waters*. Science, 133, 1702-1703.

Craig, H., 1963: *The isotopic geochemistry of water and carbon in geothermal areas. In: Tongiorgi, E. (ed.), Nuclear geology on geothermal areas*. Consiglio Nazionale delle Ricerche, Laboratorio di Geologia Nucleare, Pisa, 17-53.

Cumming, W., 2009: *Geothermal Resource Conceptual Models Using Surface Exploration Data*, Proceedings, Thirty-Fourth Workshop on Geothermal Reservoir Engineering Stanford,SGP-TR187, 181-215

D´Amore, F., and Truesdell, A.H., 1985: *Calculations of geothermal reservoir temperatures and steam fractions from gas compositions.* Geothermal Resources Council Transactions, 9, 305-310.

Darling, G., Ármannsson, H., 1989: *Stable isotopic aspects of fluid flow in the Krafla, Námafjall and Theistareykir geothermal systems of northeast Iceland*. *Chem., Geol. 79,* 197–213.

Darling, W.G., and Armannsson, H., 1990*: Indirect detection of subsurface outflow from rift valley lakes*. Journal of hydrology, vol 113.297-305.

Deocampo, D.M., 2004a: *Hydrogeochemistry in the Ngorongoro Crater, Tanzania, and implications for land use in a World Heritage Site*. Applied Geochemistry 19: 755–767.

Deocampo, D.M., 2004b: *Authigenic clays in East Africa: regional trends and paleolimnology at the Plio-Pleistocene boundary, Olduvai Gorge, Tanzania.* Journal of Paleolimnology 31: 1–9.

DePaolo D. J., 1981: *A Neodymium and Strontium Isotopic Study of the Mesozoic CalcAlkaline Granitic Batholiths of the Sierra Nevada and Peninsular Ranges, California* Journal of geophysical research, vol. 86, no. b11, pages 10470-10488

DePaolo, D. J., and Wasserburg, G. J., 1977: *The sources of island arcs as Indicated by Nd and Sr isotopic studies* Geophys Res. Lett.,4 , 465-468

Dodson R.G., 1963: *Geology of South Horr Area. Report of the Geological survey of Kenya, No 60*

Dunkelman, T.J., Karson, J.A., Rosendahl, B.R. 1988. *Structural style of the Turkana Rift, Kenya*. Geology 16, 258 – 261.

Dunkelman, T.J., Rosendahl, B.R., Karson, J.A., 1989: *Structure and stratigraphy of the Turkana rift from seismic reflection data.* J. Afr. Earth Sci. 8, 489–510.

Dunkley P.N, Smith M, Allen D J, Darling, W, G., 1993: *Geothermal activity and geology of the northern sector of the Kenya Rift Valley,* Kenya Ministry of Energy, British Geological Survey Research Report SC/93/1

ELC, 2013: *Consultancy Services for the Feasibility Study of the 400 MW Menengai Phase 1 Geothermal Power* (unpublished report)

Ellis, A.J., 1962: *Interpretation of gas analysis from the Wairakei hydrothermal area.* N.Z. J. Sci., 5, 434-452.

Ellis, A.J., and Mahon, W.A.J., 1964: *Natural hydrothermal systems and experimental Hot-water/rock interaction* Geochim. Cosmochim. Acta, 28,1323-1357.

Ellis, A. J., .and Mahon, W.A. J., 1967: *Natural hydrothermal systems and experimental hot-water/rock interactions (Part II)*. Geochim. Cosmochim. Acta, 31, 519-538.

EGS.,*2010: Final Report Geothermal Exploration in Montserrat, Caribbean, Prepared for Minister of Communications and Works Government of Montserrat, Caribbean.* Santa Rosa, California

Erxleben, A., 2009: *Atomic absorption spectroscopy*, available on *URL:* http://www.nuigalway.ie/chemistry/level2/courses/CH205_atomic_absorption_spectroscopy.pdf last accessed 16/6/2013

Ferguson A.J.D. and Harbott B.J., 1982. *Geographical, physical and chemical aspects of Lake Turkana, In: Lake Turkana: A Report on the Findings of the Lake Turkana Project, 1972-1975, (Edited by A.J. Hopson).* Overseas Development Administration, London, pp. 1-107.

Fournier, R.O 1977: *Chemical geothermometers and mixing model for geothermal systems*. Geothermics, 5, 41-50

Fournier, R.O., 1979: *A revised equation for Na-K geothermometer*. Geothermal Resources Council, Trans., 3, 221-224.

Fournier, R.O., 1991: *Water geothermometers applied to geothermal energy; Applications of geochemistry in geothermal reservoir development* (Co-ordinator: D' Amore, F.) UNITAR publication, Rome, 37-69.

Fournier, R.O., and Potter, R.W., 1982: *A revised and expanded silica (quartz) geothermometer,* Geothermal Resources Council, Bull., 11, 3-9.

Fournier, R.O., and Truesdell, A.H., 1973: *An empirical Na-K-Ca geothermometer for natural waters*. Geochim. Cosmochim. Acta, 37, 515-525

Fournier, R.O. and Truesdell, A.H., 1974: *Geochemical indicators of subsurface temperature - Part 2, estimation of temperature and fraction of hot water mixed with cold water*. J. Res. U.S. Geol. Survey, 2. 263-270.

Garcin, Y., Olago, D., Melnick, D., Strecker, M. R., Tiercelin, J.J., 2012: *East African mid-Holocene wet–dry transition recorded in palaeo-shorelines of Lake Turkana, northern Kenya Rift,* Earth and Planetary Science Letters, EPSL-11367

GDC, 2011: *Barrier Volcanic complex geothermal resource assessment project report*, 1st edition, (GDC unpublished internal report).

GDC, 2012: *Reconnaisance geothermal assessment of Lokitaung-Turkana*, (GDC unpublished internal report)

Gichira, J., Simiyu, C ., Kangogo, D., Noor, Yussuf., Mwakirani, R., Wamalwa, A.,2011: *Resistivity Structure of Barrier Geothermal Prospect Proceedings*, Kenya Geothermal Conference 2011, Kenyatta International Conference Centre, Nairobi,

Giggenbach, W.F., 1988: *Geothermal solute equilibria, derivation of Na-K-Mg-Ca geoindicators.* Geochem. Cosmochim. Acta, 52, 2749-2765.

Giggenbach, W.F., Minissale, A.A. and Scandiffio, G., 1988: *Isotopic and chemical assessment of geothermal potential of the Colli Albani are, Latium region, Italy*. Applied Geochemistry, 3: 475-486.

Giggenbach W. F., 1993: *Redox control of gas compositions in Philippine volcanic-hydrothermal systems*. Geothermics 22, 575–587.

Giggenbach, W. F., 1991a: *Chemical techniques in geothermal exploration; Applications of geochemistry in geothermal reservoir development* (D'Amore, F., Ed.), UNITAR/UNDP centre on small energy resources, Rome. 119-144

Giggenbach, W.F. 1991b: *The composition of gases in geothermal and volcanic systems as a function of tectonic setting, in Water-Rock Interactions*, Kharaka and Maest eds., Balkema Rotterdam, 873-878.

Giggenbach, W.F., 1980. *Geothermal gas equilibria.* Geochim. Cosmochlm. Acta, 44, pp 2021-2032.

Giggenbach, W.F. 1992a: *Isotopic shifts in waters from geothermal and volcanic systems along convergent plate boundaries and their origin*, *EPSL* 113, 495-510.

Giggenbach, W.F. 1992b: *Magma degassing and mineral deposition in hydrothermal systems along convergent plate boundaries,* SEG distinguished lecture; *Economic Geology*, 87, 1927-1944.

Giggenbach, W.F., 1993: *Redox control of gas compositions in Philippine volcanic hydrothermal system*s, Geothermics, **22,** 575- 587.

Giggenbach, W.F., 1997: *"The origin and evolution of fluids in magmatic-hydrothermal systems," in Geochemistry of Hydrothermal Ore Deposits*, 3rd edition, H.L. Barnes ed., John Wiley and Sons, NY, June 1997.

Giggenbach, W.F. and Glover, R.B. 1992: *Tectonic regime and major processes governing the chemistry of water and gas discharges from the Rotorua geothermal field*, New Zealand, Geothermics, **21**, 121-140.

Giggenbach, W.F. and Goguel, R.L. 1989: *Collection and analysis of geothermal and volcanic water and gas discharges,* DSIR report CD 2401, 4th ed., Pentone, New Zealand.

Giroud, N., 2008: *A chemical study of arsenic, boron and gases in high-temperature geothermal fluids in Iceland.* University of Iceland, Reykjavík, PhD thesis, 128 pp.

GOK, 2005: *Turkana District Vision and Strategy 2005 -2015*, available on http://www.aridland.go.ke/NRM_Strategy/turkana.pdf last accessed 4/2/2013

Gunnarsson, I., Arnorsson, S., 2000: *Amorphous silica solubility and the thermodynamic properties of H_4SiO_4 degrees in the range of 0 degrees to 350 degrees C at P-sat*. Geochim. Cosmochim. Acta 64, 2295 -2307

Henley, R.W., Truesdell, A., and Barton, P.B. Jr. H., 1984: *Fluid-mineral equilibrium in hydrothermal systems*. Society of Economic Geologists, Reviews in Economic Geology, 1, 267

Hughes, R.H. and Hughes, J.S., 1992. *A Directory of African Wetlands*. IUCN, UNEP, WCMC. 820 p.

Jones, B.F., Deocampo, D.M., 2003: *Geochemistry of saline lakes*. In Surface and Groundwater, Weathering, Erosion, and Soils, Drever JI (ed.); Treatise on Geochemistry 5: 393–424.

Kallqvist, T., Lien, L. and Liti, D., 1988. *Lake Turkana Limnological Study 1985-1988*. Norwegian Institute for Water Research (NIVA) and Kenya Marine Fisheries Research Institute (KEMFRI), 1988. 98p.

Karingithi, C., 2009: *Chemical Geothermometers for geothermal exploration,* Short course II on surface exploration for Geothermal resources, UNU-GTP, Lake Naivasha-Kenya, 2-17.

Karingithi, C. W., Arnórsson, S., and Gronvold, K., 2010: *Processes controlling aquifer fluid compositions in the Olkaria geothermal system, Kenya*. J. Volcanol. Geoth. Res., 196, 57-76.

Le Bas, M.J., Le Maitre, R.W., Strekeisen,A and Zanettin,B., 1986: *A chemical classification of Volcanic rocks based on the total alkali-silica diagram*. Journal of petrology,vol 27, 745-750

Levin, N.E., Zipser, E.J., Cerling, T.E., 2009. *Isotopic composition of waters from Ethiopia and Kenya: insights into moisture sources for eastern Africa*. J. Geophys. Res. 114, D23306. doi:10.1029/2009JD012166

Malimo, S., 2012: *Aquifer fluid modelling and assessment of mineral-gas-liquid equilibria in the Námafjall geothermal system, NE-Iceland,* UNU-GTP, Msc report No.3

Mahon, W. A. J., 1967: *Natural hydrothermal systems and the reaction of hot water with sedimentary rocks*. N.Z. J. Sci., 10. 206-221.

Mahon, W. A. J., McDowell. G.D. and Finlayson, J.B., 1980: *Carbon dioxide: its role in geothermal systems*. N.Z. J. Sci., 23,133-148 pp

Melnick, D., Garcin, Y., Quinteros, J., Strecker, M. R., Olago, D., and Tiercelin, J. J., 2012: *Steady rifting in northern Kenya inferred from deformed Holocene lake shorelines of the Suguta and Turkana basins*: Earth and Planetary Science Letters, doi:10.1016/j.epsl.2012.03.007, v. 331-332, p. 335-346

Morley, C.K., Wescott, W.A., Stone, D.M., Harper, R.M., Wigger, S.T., Karanja, F.M., 1992: *Tectonic evolution of the northern Kenyan Rift*. J. Geol. Soc. London 149, 333–348.

Mortensen, A. K., and Axelsson, G. 2013: *Developing a conceptual model of a geothermal system, Short Course on Conceptual Modelling of Geothermal Systems*,UNU-GTP and LaGeo, Santa Tecla, El Salvador,1-20

Nehring, N.L., D´Amore, F., 1984. *Gas chemistry and thermometry of the Cerro Prieto, Mexico, geothermal field*. Geothermics 13, 75–89.

Nicholson, K.,1993: *Geothermal fluids:chemistry and exploration techniques*, Springer-Verlag Berlin Heidelberg New York ISBN 3-540-56017-3 pp

Norry,M.J.,Truckle,P.H.,Lippard,S.J.,Hawkesworth,C.J.,Weaver,S.D., and Marriner,G.F.,1980: *Isotopic and trace element evidence from lavas, bearing on mantle heterogeneity beneath Kenya.* Philosophical transactions of the Royal society of London, Vol. A297,259-271.

Oelkers E. 2001: *General kinetic description of multioxide silicate mineral and glass dissolution*. Geochim. Cosmochim. Acta, **65**, 3703-3719.

Oyuntsetseg, D 2009: *Geochemical characterization of thermal fluids from the khangay area, central mongolia* IS-108 Reykjavík, Iceland UNU-GTP Report No 10,pp 126-135

Powell, T., and Cumming, W., 2010: *Spreadsheet for geothermal water and gas geochemistry*

Proceedings of the 35th workshop on geothermal reservoir engineering, Stanford University, Stanford, SGP-TR-188

Powell, T. 2000: *A Review of Exploration Gas Geothermometry*, Proceedings, 25th Workshop on Geothermal Reservoir Engineering, Stanford University, Stanford, CA, SGP-TR-165.

Powell, T., Moore, J., DeRocher, T., McCulloch, J.,2001: *Reservoir Geochemistry of the Karaha -Telaga Bodas Prospect, Indonesia*, Geothermal Resource Council Transactions 25.

Renaut RW, Jones B, Tiercelin J-J, Tarits C. 2002: S*ublacustrine precipitation of hydrothermal silica in rift lakes: evidence from Lake Baringo, central Kenya Rift Valley*. Sedimentary Geology 148: 235–257.

Republic of Kenya, 2002. *Turkana District Development Plan, 2002-2008*. Ministry of Finance and Planning. Government Printers.

Reyes, A.G., 1990: *Petrology of Philippine geothermal system and the application of alteration Mineralogy to their assessment.* Journal of Volcanology and Geothermal Research, 43, 279-304.

Sceal, J.S.C., and Weaver,S.D.,1971: *Trace element data bearing on the origin of salic rocks from the Quaternary Volcano Paka,Gregory Rift,Kenya*.Earth and Planetary Science letters,vol.12 327-331

Sekento L.R., 2012: *Geochemical and isotopic study of the Menengai geothermal field, Kenya Report 31*: Geothermal training in Iceland.*2012.* UNU-GTP, Iceland

Settle, A. F., 1997: *Infrared spectroscopy Handbook of Instrumental Techniques for Analytical Chemistry*

Stockli, D., 2013: *Novel Coupled Thermochronometric and Geochemical Investigation of Blind Geothermal Resources in Fault-Controlled Dilational Corners*, Geothermal Technologies Program 2013 Peer Review, Jackson school of geosciences-University of Texas at Austin.

Sombroek, W.G.,Braun H.M.H. and Van der Pouw B.J.A., 1982. *Exploratory Soil Map and Agroclimatic Zone Map of Kenya*. Kenya Soil Survey, Ministry of Agriculture, Nairobi.

Survey of Kenya, 1977: *National Atlas of Kenya*. 3rd edition., Nairobi. Report No. E1.

Tarits, C., Renaut, R.W., Tiercelin, J. J., Hérissé, A., Cotten, J. and Cabon, J., 2006: *Geochemical evidence of hydrothermal recharge in Lake Baringo*, Central Kenya Rift Valley. *Hydrol. Process.* 20, 2027–2055.

Truckle, P.H 1956: *Geology and late canoizoic lake sediments of the Suguta trough,Kenya*, Geology department,Bedford college,London. Nature Vol 263.

Truesdell, A.H., 1976: *Summary of Section III. Geochemical techniques in exploration*. Proceedings of the 2nd United Nations Symposium on the Development and Use of Geothermal Resources, San Francisco, 53-79.

Truesdell, A.H., and Fournier, R.O., 1977: *Procedure for estimating the temperature of a hot water component in a mixed water using a plot of dissolved silica vs. enthalpy*. U.S. Geol. Survey J. Res., 5, 49- 52.

Weaver, S.D., 1977: *The Quaternary caldera volcano Emuraungongolak,Kenya Rift,and the petrology of bimodal ferrobasalt-pantelleritic trachyte association*.Bulletin volcanologique,vol.40, 209-230

Weaver, S .D., Sceal, J.S.C and Gibson,I 1972: *Trace element data relevant to the origin of trachytic and pantelleritic lavas in the East African Rift System.* Contributions to mineralogy and petrology, vol.36, 181- 194.

White, F., 1983: *The Vegetation of Africa*. UNESCO, 355 pp.

APPENDIX I

Sampling procedure of fumaroles and hot springs

a) Criteria for selecting the best fumarole or spring for sampling

The criteria used to select hot springs and fumaroles for sampling include temperature, flow rate, geographic distribution, whether the water issues from soil or directly from the bedrock and any hydrogeological observations that might indicate mixing of the geothermal water with surficial water. Generally, the most favourable sites are springs with the highest temperature, the highest flow rate, the smallest aperture and minimum contact with any soil (Arnórsson et al., 2006). The following criteria are recommended when selecting springs and fumaroles for sampling (Arnórsson et al., 2000):

- High temperature
- High flow rate
- Neutral to alkaline pH
- High electrical conductivity
- Location
- Well defined outlet

When fumaroles and mud pools or springs of muddy water are located close to each other, the fumaroles should be sampled preferentially. Most likely the muddy springs represent steam heated waters. On site pH measurements will help in identifying the steam heated waters. When making a final selection of a sample site in the field, it is convenient to measure the temperature of the water and its electrical conductivity. The spring with the highest temperature and highest electrical conductivity should be selected. Samples should be collected as far as possible from narrow vents rather than large pools. Exposure of the thermal water to the atmosphere in large pools may cause changes in its chemistry and isotope composition (Arnórsson et al., 2000).

Sampling and analysis of ground and surface waters is important for evaluation of possible mixing of the geothermal water with such shallow water in upflow zones. The selection of fumaroles for sampling is not as straightforward as that of hot springs. It is generally best to sample small outlets, which discharge steam at considerable velocity, in areas of the most intense acid surface alteration. Sampling fumarole steam provides information on individual gas concentrations in the steam and is for this reason also preferred to the sampling of gases bubbling through steam-heated or hot spring water. The latter only provide information on the relative amounts of the gases in the gas phase and not their absolute concentrations in the steam (Arnórsson et al., 2006).

b) Procedure and Layout of equipment for fumarole discharge sampling

- Select a suitable fumarole for sampling by measuring the temperature using a thermocouple and a probe
- Place the funnel upside down and make some mud and cover it firmly to avoid atmospheric incursion into the funnel.
- Fix the silicon tubing (can with stand high temperatures) to the funnel
- Fix the cooling coil of stainless steel to the tubing
- Immerse the cooling coil in a bucket with water in order to condense the steam
- Fix another tubing to the outlet of the cooling coil
- Fix a plastic sampling bulb to the cooling or washing bottle (approximately 300 ml) for collection of condensate
- Attach a hand pump or a peristalitic pump for acceleration of the collection of the condensate into the sampling bulb
- Before collecting a sample, it is necessary to allow steam to pass through the tubing and the sample ports of the gas sampling bulb, and through the wash bottle when used, to displace any air in the system
- Transfer the sample in the sampling bulb or the wash bottle into the 250ml or 500ml sampling bottles for analysis of various parameters
- Set a side a sample for onsite analysis of H_2S
- When sampling for gas, remove the stainless cooling coil and attach the evacuated giggebach gas flask containing 50 ml of 40% NaOH solution with cold water continuously pouring on top of the flask to cool it
- Immerse the gas flask into a bucket with water or continously pour water on the flaks to cool it when sampling
- Allow gas to enter the gas flask till no bubbles is seen into the solution of NaOH

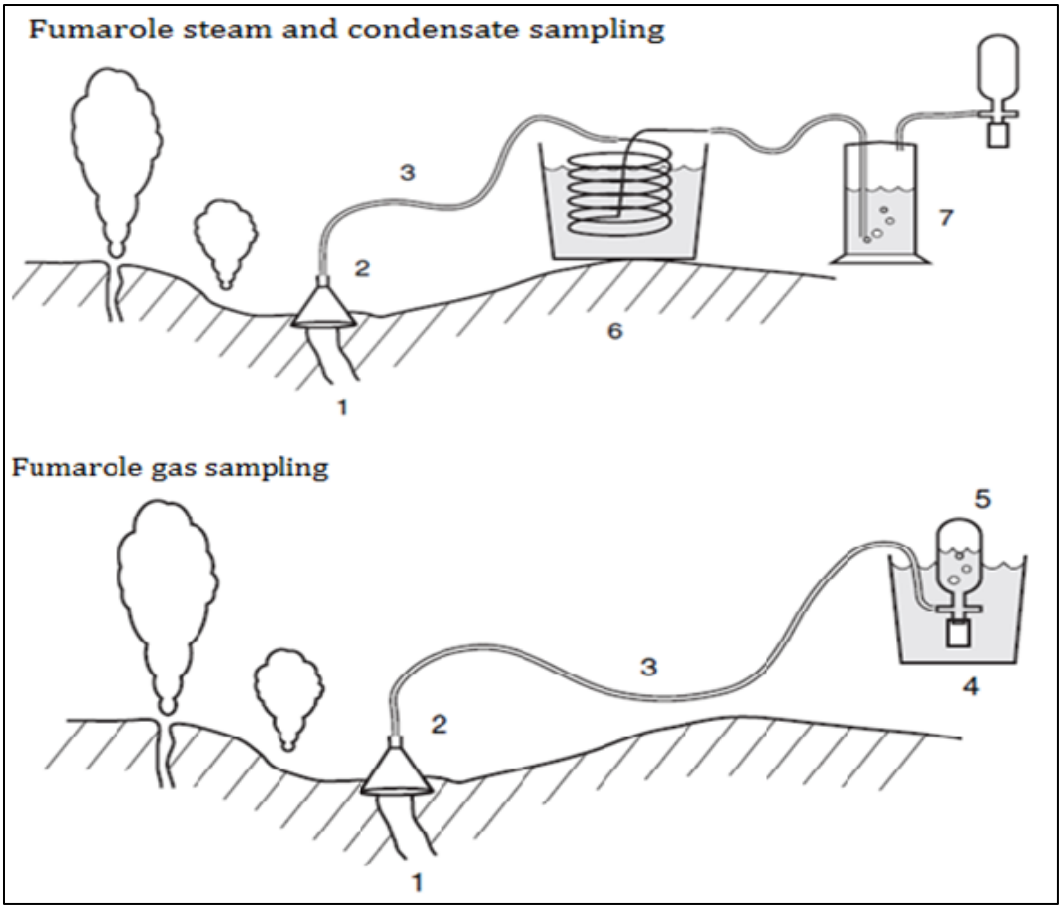

The layout of the apparatus needed to collect samples of hot-spring water (Modified after Arnórsson et al., 2006). Where 1 is: fumarole, 2: funnel, 3: silicon tubing, 4: bucket, 5: evacuated gas flask, 6: stainless steel and cooling coil.

.

c) Procedure and Layout of equipment for a hot spring discharge sampling

- Select a suitable hot spring for sampling by measuring the temperature using a thermocouple and a probe and the electrical conductivity using a conductivity meter.
- Place the funnel upside down and and hold firmly on the hot springs to prevent atmospheric air incursion
- Fix the silicon tubing (can with stand high temperatures) to the funnel
- Fix the cooling coil of stainless steel to the tubing
- Immerse the cooling coil in a bucket with water in order to condense the steam
- Fix another tubing to the outlet of the cooling coil
- Fix a plastic sampling bulb to the cooling or washing bottle (approximately 300 ml) for collection of condensate

- Attach a hand pump or a peristalitic pump for acceleration of the collection of the condensate into the plastic sampling bulb
- Attach a Teflon filter holder (4) with 20 cm diameter 0.2 μm filter membrane with a funnel or a 0.2 to 0.45 μm cellulose acetate membranes into low density polyethylene bottles using a polypropylene filter holder into the sampling bulb of wash bottle
- Before collecting a sample, it is necessary to allow steam to pass through the tubing and the sample ports of the water/ gas sampling bulb, and through the wash bottle when used, to displace any air in the system
- Transfer the sample in the sampling bulb or the wash bottle into the 250ml or 500ml sampling bottles for analysis of various parameters
- Set a side a sample for onsite analysis of H_2S
- When sampling of gas, remove the stainless cooling coil and attach the giggebach gas flask containing 50 ml of 40% NaOH solution with cold water continuously pouring on top of the flask to cool it. When sampling of gas from hot springs, the gas sampling bulb, which must have a stopcock at both ends, should not be evacuated (Arnosson et al.,2006)
- Immerse the gas flask into a bucket with water or continously pour water on the flaks to cool it when sampling
- Allow gas to enter the gas flask till no bubbles is seen into the solution of NaOH

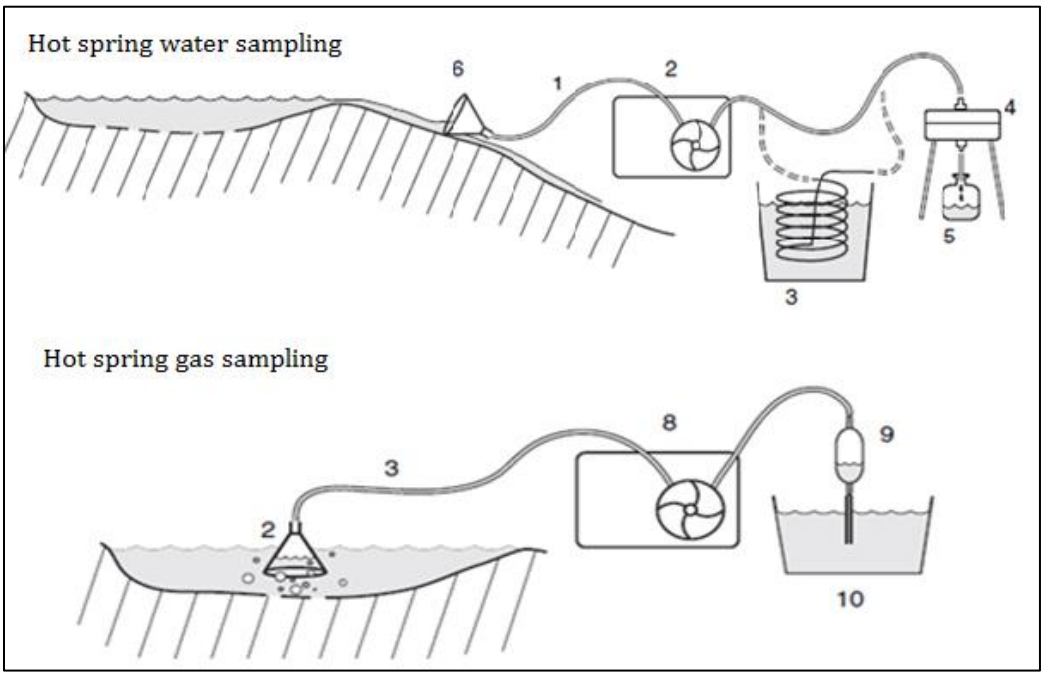

The layout of the apparatus needed to collect samples of hot-spring water (Modified after Arnórsson et al.2006). Where 1 is: silicon tubing, 2: funnel/ peristaltic pump, 3: stainless steel cooling coil, 4: polypropylene filter holder, 5: sampling bottle, 6: stainless steel and cooling coil. 8: peristaltic pump for gas sampling, 9: gas flask, 10: bucket and water.

APPENDIX II

Chemistry of the Lake Turkana and Parkati well

Hot springs	Sampling Temp (°C)	Cond (µΩ/cm)	TDS (ppm)	pH/20°C	Concentration (ppm)												
					B	SO_4	Cl	CO_2	F	H_2S	SiO_2	Al	Ca	Li	Na	K	Mg
Logipi NE	69.8			8.85	6.39	920	920	5720	82		30.8		0.48	0.149	6200	120	
Logipi NW	61.4			8.3	5.11	590	3420	5160	110		18.5		0.5	0.05	4170	79.4	
(Dunkley et al., 1993)																	
Lake Turkana waters																	
Lake Turkana[1]				nm	0.72	43.3	515	1580	21		25.68		3.5	0.01	985	20.5	2.5
Lake Turkana[2]				9.45	0.65	40	446	1580	10		25.252		2.4	0.01	932	19.2	2.4
Lake Turkana[3]				9.45	0.65	39.3	436	1520	11		21.828		2.4	0.01	909	18.8	2.4
Lake Turkana (GDC, 2012)		3510		9.5/21	32.69		495.7	980.1	7.83	0.17	22		0.17		347.4	20.04	
Shallow Ground water																	
Parkati well[1]				7.5	0.03	306	217	262	1.3		121		45.7	0.013	244		
Parkati well (GDC, 2011)				7.89	0.03	236	345	631	0.97	0.136	57	0.026	44.54	0.022	127.4		

- *(Lake Turkana and Parkati well samples labeled 1, 2 and 3 after Dunkley et al., 2013)*

APPENDIX III

Stable isotope chemistry of the BVC and other water bodies (Dunkley et al., 1993)

Location	Temp (^{o}C)	$\delta^{2}H$	$\delta^{18}O$
Logipi NW[c]	61.4	15	2.2
Logipi NE[d]	69.8	14	2.3
Central Island	70.5	36	5.8
Loyangalani[d]	39.2	-21	-4
Parkati[d]	Amb	-22	-3.9
Tum[d]	Amb	-25	-5.2
Lake Turkana[c]	-	43	6.8
Lake Turkana N[d]	-	36	5.9
Lake Turkana C[d]	-	35	5.8
Kakorinya	96	-5	-3.1
Kakorinya	92.8	-30	-5.8
Kakorinya	94	-19	-4.2
Kakorinya	94.4	-17	-3.7
Kakorinya	92.9	-22	-4.3
Lake Baringo[a]	-	47	8.8
Lake Baringo[b]	-	21	-2.8
Lake Baringo[d]	-	40	7.6
Lake Baringo N[c]	-	32	5.3
Lake Baringo S[c]	-	34	5
Eliye[d]	35.4	-13	-3.2
Eliye North[d]	37.3	-11	-2.9

- *Values in per mil (‰) with respect to SMOW.*
- *Year of sampling; a:1986, b: 1988, c:1989, d: 1991*